

T.C.
DOKUZ EYLÜL UNIVERSITY
İZMİR INTERNATIONAL BIOMEDICINE AND GENOME INSTITUTE

**IDENTIFICATION OF LONG NON-CODING
RNAs THAT HAVE POTENTIAL TO BE NOVEL
DIAGNOSTIC, PROGNOSTIC BIOMARKERS OR
THERAPEUTIC TARGETS IN MANTLE CELL
LYMPHOMA THROUGH WHOLE-
TRANSCRIPTOME SEQUENCING**

DENİZ KURŞUN

MOLECULAR BIOLOGY AND GENETICS
MASTER OF SCIENCE THESIS

İZMİR – 2019

Thesis Code: DEU.İBG.MSc-2016850033

T.C.
DOKUZ EYLÜL UNIVERSITY
IZMIR INTERNATIONAL BIOMEDICINE AND GENOME INSTITUTE

**IDENTIFICATION OF LONG NON-CODING
RNAs THAT HAVE POTENTIAL TO BE NOVEL
DIAGNOSTIC, PROGNOSTIC BIOMARKERS OR
THERAPEUTIC TARGETS IN MANTLE CELL
LYMPHOMA THROUGH WHOLE-
TRANSCRIPTOME SEQUENCING**

MOLECULAR BIOLOGY AND GENETICS
MASTER OF SCIENCE THESIS

DENİZ KURŞUN

Advisor: Assoc. Prof. Dr. CAN KÜÇÜK

(This Project was supported by TÜBİTAK with project number:116S625)

Thesis Code: DEU.İBG.MSc-2016850033

Dokuz Eylül University İzmir International Biomedicine and Genome Institute Department of Genomics and Molecular Biotechnology, Molecular Biology and Genetics graduate program Master of Science student Deniz KURŞUN has successfully completed her Master of Science thesis titled **'IDENTIFICATION OF LONG NON-CODING RNAs THAT HAVE POTENTIAL TO BE NOVEL DIAGNOSTIC, PROGNOSTIC BIOMARKERS OR THERAPEUTIC TARGETS IN MANTLE CELL LYMPHOMA THROUGH WHOLE-TRANSCRIPTOME SEQUENCING'** on the date of 22/11/2019.

CHAIR

Assoc. Prof. Dr. Can KÜÇÜK



MEMBER

Assoc. Prof. Dr. Duygu SAĞ WINGENDER
Dokuz Eylül University İzmir International
Biomedicine and Genome Institute
Department of Genome Sciences and
Molecular Biotechnology



MEMBER

Asst. Prof. Dr. Melis KARTAL
YANDIM
Izmir Economy University Faculty of
Medicine Department of Basic Medical
Sciences

SUBSTITUTE MEMBER

Prof. Dr. İnci ALACACIOĞLU

Dokuz Eylül University Oncology Institute
Department of Clinical Oncology

SUBSTITUTE MEMBER

Prof. Dr. Mahmut TÖBÜ

Ege University Faculty of Medicine,
Department of Internal Medicine

Dokuz Eylül Üniversitesi İzmir Uluslararası Biyotıp ve Genom Enstitüsü Genom Bilimleri ve Moleküler Biyoteknoloji Anabilim Dalı, Moleküler Biyoloji ve Genetik Yüksek Lisans programı öğrencisi Deniz KURŞUN '**Mantle hücreli lenfomalarda özgün tanı, prognoz belirteci veya tedavi hedefi olma potansiyeline sahip uzun kodlamayan RNA'ların tüm transkriptom dizi analizi yoluyla belirlenmesi**' konulu Yüksek Lisans tezini 22/11/2019 tarihinde başarılı olarak tamamlamıştır.

BAŞKAN

Doç. Dr. Can KÜÇÜK



ÜYE

Doç. Dr. Duygu SAĞ WINGENDER

Dokuz Eylül Üniversitesi İzmir Uluslararası
Biyotıp ve Genom Enstitüsü Genom Bilimleri ve
Moleküler Biyoteknoloji Anabilim Dalı



ÜYE

Dr. Öğr. Üyesi Melis KARTAL YANDIM
İzmir Ekonomi Üniversitesi Tıp Fakültesi,
Temel Tıp Bilimleri, Tıbbi Biyoloji Bölümü

YEDEK ÜYE

Prof. Dr. İnci ALACACIOĞLU

Dokuz Eylül Üniversitesi Onkoloji Enstitüsü
Klinik Onkoloji Anabilim Dalı

YEDEK ÜYE

Prof. Dr. Mahmut TÖBÜ

Ege Üniversitesi Tıp Fakültesi, Dahili Tıp
Bilimleri Bölümü, İç Hastalıkları Ana
Bilim Dalı

TABLE OF CONTENTS

INDEX OF FIGURES	III
INDEX OF TABLES	IV
LIST OF ABBREVIATIONS	V
ACKNOWLEDGEMENT	VI
1.INTRODUCTION AND AIMS	3
1.1.Statement and Importance of the Problem	3
1.2. Aims of the Study	3
1.3. Hypothesis of the Study	3
2. GENERAL INFORMATION	4
2.1. Normal B-Cell Development	4
2.2. Lymphoid Neoplasms	9
2.3. Mantle Cell Lymphoma	10
2.4. Emerging Roles of Long non-coding RNAs as Cancer Biomarkers	13
3. MATERIALS AND METHODS	17
3.1. Type of the Study	17
3.2. Time and Location of the Study	17
3.3. Population and Sample of the Study	17
3.4. Materials of the Study	18
3.4.1 Solutions	18
3.4.2. Chemicals	18
3.4.3. Kits	18
3.4.4. FACS Antibodies	19
3.4.5. Equipments	19
3.5. Variables of the Study	20
3.6 Data Collection Tools	20
3.6.1. Collection of MCL tumor tissue samples and obtaining FFPE sections	20
3.6.2. RNA isolation from MCL tumor FFPE tissue sections	21
3.6.3. Obtaining B cell subtypes from reactive tonsil tissues by FACS	22
3.6.4. RNA isolation from reactive tonsil B cell subtypes	25
3.6.5. Quality controls of isolated MCL RNAs (running on TAE gel)	26

3.6.6. Whole Transcriptome Sequencing	27
3.6.7. Analysis of Differentially Expressed lncRNAs and mRNAs in MCL.....	30
3.6.8. Transcript Abundance Estimation with Cufflinks	33
3.6.9. Cross-validation of selected lncRNA transcripts' expression by qRT-PCR.....	33
3.6.10. Pathway analysis of MCL-related genes.....	37
3.6.11. Survival Analysis.....	37
3.7. Study Plan and Calendar	38
3.8. Data Evaluation	38
3.9. Limitations of the Study	39
3.10. Ethics Committee Approval	39
4. RESULTS	40
4.1. FACS Analysis of Tonsil B cell Subtypes.....	40
4.2. Quality control of raw sequence data	41
4.3. Confirming the strand specificity orientation of the RNA-seq data	43
4.4. Read mapping and Quality Control.....	43
4.5. Identification of differentially expressed lncRNAs in MCL cases	45
4.6. Identification of differentially expressed mRNAs	49
4.7. Quality control of transcript expression analysis of whole transcriptome data obtained with RNA-Seq.....	53
4.8. Cross-validation of selected lncRNA transcripts' expression by qRT-PCR.....	56
4.9. Pathway analysis of MCL-related genes.....	59
4.10. ROC and Survival Analysis.....	65
5. DISCUSSION	70
6. CONCLUSION AND FUTURE ASPECTS	73
7. REFERENCES	74
8. APPENDIX.....	82
8.1. Curriculum Vitae.....	82
8.2. Ethics Comittee.....	84

INDEX OF FIGURES

Figure 1: Illustration of BCR gene recombination events in normal B cell development.....	5
Figure 2: Demonstration of germinal center reactions	8
Figure 3: LncRNAs which are associated with hallmarks of cancer	15
Figure 4: Schematic depiction of the RNA isolation process from B-cell subsets by RNeasy Mini kit.....	26
Figure 5: Integrity checks of RNAs isolated from MCL cases (TAE gel images).....	27
Figure 6: TruSeq Stranded Total RNA Kit Library Preparation	29
Figure 7: RNA-seq data analysis pipeline.....	30
Figure 8: Sorting gates strategies used in multicolor FACS analysis to isolate B-cell subsets.	40
Figure 9: Per base sequence quality of MCL41 sample.....	42
Figure 10: MultiQC results of HISAT2 alignment scores	44
Figure 11: Heatmap of sample-to-sample distances of lncRNA annotated MCL and control samples.....	47
Figure 12: PCA plot of lncRNA annotated MCL and control samples	48
Figure 13: MA-plot of lncRNA annotated MCL and control samples	49
Figure 14: Heatmap of sample-to-sample distances	51
Figure 15: PCA plot of MCL and control samples.....	52
Figure 16: MA-plot of MCL and control samples.....	53
Figure 17: RNA-Seq expression of CCND1 and SOX11 transcripts in MCL cases.....	55
Figure 18: RNA-Seq expression of MALAT1 and SNHG5 lncRNAs in MCL cases.....	56
Figure 19: Comparison of SNHG5 expression levels in MCL cases by RNA-Seq and qRT-PCR methods	58
Figure 20: Relative MALAT1 expression in MCL samples (n=18) compared to control samples (n=3)	59
Figure 21: KEGG Pathway analysis of upregulated differentially expressed mRNAs in MCL	60
Figure 22: Gene Ontology analysis of upregulated differentially expressed mRNAs with the most enriched GO term associated with the biological process	62
Figure 23: Reactome pathway analysis of downregulated differentially expressed mRNAs in MCL.	63
Figure 24: Gene Ontology analysis of downregulated differentially expressed mRNAs with the most enriched GO term associated with the biological process	64
Figure 25: ROC Curves of AC010983.1 (A), LINC01268 (B), PWRN2 (C), MAGI1-IT1 (D) lncRNAs (AUC: area under the ROC curve)	65
Figure 26: ROC curves of SOX11(A), EZH2 (B), and IL33 (C) mRNAs (AUC: area under the ROC curve).....	67
Figure 27: Kaplan Meier graphs of AC010983.1 (A) LINC01268 (B) PWRN2 (C) MAGI1-IT1 (D) lncRNAs	68
Figure 28: Kaplan Meier graphs of SOX11(A), EZH2 (B), and IL33 (C) mRNAs	69

INDEX OF TABLES

Table 1: MCL international prognostic index	12
Table 2: Immunophenotypic profile and used FACS antibodies for B-cell subsets.....	24
Table 3: Designed q-RT-PCR Primer List	34
Table 4: Genomic DNA elimination reaction components	35
Table 5: Reverse-Transcription Master Mix Componets	35
Table 6: Thermal cycler protocol.....	36
Table 7: qPCR reaction components.....	36
Table 8: qPCR cycling program	37
Table 9: The top 20 upregulated DElncRNAs in MCL	45
Table 10: The top 20 downregulated DElncRNAs in MCL.....	46
Table 11: The most dysregulated DEmRNAs in MCL.....	50
Table 12: Details of the ROC Curve Analysis of Upregulated DElncRNAs	66
Table 13: Details of the ROC Curve Analysis of Upregulated DEmRNAs.....	67

LIST OF ABBREVIATIONS

BAM	Binary alignment map
APC	Antigen-Presenting Cells
AUC	Area Under Curve
BCR	B cell receptor
BM	Bone Marrow
CB	Centroblast
CC	Centrocyte
CCND1	Cyclin D1
cDNA	Complementary DNA
cMCL	Conventional Mantle Cell Lymphoma
CSR	Class switch recombination
DElncRNA	Differentially expressed long non-coding RNA
DEmRNA	Differentially expressed mRNA
DLBCL	Diffuse Large B cell lymphoma
FACS	Fluorescence-Activated Cell Sorting
FDC	Follicular Dendritic Cell
FDR	False Discovery Rate
FPKM	Fragments Per Kilobase of Transcript per Million Mapped
GC	Germinal center
GO	Gene Ontology
HSC	Hematopoietic stem cell
Ig	Immunoglobulin
IgHV	Immunoglobulin heavy chain variable
KEGG	Kyoto Encyclopedia of Genes and Genomes
lincRNA	Long intergenic noncoding RNA
lncRNA	Long noncoding RNA
MBC	Memory B cell
MCL	Mantle Cell Lymphoma
MIPI	MCL international prognostic index
NBC	Naive B cell
NGS	Next-generation sequencing
NHL	Non-Hodgkin's Lymphoma
nnMCL	Non-nodal Mantle Cell Lymphoma
OS	Overall Survival
RNA-seq	RNA sequencing
ROC	Receiver Operating Characteristics
SHM	Somatic hypermutation
V(D)J	Variable Diversity Joining
WHO	World Health Organization
WTS	Whole Transcriptome Sequencing

IDENTIFICATION OF LONG NON-CODING RNAs THAT HAVE POTENTIAL TO BE NOVEL DIAGNOSTIC, PROGNOSTIC BIOMARKERS OR THERAPEUTIC TARGETS IN MANTLE CELL LYMPHOMA THROUGH WHOLE-TRANSCRIPTOME SEQUENCING

Deniz Kurşun, Izmir International Biomedicine and Genome Institute, Dokuz Eylül University Health Campus, Balçova, 35340, Izmir / Turkey, deniz.kursun@msfr.ibg.edu.tr

ABSTRACT

Mantle cell lymphoma (MCL) is a B-cell non-Hodgkin's lymphoma (NHL) which is considered as an incurable lymphoid neoplasm with a continuous relapse pattern and a median survival of only 3-5 years. Therefore, there is an urgent need to elucidate the MCL disease pathobiology and identify novel biomarkers and therapeutic target in order to optimize the treatment and improve the prognosis of MCL patients. Long noncoding RNAs (lncRNAs) have been shown to involve the development of many cancers and some of them are used as novel biomarkers. However, there are very few reports of lncRNAs that are related to the MCL pathogenesis and prognosis.

In this study, we aimed to identify lncRNAs that have the potential to be novel diagnostic, prognostic biomarkers or therapeutic targets in MCL through whole-transcriptome sequencing. We examined the lncRNA and also mRNA expression profile of 18 MCL samples and compared with 3 control samples. A total of 1149 significantly differentially expressed lncRNAs were detected with 322 of lncRNAs upregulated and 827 of lncRNAs downregulated in MCL. We analyzed some selected lncRNAs in MCL patient tumor samples - for cross-validation of WTS results - by qRT-PCR. We also performed pathway analysis to interpret the differential expression data. And we found that upregulated mRNAs were mainly involved in angiogenesis and pathways in cancer. We examined the diagnostic value of differentially expressed AC010983.1, LINC01268, PWRN2, MAGI1-IT1 lncRNAs and SOX11, EZH2 and IL33 mRNAs by ROC curve analysis. Despite a high area under the curve value of selected transcripts, according to the log-rank test of Kaplan Meier curves, p values were not significant ($P > 0.05$). However, our present study showed the potential value of significantly differentially expressed lncRNAs and mRNAs on MCL patient prognosis which should be further investigated with increased sample number and functional assays.

Keywords: MCL, NHL, RNA-seq, lncRNA

Mantle hücreli lenfomalarda özgün tanı, prognoz belirteci veya tedavi hedefi olma potansiyeline sahip uzun kodlamayan RNA'ların tüm transkriptom dizi analizi yoluyla belirlenmesi

Deniz Kurşun, Izmir International Biomedicine and Genome Institute, Dokuz Eylül University Health Campus, Balçova, 35340, Izmir / Turkey, deniz.kursun@msfr.ibg.edu.tr

ÖZET

Mantle hücreli lenfoma (MCL), sürekli nüks paterni ve sadece 3-5 yıl ortanca sağkalım ile tedavi edilemeyen bir lenfoid neoplazmı olarak kabul edilen B hücreli Hodgkin olmayan lenfoma alt türüdür (NHL). Bu nedenle, MCL hastalarının tedavisinin optimize edilmesi ve prognozlarının iyileştirilebilmesi için MCL patolojisinin aydınlatılarak yeni biyobelirteçlerin keşfedilmesi ve tedavi hedeflerinin belirlenmesi gerekmektedir. Uzun kodlayıcı olmayan RNA'ların (lncRNA'lar) birçok kanserin gelişimine katkı koyduğu ve bazılarının yeni biyobelirteçler olarak kullanıldığı gösterilmiştir. Bununla birlikte, MCL patogenezi ve prognozu ile ilgili çok az sayıda lncRNA literatürde rapor edilmiştir.

Bu çalışmada, tüm transkriptom dizilime yoluyla MCL'de yeni tanısal, prognostik biyobelirteçler veya terapötik hedefler olma potansiyeli olan lncRNA'ları belirlemeyi amaçladık. 18 MCL numunesinin lncRNA'sını ve ayrıca mRNA ekspresyon profilini inceledik ve 3 kontrol numunesi ile karşılaştırdık. Toplamda 1149 anlamlı şekilde farklı şekilde eksprese edilen lncRNA'lar belirledik. Belirlenen bu lncRNA'lardan 322 tanesi upregüle, 827 tanesi ise kontrol örneklere göre downregüle olmuştu. MCL hasta tümör numunelerindeki bazı seçili lncRNA'ları –WTS sonuçlarının çapraz validasyonu amacıyla qRT-PCR ile analiz ettik. Farklı şekilde eksprese edilen genleri yorumlamak için yolak analizi gerçekleştirdik ve upregüle edilmiş mRNA'ların çoğunlukla anjiyogenez ve kanserdeki yolaklarla ilişkili olduğunu gözlemledik. AC210983.1, LINC01268, PWRN2, MAGI1-IT1 lncRNA'ların ve SOX11, EZH2 ve IL33 mRNA'ların MCL prognozunu belirleyebilecek transkript seviyelerini ROC eğrisi analizi ile inceledik. Kaplan Meier eğrileri, P değeri anlamlı değildi ($P > 0.05$). Bununla birlikte, bu çalışmamız, MCL hasta prognozunda anlamlı şekilde farklı şekilde eksprese edilen lncRNA'ların ve mRNA'ların, artan numune sayısı ve fonksiyonel analizlerle daha fazla araştırılması gereken potansiyel değerini göstermiştir.

Anahtar kelimeler: MCL, NHL, RNA dizileme, lncRNA

1.INTRODUCTION AND AIMS

1.1.Statement and Importance of the Problem

Mantle cell lymphoma (MCL) is a rare B-cell non-Hodgkin's lymphoma (NHL) which is considered as an aggressive, incurable lymphoid neoplasm with a continuous relapse pattern and a median survival of only 3-5 years (Jares, Colomer, & Campo, 2007; Swerdlow et al., 2016). MCL is a heterogeneous disease with a broad spectrum of clinical, pathological, and biological features; hence, clinical treatment options are also variable (Campo, 2014). Conventional MCL is treated with a front-line combination of chemotherapy or intensive chemo-immunotherapy followed by stem-cell transplantation as consolidation therapy. However, along with severe side-effects of chemotherapy regimens, resistance to these therapies occurs and tumor eventually relapse although most of the time patients initially respond to these therapies (Wu et al., 2016). Therefore, there is an urgent need to elucidate the MCL disease pathobiology and identify of novel biomarkers and therapeutic target to optimize the treatment and improve the prognosis of MCL patients (Ahmed, Zhang, Nomie, Lam, & Wang, 2016).

1.2. Aims of the Study

The aims of this study are as follows: 1) identification and quantification of the dysregulated long non-coding RNAs that have potential to be novel diagnostic, prognostic, and therapeutic targets in MCL disease through whole transcriptome sequencing; 2) investigation of the association between up or down-regulated lncRNA or mRNAs with MCL patient prognosis.

1.3. Hypothesis of the Study

There are dysregulated oncogenic lncRNAs in MCL cases, which promote MCL tumorigenesis and/or predict patient survival.

2. GENERAL INFORMATION

2.1. Normal B-Cell Development

The vast majority of the worldwide incidence of lymphoid malignancies are derived from B-cells. Therefore, to better elucidate the mechanism of B-cell pathogenesis, it is necessary to understand the normal B-cell development and function (Evans & Hancock, 2003).

There are two types of lymphoid organs: primary – including bone marrow and thymus- and secondary lymphoid organs -including spleen and lymph nodes. Lymphocyte generation and maturation occur within primary lymphoid organs. Then through blood circulation, mature lymphocytes migrate to secondary lymphoid tissues where they encounter antigens that activate them. This encounter, in turn, leads to proliferation and differentiation of this lymphocyte into effector and memory cells (Abbas, Abul K, Lichtman, Andrew H, Pillai, 2018; Evans & Hancock, 2003).

In humans, B-cells develop from hematopoietic stem cells (HSCs) in the fetal liver and after birth, most of their differentiation and maturation occurs in the bone marrow (Galy, Travis, Cen, & Chen, 1995). This process is mostly stimulated by hematopoietic cytokines such as colony-stimulating factors which are mostly produced by the stromal cells in the bone marrow (Abbas, Abul K, Lichtman, Andrew H, Pillai, 2018; Lebien, 2000). Hematopoietic stem cells (HSCs) are multipotent and have the capacity to self-renew and depending on the received stimuli give rise to all types of blood cells, including lymphocytes. By transducing the essential B-cell development signals HSCs differentiate into common lymphoid precursors (CLPs) which can rise to B cells, T cells, natural killer (NK) cells and dendritic (DC) cells; and they lose the myeloid potential. Progenitor B cells (Pro-B) are the first precursor B cells which are differentiated from the CLPs and play a cardinal role in the humoral responses against the foreign antigens (Lebien, 2000; Rolink & Melchers, 1991).

Another cardinal step of B lymphocyte development is the antigen receptor gene rearrangements encoding the B cell receptor (BCR)/Immunoglobulin (Ig). This process paves the way for a highly diverse array of the adaptive immune repertoire. BCRs are composed of two polypeptide chains, heavy and light chain, which are joined by disulphide bonds (Schatz & Ji, 2011). The first step of normal B cell differentiation is the somatic recombination of V(D)J (variable, diversity and joining) genes in the (Ig) heavy gene locus of pro-B cells (**Figure 1**). V(D)J recombination is an error-prone process and also an important source of chromosomal aberrations and therefore may contribute to the development of lymphomas and leukaemias (Mills, Ferguson, & Alt, 2003). VDJ recombination process is initiated by an important protein complex: recombination activating genes 1 (RAG1) and RAG2. Precursor B cells express the following specific markers: CD34 and terminal deoxyribonucleotide transferase (TdT). TdT is an important molecule which adds untemplated “N” nucleotides to the free 3 termini of the coding ends following their cleavage by RAG1/2 recombinases (Nemazee, 2006; Punt, Stranford, Jones, & Owen, 2018; Schatz & Ji, 2011).

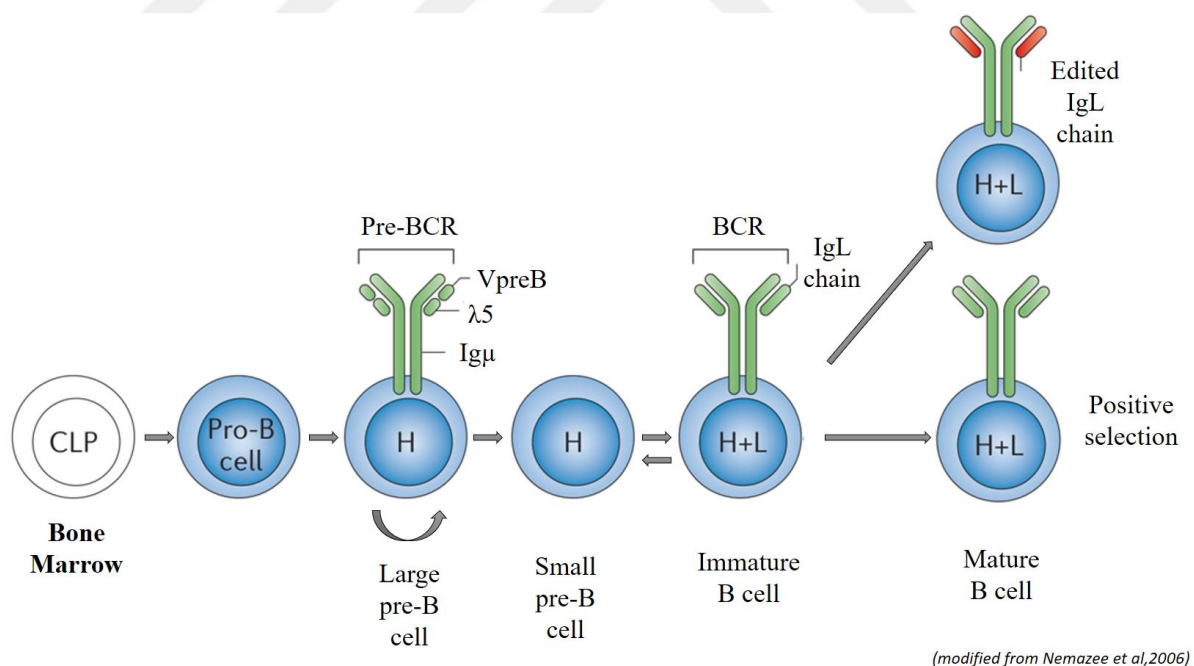


Figure 1: Illustration of BCR gene recombination events in normal B cell development

Pro-B cells carry out the DH-JH rearrangements and do not express Ig on their surface. The following precursor stage (Pre-B cells) includes VH rearrangement to the DH–JH segment and then Ig Kappa (IgK) and Ig Lambda (IgL) genes are rearranged (Jares, Colomer, & Campo, 2012). Ig heavy chain (μ) in pre- B cells are then associates with the surrogate light chains consisting of VpreB, $\lambda 5$: to form the pre-B cell receptor (pre-BCR) which is expressed on the cell surface. This process along with the expression of Ig-a (CD79a) and Ig-b (CD79b) promotes the cell differentiation from the pre-B cell to the generation of a diverse population of IgM⁺ immature B cells. Accordingly, BCR expression is essential for B cell development and survival in the periphery. Self-reactive immature B cells are subjected to negative selection at this checkpoint of B-cell tolerance (Pelanda & Torres, 2012). On passing the checkpoint, IgM⁺ immature B cells migrate to the spleen where they differentiate into distinct transitional B cell stages and can eventually differentiate into circulating follicular B cells or marginal zone (MZ) B cells (Matthias & Rolink, 2005; Song & Matthias, 2018).

Antigen inexperienced, mature B cells with surface-bound IgM⁺, IgD⁺ (naive B cells) recirculate between the blood and the lymphoid organs until they are activated by antigens to proliferate and differentiate into effector and memory cells. Naive B cells exist at very low frequencies and rarely if ever divide (Luckey et al., 2006). Upon antigen binding, naive B cells travel to secondary lymphoid tissues and undergo further differentiation to form germinal centres.

Naive B cells are activated by antigen receptor stimulation in two different ways: T-cell independent and T-cell dependent activation (Mesin, Ersching, & Victora, 2016). In the absence of MHC class II T helper cells, BCRs interact with foreign antigens that have organized and highly repetitive epitope units which allow for the crosslinking of multiple BCRs, providing the first signal for activation. Since the T cells are not involved, the second signal for activation comes from the other molecules such as interactions of toll-like receptors (TLRs) and PAMPs (Pathogen-associated molecular pattern). Upon activation, B cells undergo clonal proliferation and differentiate into plasma cells which produce large numbers of antibodies with low-affinity IgM. After differentiation, the surface BCRs disappear and the plasma cell secretes pentameric IgM molecules that have the same antigen specificity as the BCRs. The T cell-independent response is short-lived and does not result in the production of memory B cells. Thus, it will

not result in a secondary response to subsequent exposures to T-independent antigens (Hess et al., 2013; Vos, Lees, Wu, Snapper, & Mond, 2000).

The other type of naive B cell activation is the T-cell dependent activation which requires the interaction of co-stimulatory surface BCRs with ligands expressed by T cells and /or antigen-presenting cells (APCs). Activated B cells proliferate rapidly and form germinal centres (GCs) in the follicles of the peripheral lymphoid tissues, including the lymph nodes, tonsils, spleen and Peyer's patches (De Silva & Klein, 2015; Lebien, Thomas, & Tedder, 2008).

In the germinal centers, B cells undergo clonal expansion and experience two key processes, somatic hypermutation (SHM) and class-switch recombination (CSR) in order to increase antigen affinity. During GC reactions an active positive selection occurs by which B cells are selected for survival and proliferation on the basis of their increased affinity for antigens, this process is termed as affinity maturation. SHM process occurs at the Ig VH region by introducing mostly single nucleotide substitutions and generates mutant GC B cell clones that have a diverse range of affinities for the antigens. CSR occurs at the IgH locus, via a DNA-level mechanism which mediates isotype switching (or class switching) of antibodies from IgM and IgD to either IgG, IgA or IgE. CSR and SHM are mediated by a genome mutator enzyme, termed activation-induced cytidine deaminase (AID). All these processes shape the antibody response producing GC B cells with high-affinity, class-switched antibodies that can differentiate into either antibody-secreting plasma cells or long-lived memory B cells. GC microenvironment is cardinal for the humoral immunity for being the main source of memory B cells and plasma cells that produce high-affinity antibodies (Lebien et al., 2008; Recaldin & Fear, 2016; Shen et al., 2004). The GC reactions are briefly depicted in **Figure 2**.

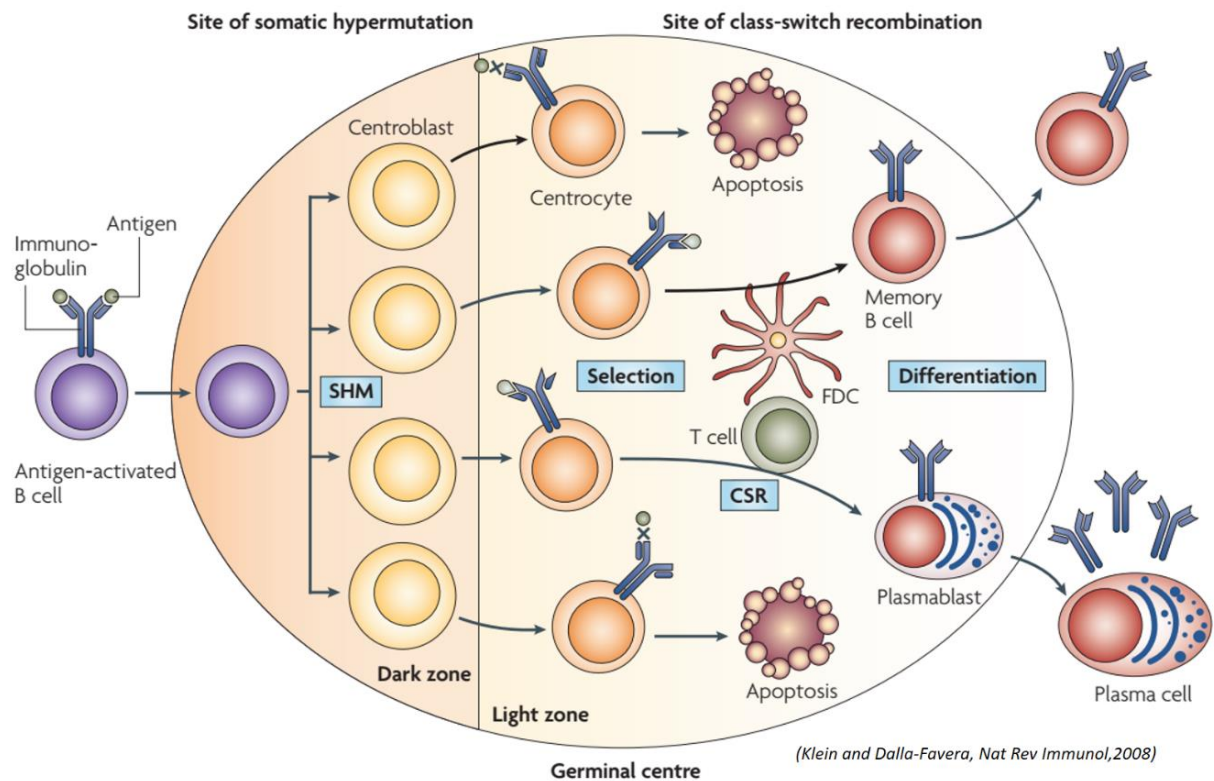


Figure 2: Demonstration of germinal center reactions

T-cell co-stimulated naive B cells move to the center of the primary follicle where they further associate FDCs. Rapidly proliferating B cells push the IgM⁺ IgD⁺ B cells aside, leading to secondary follicle formation to form the mantle zone around the GC. After several days of cell proliferation, the specific GC structure becomes evident: a dark region containing densely packed proliferative B cells known as centroblasts and a light region of smaller, non-cycling centrocytes within a network of FDCs, T cells and macrophages. In the dark zone, CBs undergo clonal selection and SHM processes and then move to the light zone, where the modified BCR of the light zone B cells are selected for improved binding to the antigen. The positive selection is followed by the recirculation of cells from light zone to dark zone where they are subjected to further SHM and proliferation; in order to generate antibodies with high affinity. Then, according to received stimuli, CCs differentiate into antibody-secreting plasma cells or memory-B cells and leave the GC (De Silva & Klein, 2015; Victora et al., 2012).

All these reactions are regulated by several important transcriptional factors including Paired box protein 5 (PAX5) also known as 'B-cell identity gene' a gene compulsory for B-cell lineage commitment. B cell lymphoma 6 (BCL-6) is an essential gene for dark zone gene expression programme and thus for the SHM process. REL and MYC genes play an important role during light and dark zone recirculation process. Interferon-regulatory factor 4 (IRF4) gene is required in CSR reactions as well as for the generation of plasma cells which are derived from GC. B lymphocyte-induced maturation protein 1 (BLIMP1) is also required for plasma cell differentiation (De Silva & Klein, 2015; Klein & Dalla-Favera, 2008; Shen et al., 2004; Song & Matthias, 2018).

2.2. Lymphoid Neoplasms

Lymphoid neoplasms originate from malignant transformation of normal lymphocytes at different developmental and/or maturation stages and altogether represent the fourth most common cancer (Morton et al., 2007; Teras et al., 2016). Lymphoid neoplasms exhibit a very diverse and heterogenic group of malignancies including Hodgkin and non-Hodgkin lymphomas (NH, NHL), lymphocytic leukaemias, and plasma cell neoplasms (Jiang, Bennani, & Feldman, 2017; Morton et al., 2007; Teras et al., 2016). Among these, NHL is the most common subtype and ranks as 6th most common cancer in the UK (Bowzyk Al-Naeab, Ajithkumar, Behan, & Hodson, 2018).

Similar to most type of cancers, activation of proto-oncogenes and derangement of tumor suppressor genes occurs during lymphomagenesis. On the other hand, the genome of the lymphoma cells is relatively more stable than most types of carcinoma cells (epithelial cancer cells). The act of enzymes which are responsible for immunoglobulin gene recombinations may cause DNA double-strand breaks which in turn may cause chromosomal translocations. Indeed, one of the major mechanism of proto-oncogene activation is chromosomal translocations. There is a tendency for the juxtaposition of the proto-oncogene to heterologous regulatory sequences (Evans & Hancock, 2003; Shankland, Armitage, & Hancock, 2012).

The vast majority of NHL arises from B-cells at various stages (Evans & Hancock, 2003). Normal B cells undergo somatic hypermutations, clonal expansion and class switch

recombination in germinal centres. Consequently, the germinal centre is thought to be the origin of various types of lymphoma, involving diffuse large B cell lymphoma (DLBCL) and follicular lymphoma. (Küppers, 2005; Shankland et al., 2012). Since the IgV mutations occur inside of the GCs non-Hodgkin lymphomas can be divided into two categories: with and without IgV mutations. Most of the mantle cell lymphoma cases are represented without IgV mutation category (Küppers, 2005; Shankland et al., 2012).

2.3. Mantle Cell Lymphoma

Mantle cell lymphoma is a mature B-cell non-Hodgkin lymphoma which is considered as an incurable disease by the World Health Organization (WHO) (Jares et al., 2007; Swerdlow et al., 2016). The incidence of MCL is between 3-10% among all type of lymphomas and generally diagnosed with patients over 60 years-old with clear male predominance ($\geq 2:1$) (Cortelazzo, Ponzoni, Ferreri, & Dreyling, 2012; Hoster, 2011).

MCL is a heterogeneous disease with highly diverse clinical and biological subtypes. Generally, classical MCL (cMCL) follows an aggressive clinical course with a recurrent relapse pattern and a median overall survival of 3-5 years (Bertoni & Ponzoni, 2007; Dreyling et al., 2011; Rosenwald et al., 2003). Classical or conventional MCL (cMCL) is the most common subtype of MCL which originates from IgHV unmutated or minimally mutated CD5+ B cells which are not exposed to GC environment and generally represent epigenetically naive B cell-like signature. cMCL cells are generally small to medium size of lymphoid cells; however, acquiring further molecular and genetic abnormalities may result in highly aggressive cytological variants including blastoid and pleomorphic variants (Bertoni & Ponzoni, 2007; Jares et al., 2012; Swerdlow et al., 2017; Vegliante et al., 2013). Patients with cMCL usually express SOX11, a neural transcriptional factor, and generally have a very aggressive clinical course with eventual involvement of lymph nodes, gastrointestinal tract (GI) and other extranodal sites. It has been suggested that SOX11 changes the terminal B-cell differentiation program (Vegliante et al., 2013).

However, an indolent subtype of MCL is also identified with better survival. Indolent MCL patients have distinct biological and genetic features than conventional MCL (cMCL) and

typically have asymptomatic and nonnodal clinical presentation and lacks the expression of SOX11 (Dreyling et al., 2011; Fernández et al., 2010; Nodit, Bahler, Jacobs, Locker, & Swerdlow, 2003; Royo et al., 2012). This non nodal subtype of MCL (nnMCL) originates from GC-experienced cells which have highly mutated IgHV regions, epigenetically represents memory B-cell (memory-like) signature and have more stable karyotype than cMCL. Indolent nnMCL patients generally have a leukemic presentation with the spleen, peripheral blood (PB) and bone marrow involvement (Swerdlow et al., 2017).

As being a highly heterogeneous disease, the clinical treatment options of MCL is also variable. MCL is treated with a front-line combination of chemotherapy or intensive chemo-immunotherapy followed by stem-cell transplantation as consolidation therapy. However, along with the severe side-effects of chemotherapeutic regimens, resistance to these therapies occur and tumor relapse although most of the time patients initially respond to these therapies (Wu et al., 2016). Therefore, there is an urgent need to develop targeted and new strategies for the treatment of MCL. To do so, the molecular basis and mechanisms of drug resistance in MCL need to be elucidated (Ahmed et al., 2016). MCL disease risk stratifications are generally assessed by MCL international prognostic index (MIPI). MCL international prognostic index (MIPI) is the first and established prognostic index for MCL patients which uses four main prognostic indexes: age, Eastern Cooperative Oncology Group (ECOG) performance status, white blood cell (WBC) count, and lactate dehydrogenase (LDH) level. Performance status which measures the ability to perform daily activities and age are direct factors for measurement of therapy tolerance whereas, LDH level and WBC count are indirect measures. Additionally, cell proliferation index (Ki-67) has also been selected that serves as an important biological marker.

Table 1: MCL international prognostic index (*adapted from Vose et al 2017*)

Points	Age (years)	ECOG PS	LDH/ULN	WBC (10^9 cells/L)
0	<50	0 - 1	<0.67	<6.7
1	50 - 59	n/a	0.67 – 0.99	6.7 – 9.99
2	60 - 69	2 - 4	1.00 – 1.49	10 – 14.99
3	>69	n/a	>1.49	>14.99

*ULN: upper limit of normal

*ECOG PS: ECOG performance status

*n/a: not available

According to this evaluation, MIPI assessed MCL patients into three risk groups: patients with 0-3 points are assigned as low risk, patients with 4–5 points assigned as intermediate risk and patients with 6–11 points are assigned as high risk (**Table 1**). Low-risk patients do not reach median overall survival (OS), and if there are no other symptoms for the treatment they may be considered only for close observation. Intermediate risk patients have a median OS of 51 months, and high-risk patients have a median OS of 29 months (Cheah, Gairdner, Wang, & Seymour, 2016; E. et al., 2008; Vose, 2017).

The primary oncogenic event and also the genetic hallmark of MCL is the chromosomal translocation which causes juxtaposition of *CCND1* (also known as *BCL1*), a cell cycle gene at chromosome 11q13 and *IgH* chain gene at chromosome 14q32. This reciprocal translocation, *t*(11;14)(q13;q32), is present in more than 90% of the MCL cases and, and leads to constitutive expression of *CCND1* gene which is not expressed in normal B cells (Jares et al., 2007; Rosenwald et al., 2003). Nonetheless, *CCND1* overexpression alone is not sufficient enough for lymphomagenesis. Secondary oncogenic events which generally targets cell cycle (*CDKN2A*, *RBI*, *BMI1*), DNA damage response (*TP53*, *ATM* and *CHK2*) and survival pathway-related genes (*BIRC3*, *BCL2* and *TNFAIP3*) are required (Jares et al., 2012; Veloza, Ribera-Cortada, & Campo, 2019).

Recently, the incorporation of conventional and novel diagnostic approaches such as genomic sequencing is used to understand the genetic mechanisms underlying disease progression, relapse and resistance to therapy on MCL patients (Inamdar et al., 2016). In a study conducted with the RNA-Seq method, 12% frequency of NOTCH1 gene mutations was detected on MCL tumor samples and cell lines (Kridel, Meissner, Rogic, Boyle, Telenius, Woolcock, Gunawardana, Jenkins, Cochrane, Ben-neriah, et al., 2012). In another NGS-based study, anti-apoptotic protein BIRC3, Toll-like receptor 2 (TLR2), chromatin-modifying WHSC1, MLL2 and MEF2B genes, as well as disease-associated mutations were detected in the NOTCH2 gene (Bea et al., 2013). A genome-sized promoter / CpG island methylation analysis study Reported 8 aberrantly methylated, MCL associated genes; hypermethylated genes: CDKN2B, MLF-1, PCDH8 and HOXD8; hypomethylated genes: CD37, HDAC1, NOTCH1 and CDK5) detected (Leshchenko et al., 2010). In addition to these studies, microRNAs with irregular expression in MCL tumors have been reported (Iqbal et al., 2012; Navarro et al., 2013).

Recently, with the advent of next-generation sequencing (NGS) technologies through whole-genome sequencing (WGS), whole-exome sequencing (WES) and miRNA expression profiling MCL disease etiology tried to be figured out (Ahmed et al., 2016; Kridel et al., 2012; Navarro et al., 2013). However, these studies have focused considerable effort on identifying MCL-related somatic mutations in protein-coding genes (Wojcik et al., 2010) and the studies performed on the non-coding portion of the human genome is rare for MCL (Hu, Gupta, Troska, Nair, & Gupta, 2017).

2.4. Emerging Roles of Long non-coding RNAs as Cancer Biomarkers

The non-coding part of the human genome is much more abundant than the coding part, but until recently these parts were generally called junk DNA and thought to have no function at the organism level. However, along with the recent advances in high throughput technologies, it was found that this non-protein-coding part of the human genome transcribed long non-coding RNAs (lncRNAs), which have various important functional roles (Kopp & Mendell, 2018; Ling et al., 2016).

lncRNAs are the common name given to transcribed RNAs that are longer than 200 bp, which do not have an open reading frame and do not encode proteins (Kapranov et al., 2007). There are tens of thousands of different lncRNAs in humans (Washietl, Hofacker, Lukasser,

Hüttenhofer, & Stadler, 2005). lncRNAs have various roles in the regulation of expression of the target gene or gene groups involving transcriptional, post-transcriptional or translational regulation and also in epigenetic modifications (Jiang, Ni, Cui, Wang, & Zhuo, 2019; Peng, Koirala, & Mo, 2017).

Studies aimed at elucidating the functions of lncRNAs revealed that these RNA species are involved in many critical biological processes involving development, cell cycle and apoptosis. Irregularity in lncRNA expression levels have been shown to be associated with many diseases, including cancer (Huarte, 2015; Ounzain et al., 2014; van deVondervoort et al., 2013).

Dysregulated gene dose and/or expression levels along with the genomic changes including SNPs (single-nucleotide polymorphisms), CNVs (copy number variations) of lncRNAs in tumor cells resulted in the association of lncRNAs with oncogenesis (Huarte, 2015; Jiang et al., 2019). Along with the recent advances in high throughput technologies, the identification of many lncRNAs which are related with the hallmarks of cancer is detected (**Figure 3**) (Schmitt & Chang, 2016). For instance, a lncRNA called HOTAIR has been found to mediate the interaction of Polycomb repressor complex (PRC2) proteins with histone modification function with chromatin, and to mediate the expression of target genes (Rinn et al., 2007).

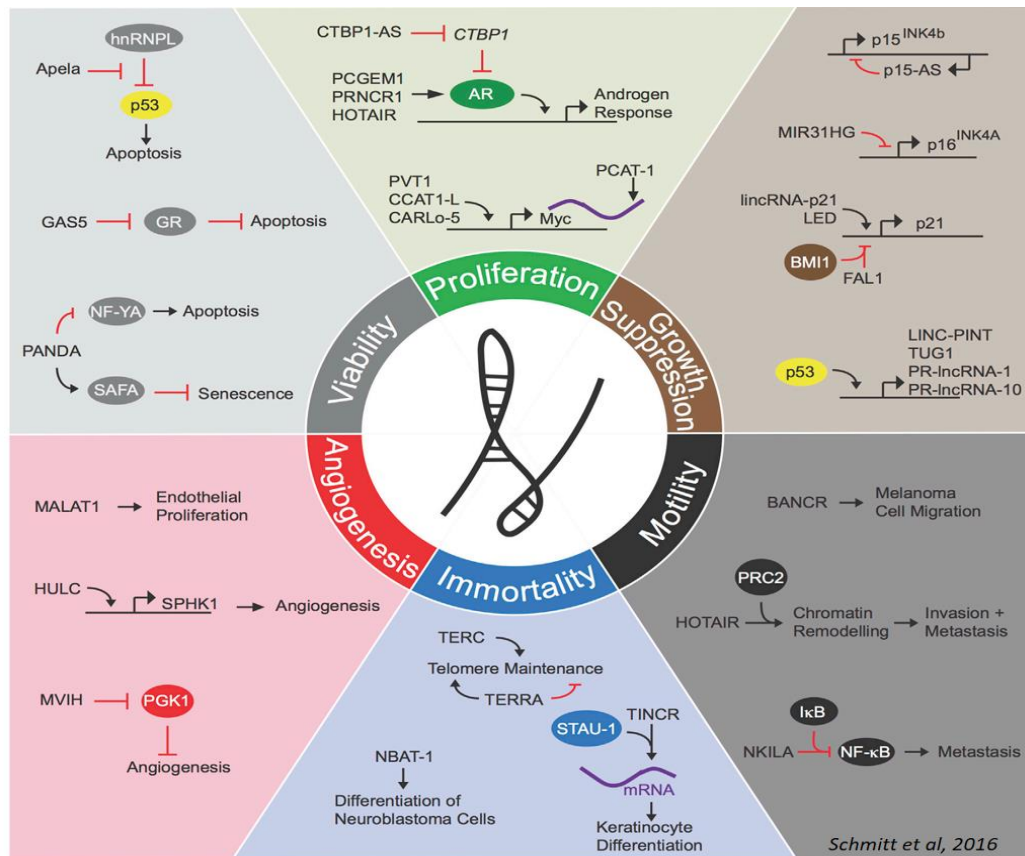


Figure 3: LncRNAs which are associated with hallmarks of cancer

Overexpression of HOTAIR lncRNA is associated with many types of cancers including breast cancer and found to have a strong role in breast cancer metastasis (Huarte, 2015; Peng et al., 2017). Overexpression of Metastasis-associated lung adenocarcinoma transcript 1 (MALAT1), an evolutionary conserved lncRNA was found to have a role in cell proliferation and /or metastasis of many types of cancers including lung, colon, prostate, pancreatic, breast cancer, and mantle cell lymphoma (Huarte, 2015; Wang et al., 2016). Even though the functional mechanism of MALAT1 in tumorigenesis is not fully understood it has been thought that this lncRNA is associated with many disease-related molecular mechanisms including epithelial-mesenchymal transition (EMT), angiogenesis, Wnt/ β -catenin pathway, PI3K/AKT pathway, and ERK/MAPK pathway.

Identification of functional lncRNAs which paves the way for tumorigenesis and metastasis make them promising therapeutic targets and also promising biomarkers in cancer diagnosis and prognosis. For instance, Prostate cancer-associated 3 (PCA3) that is a prostate cancer-specific biomarker, is the first Food and Drug Administration (FDA) approved test

based on lncRNA. Furthermore, HULC, a lncRNA which is overexpressed in hepatocellular carcinoma (HCC) and serves as a biomarker, can be detected in the blood by PCR (Schmitt & Chang, 2016).

The studies reporting lncRNAs associated with MCL disease formation and pathogenesis are recently increasing (Fan et al., 2019; Hu et al., 2017; Mu, Liu, Wu, Xia, & Fang, 2019; Y. Zhang, Lu, Du, & Zhang, 2019); however, there is only one study which used the whole transcriptome sequencing method for lncRNA profiling in four MCL cases and four control samples (Hu et al., 2017). The different aspects of this dissertation from the articles of Hu, Gupta et al. study are as follows: 1) The relationship between DElncRNAs and MCL clinical course is examined. The relationship between lncRNAs with irregular expression and patient survival was evaluated. 2) Different than the article, our study also aimed to determine the signaling pathways affected by significantly DEmRNAs.

Therefore, in this study, this multidimensional aspect of RNA-Seq method has been utilized; for differentially expressed lncRNA identification in MCL tumors using RNA-Seq sequencing data; contributing to the elucidation of MCL etiology; and to explore specific diagnostic, prognostic and therapeutic targets.

3. MATERIALS AND METHODS

3.1. Type of the Study

This is an experimental study.

3.2. Time and Location of the Study

All the experimental part of this study were conducted at the Izmir Biomedicine and Genome Center, between March 2017 and November 2019. Whole transcriptome sequencing services were obtained from Macrogen (South Korea) and Novogene (Hong Kong) companies.

3.3. Population and Sample of the Study

Between 2011 and 2017, tumor sections of formalin fixed paraffin embedded (FFPE) lymph node biopsy tissues belonging to 18 different patients diagnosed with MCL disease were obtained from the DEU Pathology department. MCL disease characterization of these samples was performed by the pathology department as part of the routine diagnostic procedure. Tumor sections were prepared from FFPE tumor tissues at approximately 8 μm thickness with a microtome device at DEU iBG-izmir Histopathology Department or DEU Medical Pathology department and placed into sterile 1.5 mL eppendorf tubes with a maximum of 5 sections per tube.

For non-lymphoma control samples, 7 fresh, reactive pediatric tonsil samples were obtained from routine tonsillectomy operations at DEU Otorhinolaryngology (Ear-Nose-Throat) department.

All these human samples were collected and processed in accordance with the ethical recommendations accepted by the DEU Noninvasive Research Ethics Board (with 2525-GOA protocol number and 2017/26-31 decision number).

3.4. Materials of the Study

3.4.1 Solutions

Solutions	Vendor/ Contents
1X PBS+5mM EDTA	250ml 1XPBS (pH 7.2-7.4) with 0,47g Na ₂ EDTA
10X ACK Lysis Buffer	43g NH ₄ Cl; 5g KHCO ₃ ; 0,186g Na ₂ EDTA and 500ml ddH ₂ O (pH7.2)
10X PBS	Gibco by Life Technologies, Carlsbad, CA, USA
RPMI	Gibco by Life Technologies, Carlsbad, CA, USA
TAE Buffer (Tris-acetate-EDTA) (50X)	Thermo Fisher Scientific, Waltham, MA, USA
Ficoll-Paque PLUS density gradient centrifugation medium	GE Healthcare, Uppsala, Sweden

3.4.2. Chemicals

Chemicals	Vendor
Ethanol Absolute	Isolab, Wertheim, Germany
Chloroform	Sigma-Aldrich ,St. Louis, Missouri, USA
TriZol	Ambion, Austin, TX, USA
β-Mercaptoethanol	Sigma-Aldrich, St. Louis, Missouri, USA
Trypan Blue Solution	Sigma-Aldrich, St. Louis, Missouri, USA
50 bp DNA Ladder	New England Biolabs, MA, USA
RedSafe Nucleic Acid Staining Solution	iNtRON Biotechnology, KOREA

3.4.3. Kits

Kit Name	Vendor	Catalog No
RNeasy Mini kit (50)	Qiagen, Hilden, Germany	74104
RNeasy FFPE kit (50)	Qiagen, Hilden, Germany	73504
QuantiTect Reverse Transcription Kit (50)	Qiagen, Hilden, Germany	205311

Maxima SYBR Green qPCR Master Mix (2X) (200)	Thermo Fisher Scientific, Waltham, MA, USA	K0251
-------------------------------------------------	-----------------------------------------------	-------

3.4.4. FACS Antibodies

Antibodies	Vendor	Catalog No
PE Mouse Anti-Human CD38 Clone HIT2 (RUO)	BD Biosciences, San Jose, CA	560981
PerCP-Cy™5.5 Mouse Anti-Human CD23 Clone M-L233 (RUO)	BD Biosciences, San Jose, CA	561166
APC Mouse Anti-Human IgD Clone IA6-2 (also known as δ -IA6-2) (RUO)	BD Biosciences, San Jose, CA	561303
PE anti-human CD38, 100 tests Reactivity: Human, Cross-Reactivity: Chimpanzee, Horse, Cow (Bovine); Clone: HIT2	Biolegend, San Diego, CA, USA	303506
PerCP/Cyanine5.5 anti-human CD23, 100 tests Reactivity: Human; Clone: EBVCS-5	Biolegend, San Diego, CA, USA	338518
APC anti-human IgD, 100 tests Reactivity: Human; Clone: IA6-2	Biolegend, San Diego, CA, USA	348222
DAPI (4',6-Diamidino-2-Phenylindole, Dilactate), 10 mg Reactivity	Biolegend, San Diego, CA, USA	422801

3.4.5. Equipments

Equipment Name	Vendor
Refrigerator (+4°C)	Bosch, Stuttgart, Germany
Refrigerator (-20°C)	Bosch, Stuttgart, Germany
Freezer (-80°C)	Eppendorf, Hamburg, Germany
MicroCL 17R centrifuge	Thermo Fisher Scientific, Waltham, MA, USA

Centrifuge 5810R	Eppendorf, Hamburg, Germany
Vortex	Thermo Fisher Scientific, Waltham, MA, USA
mySPIN™ mini centrifuge	Thermo Fisher Scientific, Waltham, MA, USA
UVC/T-AR DNA/RNA UV box	Biosan, LATVIA
SimplyApp Thermal Cycler	Applied Biosystems, Foster City, CA, USA
T100 Thermal Cycler	Bio-Rad, Hercules, CA, USA
Light Cycler 480 II	Roche Applied Science, Mannheim, Germany
BD FACSAria™ III	Biolegend, San Diego, CA, USA
NanoDrop 2000	Thermo Fisher Scientific, Waltham, MA, USA
Hemocytometer	Qiuqing Company, Shanghai, CHINA
ZEISS Axio Vert.A1 Inverted Microscope	Zeiss, Oberkochen, Germany
Precision balance	Sartorius, Göttingen, Germany
pH meter	Hanna, Rhode Island, ABD
Magnetic stirrer with heater	Thermo Fisher Scientific, Waltham, MA, USA
Gel Doc XR+ Gel documentation system	Bio-Rad, Hercules, CA, USA
Power supply unit for electrophoresis	Bio-Rad, Hercules, CA, USA

3.5. Variables of the Study

Dependent variables: Transcript expression levels of different MCL and control samples

Independent variables: Effect of differential expression on prognosis of MCL patients.

3.6 Data Collection Tools

3.6.1. Collection of MCL tumor tissue samples and obtaining FFPE sections

Between 2011 and 2017, tumor sections of FFPE lymph node biopsy tissues belonging to 18 different patients diagnosed with MCL disease were obtained from the DEU Pathology department. The lymph node biopsies were abundant in tumor tissue. Tumor sections were prepared from FFPE tumor tissues at approximately 8 µm thickness with a microtome device at DEU iBG-izmir Histopathology Department and placed into sterile 1.5 mL eppendorf tubes

with a maximum of 5 sections per tube. Tubes containing tumor tissue sections of each patient were stored at + 4 ° C until RNA isolation.

3.6.2. RNA isolation from MCL tumor FFPE tissue sections

As a clinical diagnostic process, tumor biopsies are routinely fixed in formalin and embedded in paraffin blocks and kept in pathology archives for long term storage. FFPE sections represent an invaluable source for research and allow for long term follow up. However, nucleic acids in FFPE tissue samples are adversely affected during this fixation procedures. The extent of nucleic acid degradation depends on many factors such as sample type and age, fixation and paraffin embedding conditions, storage time and temperature (Antica, Paradzik, Novak, Dzebro, & Dominis, 2010; Bohmann et al., 2009; Deben et al., 2013). von Ahlfen et al demonstrated that RNA integrity is better preserved when the FFPE tumor samples are kept at +4 °C (von Ahlfen, Missel, Bendrat, & Schlumpberger, 2007). Hence, in order to minimize the RNA degradation, after obtaining the FFPE tumor sections of each patient were stored at + 4 ° C until RNA isolation.

RNA isolation from 18 collected FFPE tumor tissue sections of each MCL patient was performed using the RNeasy FFPE kit (Qiagen, Cat no: 73504) by following the manufacturer's instructions. The RNeasy FFPE Kit was specifically designed for the purification of total RNA from formalin-fixed, paraffin-embedded tissue sections. This kit has been optimized to reverse the chemical modification and crosslinking caused by formaldehyde fixation process as much as possible, without further RNA degradation (Belder et al., 2016; Deben et al., 2013).

The RNA isolation procedure can be summarized as follows: First, paraffin was removed from the FFPE tissue sections by adding 320 µl Xylene solution for deparaffinization. Then, samples are incubated at 56°C for 3 minutes, then allowed to cool at room temperature. Next, 240 µl PKD lysis buffer was used to separate the RNA from the sections and centrifuged for 1 minute at 11,000 x g. After centrifugation, 10 µl proteinase K is added to the lower, clear phase and mixed gently by pipetting up and down about 30-40 times. Then, samples are incubated in a shaking incubator at 56°C for 15 minutes, then at 80°C for 15 minutes with shaking speed of 350 rpm. The 15 minutes incubation at 80°C is very crucial to reverse the crosslinking of RNA caused by the formalin, improving the RNA quality. After this step, the lower, uncolored phase is transferred into a new 1,5 ml microcentrifuge tube and incubated on

ice for 3 minutes. Then, centrifuged for 15 minutes at 20,000 x g (13,500 rpm). After centrifugation, the supernatant is carefully transferred into a new 2 ml microcentrifuge by avoiding disturbing the pellet. Next, DNase Booster Buffer equivalent to a tenth of the total sample volume (approximately 18 µl) and 10 µl DNase I stock solution is added and mixed by inverting the tube and centrifuged briefly to collect residual liquid from the sides of the tubes. It is then followed by incubation at room temperature for 15 minutes. 500 µl RBC buffer and 1200 µl ethanol (100%) were added to the sample to adjust binding conditions, and the lysate mixed thoroughly. Then, 700 µl of the sample was transferred to an RNeasy MinElute spin column and centrifuged for 15 seconds at ≥ 8000 x g and flow through is discarded. This step was repeated until the whole sample is passed through the column. 500 µl buffer RPE was added twice to wash the spin column and centrifuged firstly for 15 seconds at ≥ 8000 x g and then for 2 minutes at ≥ 8000 x g. In order to eliminate the residual ethanol and dry the silica membrane, spin-column was centrifuged at full speed for 5 minutes.

Finally, the RNeasy spin column was placed in a new 1.5 ml collection tube and RNA was eluted in 30 µl RNase-free water by centrifugation at full speed for 1 minute. The concentration and purity of the isolated RNA samples were determined spectrophotometrically with the Thermo Nanodrop 2000 instrument and stored at -80°C until use. RNA samples with A260/A280 ratios between 1.8–2.2 and A260/230 ratios above 2 were considered pure.

3.6.3. Obtaining B cell subtypes from reactive tonsil tissues by FACS

Fresh tonsil tissues were obtained from routine tonsillectomy operations in DEU ENT department. Tonsils were collected and processed in accordance with the ethical recommendations accepted by the local ethics committee. Two types of B cells (Naive B cells and memory B cells) were isolated from seven tonsillectomy specimens as control samples.

The first few samples obtained from DEU ENT department were used for experimental optimization. As a result of these trials, the optimized workflow was determined as follows: Immediately after surgical removal tonsil tissues were placed in 1X PBS solution and transported first to DEU Pathology department and then to iBG-center, on ice. In the pathology

department of DEU, half of a pair of tonsillar tissues were cut for diagnostic purposes and other halves were used in the experimental procedures which were performed in the iBG-center.

In order to prepare cell suspension from tonsil tissues, tissue homogenization was performed first with the help of a forceps and a metal mesh and 50 mL of cell suspension were prepared using 1 X PBS + 5 mM EDTA solution. The tonsil cell suspension was passed through a 100-micron filter (Corning Ref no: 352360) to eliminate cell clumps and debris. After this step, two different methods were used for the preparation of tonsil cells for fluorescence-activated cell sorting (FACS) analysis: Mononuclear cell (MNC) recovery by Ficoll-Paque PLUS density gradient centrifugation medium and ACK lysis method. MNCs recovery by Ficoll-Paque was performed according to the manufacturer's instructions. Nevertheless, ACK lysis method gave better yield in terms of tonsil cell number.

ACK lysis method can be summarized as follows: The 50 mL tonsil cell suspension was incubated for 15 minutes in 1X ACK lysis buffer at a ratio of 1: 4 (10 ml tonsil cell suspension and 40 ml 1X ACK buffer in each five falcon tubes). After centrifugation and washing with 1X PBS + 5mM EDTA solution, cell pellet suspended in 20 mL of 1XPBS + 5MmEDTA solution was prepared. After cell counting with trypan blue, direct immunofluorescence staining of tonsillar cells was performed for cell sorting.

It has been known that conventional MCL has a naive B cell-like signature and nonnodal leukemic type of MCL have memory B-cell like signature (Veloza et al., 2019). Therefore, naive B cells and memory B cells were sorted from tonsil B-cell suspension. The B lymphocyte subtypes and the differentiating antibodies used during cell sorting is listed in **Table 2** The flow cytometer antibodies were chosen as PE, PerCP-Cy™ 5.5 and APC which has four different fluorescent channels.

Table 2: Immunophenotypic profile and used FACS antibodies for B-cell subsets

Cell Type	Immunophenotypic Profile	FACS Antibodies
Naïve B cell	IgD ⁺ / CD23 ⁻	APC Mouse Anti-Human IgD; PerCP-Cy TM 5.5 Mouse Anti-Human CD23
Memory B cell	IgD ⁻ / CD38 ⁻	PE Mouse Anti-Human CD38; APC Mouse Anti-Human IgD

In FACS analysis, it is important to locate the cells labelled with antibodies as well as the non-labelled, i.e. negative population. To be able to locate the negative population, an unstained sample was used as a negative control in each experiment. This unstained control sample allows to determine the background fluorescence level or autofluorescence level and to properly adjust the voltages and negative gates. Besides, since multiple fluorochromes were used with the FACS device, fluorescence compensation beads were used to correct the spectral overlap between the fluorochromes when interpreting the signals obtained (Cossarizza et al., 2017; Tung, Parks, Moore, Herzenberg, & Herzenberg, 2004). Compensation tubes are prepared according to the manufacturer's protocol (Anti-Mouse Ig, κ /Negative Control Compensation Particles Set, cat no: 552843).

Thirty million cells for each tonsillar sample were prepared for flow cytometry. Both stained and unstained samples were prepared. The cells are stained with an antibody cocktail containing antibodies against; CD38, CD23 and IgD. Stained cells were incubated in the dark and on ice for 20 minutes. The cells were then washed once with 6 mL of 1X PBS + 5 mM EDTA and centrifuged at 400 g for 10 minutes. The cells were then resuspended in 1 mL of 1X PBS + 5 mM EDTA. Finally, 6 μ l DAPI was added to both stained and unstained tubes for labelling and filtering out the non-viable cells. For each B cell subtype, 1 mL of RPMI was put into FACS tubes and cell sorting procedures were performed by FACS Aria III device by iBG flow cytometer service unit specialist Dr. Xiaozhou Hu.

3.6.4. RNA isolation from reactive tonsil B cell subtypes

The RNA isolation from the five reactive tonsil B cell subtypes was obtained by using Trizol and RNeasy Mini Kit (Qiagen) and only RNeasy Mini kit were used for the other two samples.

RNA isolation from reactive tonsil B cell subtypes was performed by using both Trizol (Ambion) and RNeasy Mini Kit (Qiagen Cat No: 74104). Details of RNA isolation procedures using Trizol and RNeasy Mini Kit are as follows: After FACS sorting, four B cell subtypes were transferred to eppendorf tubes and centrifuged at 500g for 5 minutes. The supernatant was then discarded and cell pellets of each subtype were resuspended with an appropriate amount of Trizol. 20% by volume chloroform (0.2 ml chloroform to 1 ml Trizol) was added and mixed and incubated at room temperature for 2-3 minutes. It was then centrifuged at 12,000g for 15 minutes at 4 ° C. After centrifugation, the supernatant containing RNA was transferred to new 1.5 mL tubes. Then 70% of ethanol was added dropwise and stirring for each tube. For further purification of RNA with RNeasy mini-column, the RNA-ethanol mixture was transferred to the RNA-mini column and isolation procedures carried out in accordance with the manufacturer's protocols Thermo Nanodrop 2000 instrument was used to measure the concentration and purity of the isolated RNA.

RNA isolation from tonsil B cell subsets using only the Qiagen RNeasy Mini kit (Cat No: 74104) was depicted in **Figure 4** and conducted as follows: Cells belonging to four different B cell subtypes separated by FACS were transferred to 15 ml tubes from flow tubes and was centrifuged for 10 minutes at 300g. The supernatant was carefully removed with a serological pipette. Homogenization was achieved in the presence of RLT buffer containing a highly denaturing guanidine-thiocyanate which immediately deactivates RNases to ensure purification of intact RNA. Ethanol was added to ensure proper binding conditions and the samples were then transferred to an RNeasy Mini spin column where the total RNA was washed efficiently to which the membrane was bound. After washing in RW1 and RPE buffer solutions, high-quality RNA was eluted in 30 µl of RNase-free water. Elution was performed twice using different collection tubes to maximize the amount of RNA obtained. The concentration and purity of the isolated RNA samples were determined spectrophotometrically with the Thermo Nanodrop 2000 instrument.

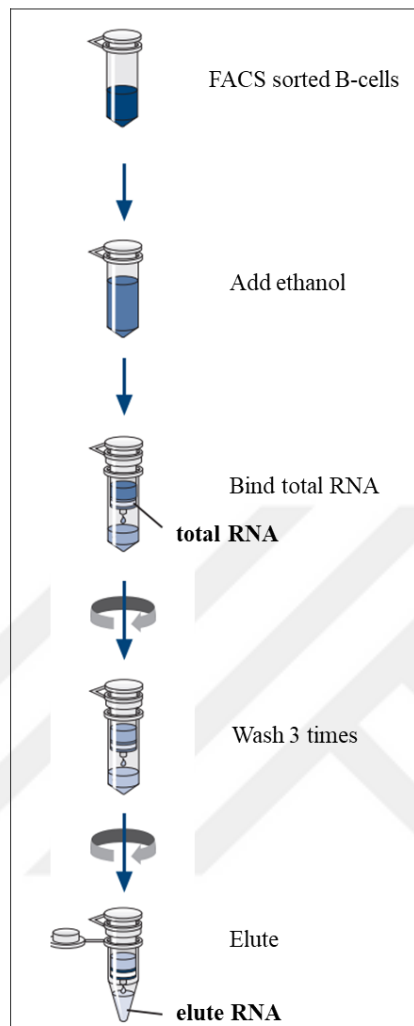


Figure 4: Schematic depiction of the RNA isolation process from B-cell subsets by RNeasy Mini kit

3.6.5. Quality controls of isolated MCL RNAs (running on TAE gel)

To assess the quality of the isolated RNA, MCL RNAs with high concentrations were run by gel electrophoresis. Total RNA quality control was carried out as follows: 500 ng of RNA was run on a 1% agarose TAE (Tris-Acetate-EDTA) gel for 20 minutes, and the 28S and 18S bands were still visible and evaluated under UV light (**Figure 5**). And it was observed that the RNA samples tested were of sufficient integrity for sequencing.

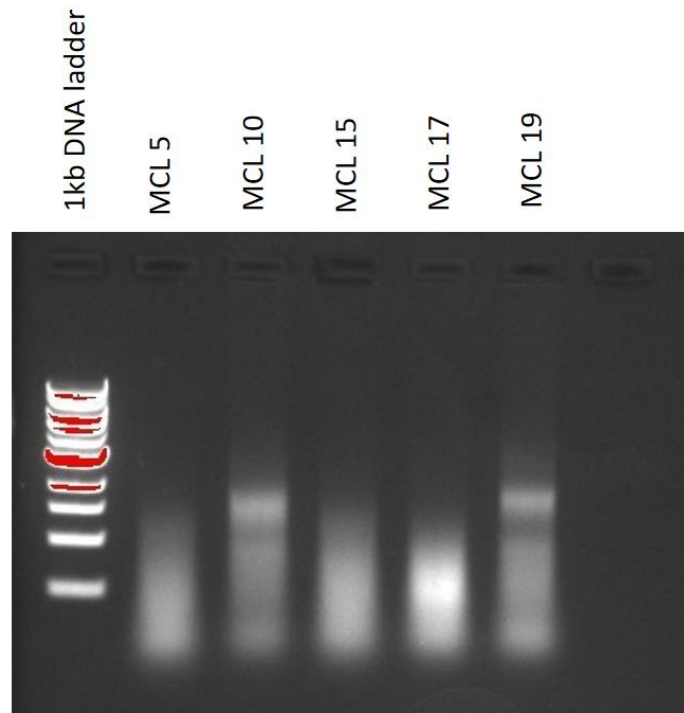


Figure 5: Integrity checks of RNAs isolated from MCL cases (TAE gel images)

3.6.6. Whole Transcriptome Sequencing

Samples with sufficient RNA in terms of quantity and quality were sent to Macrogen (South Korea) company for the first batch and Novogene (Hong Kong) company for the second and third cargoes for whole transcriptome sequencing purposes.

Prior to whole transcriptome sequencing library preparation, RNA quantification and integrity assessments were performed at Macrogen or Novogene companies using the Agilent 2100 Bioanalyzer (Agilent Technologies, Santa Clara, CA, USA). Since the samples underwent routine FFPE treatment the RIN scores, of MCL RNA samples, were estimated - as expected - as values between 2-3 (data not shown). This observation is similar to the RIN scores observed in FFPE RNA samples specified in the technical note "Evaluating RNA Quality from FFPE Samples" from the Illumina next-generation sequencing company (<https://www.illumina.com/documents/products/technotes/technote-expression-analysis-ffpe-samples.pdf>). In the same technical note, it was stated that FFPE RNA samples should be evaluated using a different method called DV200. The DV200 method determines the suitability of samples for WTS by determining the ratio of RNA fragments longer than 200

bases to total RNA fragments. According to the DV200 measurements, all FFPE RNA samples were found to have sufficient quality and quantity of RNA for NGS library formation.

Sequencing of MCL samples (n=10) at Macrogen company was performed using the Illumina HiSeq platform and the TruSeq Stranded Total RNA with Ribo-Zero kit. Paired-end readings of 100 base pairs were obtained. For the sequencing at Novogene company, paired-end readings of 150 base pairs were obtained using the Illumina HiSeq platform. TruSeq Stranded Total RNA with Ribo-Zero kit was used for all FFPE samples (n=8) and one control sample, and for two of the control samples NEBNext Ultra II Directional RNA Library Preparation Kit for Illumina were used.

Strand information is not preserved for conventional libraries for Illumina RNA-seq in which the originally transcribed cDNA strand information is lost. Non-stranded libraries generally perform well in gene quantification, however, crucial information is lost specifically for anti-sense transcription, which is increasingly gaining importance (Z. Wang, Gerstein, & Snyder, 2010; Zhong et al., 2011). Nevertheless, stranded library preparation protocols preserve the strand information which significantly enhances the value of RNA-seq and help improve accurate identification of the antisense transcripts which is also important for lncRNA detection (Hou et al., 2015; Levin et al., 2010).

In this study, Truseq stranded total RNA with Ribo-zero Human library preparation kit (Illumina company) was used during the preparation of FFPE RNAs and a control RNA sample for sequencing. This kit is suitable for FFPE samples but is also suitable for simultaneous sequencing of mRNAs and small RNAs as well as lncRNAs. First, ribosomal RNA (rRNA) from total RNA were filtered out in the samples; and then, respectively, RNA cleavage, complementary DNA (cDNA) formation, adenosine nucleotide insertion to the 3' ends of cDNA, and finally, insertion and sequencing of the adapter sequences into cDNA ends was performed. The schematic depiction of WTS analysis with TruSeq Stranded Total RNA Kit is shown in **Figure 6**.

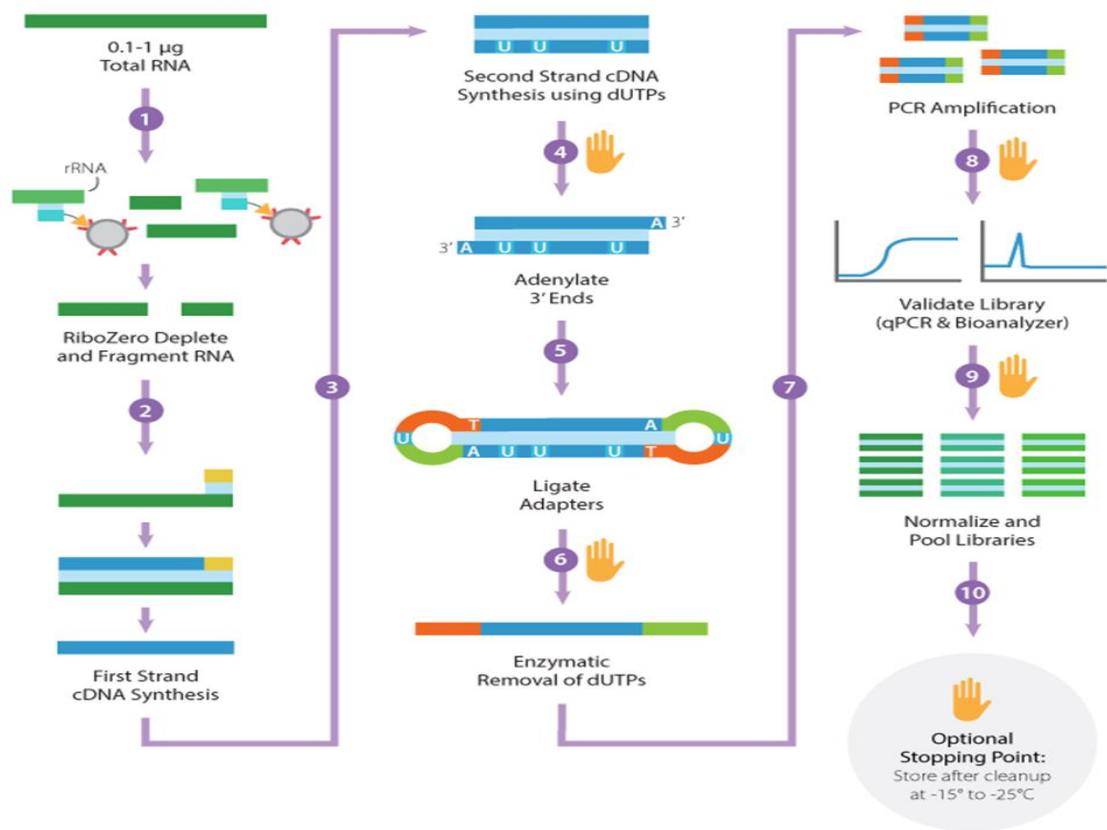


Figure 6: TruSeq Stranded Total RNA Kit Library Preparation

Strand information is also preserved for NEBNext Ultra II Directional RNA Library Prep Kit which was used for the library preparation of the two control samples. Preparation of cDNA library steps before next-generation sequencing are respectively as follows: **1)** rRNA elimination in total RNA using the rRNA removal kit; **2)** RNA fragmentation and random priming; **3)** First and second-strand cDNA synthesis; **4)** End repair of cDNAs and dA-Tailing (addition of adenine nucleotides); **5)** NEBNext adapter ligation; **6)** cDNA libraries were prepared after size selection and PCR enrichment experiments.

The raw data obtained as a result of sequencing in both companies were delivered to our laboratory in “FASTQ” format.

3.6.7. Analysis of Differentially Expressed lncRNAs and mRNAs in MCL

Raw data in FASTQ format obtained from sequencing companies were transferred to Galaxy NGS array analysis platform (<https://usegalaxy.org/>) and subsequent RNA-seq analyses were performed at the Galaxy environment. Galaxy is an open access, user-friendly platform for genomic data analysis (Goecks, Nekrutenko, Taylor, & The Galaxy Team, 2010).

The main steps of identification of differentially expressed lncRNAs (DElncRNAs) and mRNA (DEmRNAs) analysis are demonstrated in **Figure 7**. After the quality check of the raw data and adaptation into Galaxy environment, splice aware mapping tools were used to align RNA-seq reads into reference genome and reads were counted in order to estimate the differentially expressed genes. Ultimately, pathway enrichment analysis was performed to examine genes involved in signalling pathways or biological processes that may be related to mantle cell lymphoma.

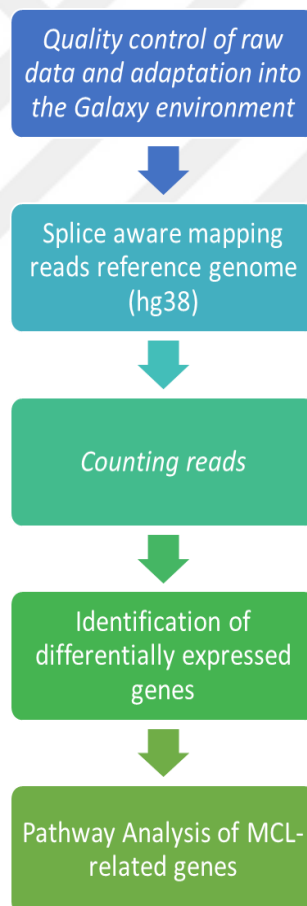


Figure 7: RNA-seq data analysis pipeline

Quality control of raw data and adaptation into the Galaxy environment

The preliminary quality control (QC) from raw data reads was performed by using **FASTQC** tool (Galaxy version 0.72+galaxy1) with default settings (Andrews, 2010). FASTQC tool creates a read quality report including, per base sequence quality, per sequence quality scores, sequence duplication levels and more.

The balance between RNA-Seq, sensitivity (number of aligned reads) and specificity (number of correctly aligned reads) generally are adversely affected when the datasets are trimmed. Besides, the alignment tools such as Tophat and HISAT2 overcomes poor quality reads, hence making trimming superfluous (Del Fabbro, Scalabrin, Morgante, & Giorgi, 2013). Therefore, after quality control step, trimming of our raw data RNA-seq reads were not performed.

FASTQ Groomer (Galaxy Version 1.1.1) tool is used to verify the FASTQ format and adaptation of raw reads into the Galaxy environment (Blankenberg et al., 2010).

Infer Experiment (Galaxy version 2.6.4.1) module of RSeQC tool was used to confirm the strand specificity orientation of the RNA-seq data. The bam file of HISAT2 was used as input, and “hg38_RefSeq.bed.gz” file (<https://www.ncbi.nlm.nih.gov/refseq/>) was used as reference gene model.

Mapping reads to a reference genome

After raw data upload and grooming steps, RNA-seq reads were mapped to the reference genome (UCSC GRCh38 / hg38) using two different splice aware mapping tool **HISAT2** (Kim, Langmead, & Salzberg, 2015).

After grooming step, RNA-seq reads were aligned to the most current human reference genome (UCSC GRCh38 / hg38) using **HISAT2** (Galaxy Version 2.1.0+galaxy4), a software package capable of rapid alignment to the reference genome. HISAT2 is a fast and effective splice alignment tool which uses the Burrows-Wheeler transform (BWT) and the Ferragina-Manzini (FM) indexing scheme (Kim et al., 2015). The following parameters were used when running HISAT2: Select a reference genome: hg38; Is this a single or paired library: paired;

Specify strand information: Reverse (RF); Output alignment summary in a more machine-friendly style: True; Print alignment summary to a file: True.

Counting reads

featureCounts (Galaxy Version 1.6.3+galaxy2) tool was used to measure gene expression in RNA-Seq data from BAM files of mapping output and to generate count matrix (Liao, Smyth, & Shi, 2014).

For lncRNA annotation, following parameters were used: Specify strand information: Stranded (Reverse); Gene annotation file: “gencode.v29.long_noncoding_RNAs.gff3.gz”; Count fragments instead of reads: Enabled; GFF gene identifier gene_name; Minimum mapping quality per read; 12.

For mRNA annotation, following parameters were used: Specify strand information: Stranded (Reverse); Gene annotation file: “gencode.v29.gff3.gz”; Count fragments instead of reads: Enabled; GFF gene identifier gene_name; Minimum mapping quality per read; 12

Differential expression analysis

DESeq2 (Galaxy Version 2.11.40.2) tool (Love, Huber, & Anders, 2014) was used for the identification of differentially expressed lncRNAs and mRNAs and visualization of the results. The input parameters are as follows: 1. Factor level: feature counts files of 18 MCL samples, 1. Factor level: feature counts files of 3 control samples; Files have header? : Yes; Output normalized counts table: Yes; Fit type: Parametric.

3.6.8. *Transcript Abundance Estimation with Cufflinks*

Gene expressions (transcript abundances) of normal and tumor samples were also estimated as read counts normalized per kilobase of feature length per million mapped fragments. After FASTQ groomer step the reads were aligned to the reference genome (UCSC GRCh38 / hg38) using another splice aware mapping tool **Tophat** (Galaxy version 2.1.1). Then, **Cufflinks** (Galaxy version 2.2.1.2) tool was used to estimate the gene expression values as FPKM (Fragments Per Kilobase Per Million Mapped Fragments) values (Trapnell, Pachter, & Salzberg, 2009).

The estimated FPKM values were then used for quality control of transcript expression analysis of whole transcriptome data obtained with RNA-Seq. Pearson correlation analysis of FPKM values of different housekeeping genes in pairs was performed. Then, housekeeping genes' normalized FPKM values of selected transcripts were compared between MCL samples and control sample.

3.6.9. *Cross-validation of selected lncRNA transcripts' expression by qRT-PCR*

lncRNA transcripts which found to be differentially expressed were cross-validated by SYBR green qRT-PCR assay.

Primer design for selected lncRNAs

Primers were specifically designed for each gene using the IDT PrimerQuest program (**Table 3**). Since the short amplicon size more efficient for q-RT-PCR analysis of FFPE-derived RNAs the length of the primers was designed between 18-25 bp, and the amplicon size was chosen between 80-90 bp. The primers were synthesized by Sentebiolab Biotech company (Ankara).

Table 3: Designed q-RT-PCR Primer List

Gene Name	Forward Sequence (5'→3')	Reverse Sequence(3'→5')	Amplicon Length	Optimized Working Tm
SNHG5	TGTCTTCAGTGGCAC AGT	CCATTAAATATTCTCCCA GATGTTC	85 bp	54 °C
MALAT1	GAGAGATGAGTTGGG ATCAAGTG	GAGATACCTGTCTGAGGC AAAC	78 bp	54 °C
ROR1-AS1	ACTTCCTGGCCTTGGT TTC	CCCAAGAGCTTCGGTTTC C	95 bp	54 °C
MAST4- AS1	ATGGCCGGCAACTAC AG	TGTCCACCTTGATTACTC TTCTC	90 bp	54 °C
FTX	GAATGTCCTTGTGAG GCAGTTG	TGGTCACTCACATGGATG ATCTG	97 bp	54 °C

Resuspending PCR primers

q-RT-PCR primers were received in a lyophilized state. To be able to decrease the number of re-freezing and re-thawing of primers, a master stock of 50 μ M were prepared and then diluted to 10 μ M working stock. The procedure can be briefly explained as follows: First, the forward and reverse primer tubes were spun down before opening to ensure that dried pellet is at the bottom not dislodged, which may happen during shipping. Then, ultrapure water was added to lyophilized primers to prepare 50 μ M stock solution. The added water amount was determined by simply multiplying the number of nmol of primer in the tube by 10. After that, 10 μ M of working stock was prepared by adding 10ul Forward primer, 10ul Reverse primer and 80ul ddH₂O.

cDNA synthesis

cDNA (complementary DNA) synthesis of extracted RNA from both MCL tumor samples and B-cell subsets was performed by QuantiTect Reverse Transcription Kit (Qiagen, Cat no: 205311). This kit is composed of two main steps: gDNA (genomic DNA) elimination and reverse transcription (RT). cDNA synthesis procedure can be summarized as follows: Firstly, gDNA elimination reaction components were prepared according to **Table 4**. Next, 14 μ l mix, incubated for 2 min at 42°C, then placed immediately on ice. Then, the reverse-transcription master mix was prepared on ice according to **Table 5**. The reverse-transcription master mix contains all components required for first-strand cDNA synthesis except template RNA. The RT master mix comprises all the components necessary for the synthesis of the first stranded cDNA, except for template RNA. After that, 6 μ l of RT master mix is added to the first mix (14 μ l). Lastly, the volume of reaction (20 μ l) was incubated for 30 minutes at 42°C and then, for 3 minutes at 95°C. The final cDNA concentration was between **30-40 ng** among samples.

Table 4: Genomic DNA elimination reaction components

Component	Volume/Reaction
gDNA Wipeout Buffer, 7x	2 μ l
Template RNA	Variable (up to 1 μg*)
RNase-Free Water	Variable
Total Volume	14 μl

Table 5: Reverse-Transcription Master Mix Componets

Component	Volume/Reaction
Quantiscript Reverse Transcriptase	1 μ l
Quantiscript RT Buffer, 5x	4 μ l
RT Primer Mix	1 μ l
Total Volume	6 μl

After completion of the reactions, all samples were diluted 1:10 with molecular grade water and stored in -20 °C for future use in the q-RT-PCR assay.

Optimization of primers with gradient PCR

Before the assay set of gene expressions were analyzed, optimization of parameters such as cDNA amount, primer amount, annealing temperatures was performed with designed primer pairs. The optimum primer annealing temperature was determined with gradient PCR. 2 ul of cDNA (1:10 diluted) was used to amplify primer mix (forward and reverse), the thermal cyclers protocol is shown in **Table 6**. After PCR, 10 ul of the sample was run in 1.7% Agarose gel for 20-30 min.

Table 6: Thermal cyclers protocol

94 °C	20 sec	35 cycle
54-56-58-60-62-64 °C	20 sec	
72 °C	20 sec	

Quantitative Real-Time PCR (q-RT-PCR)

The q-RT-PCR analysis was conducted by using Maxima SYBR Green qPCR mix (Thermo Fisher Scientific, Waltham, MA, USA) according to manufacturer's recommendations –depicted in **Table 7**. qPCR reactions were conducted by using the LightCycler 480 II (Roche Applied Science, Mannheim, Germany), the cycling program is demonstrated at **Table 8**.

Table 7: qPCR reaction components

Component	20 µL reaction
2X master mix	10 µL
Primer mix (in H ₂ O)	1 µl
cDNA	9 µl

Table 8: qPCR cycling program

Program	Cycle	Temperature	Time
Pre-incubation	1	95 °C	5min
Amplification	45	95 °C	10 sec
		54 °C	10 sec
		72 °C	10 sec
Melting Curve	1	95 °C	5 sec
		65 °C	1 min
		97 °C	Continuous
Cooling	1	40 °C	30 sec

qRT-PCR data analysis was performed using the reference Ct method using two reference genes (Rao et al., 2013). Statistical significance was tested between two groups by student's two-tailed t-test and 3 techniques were used for each case.

3.6.10. Pathway analysis of MCL-related genes

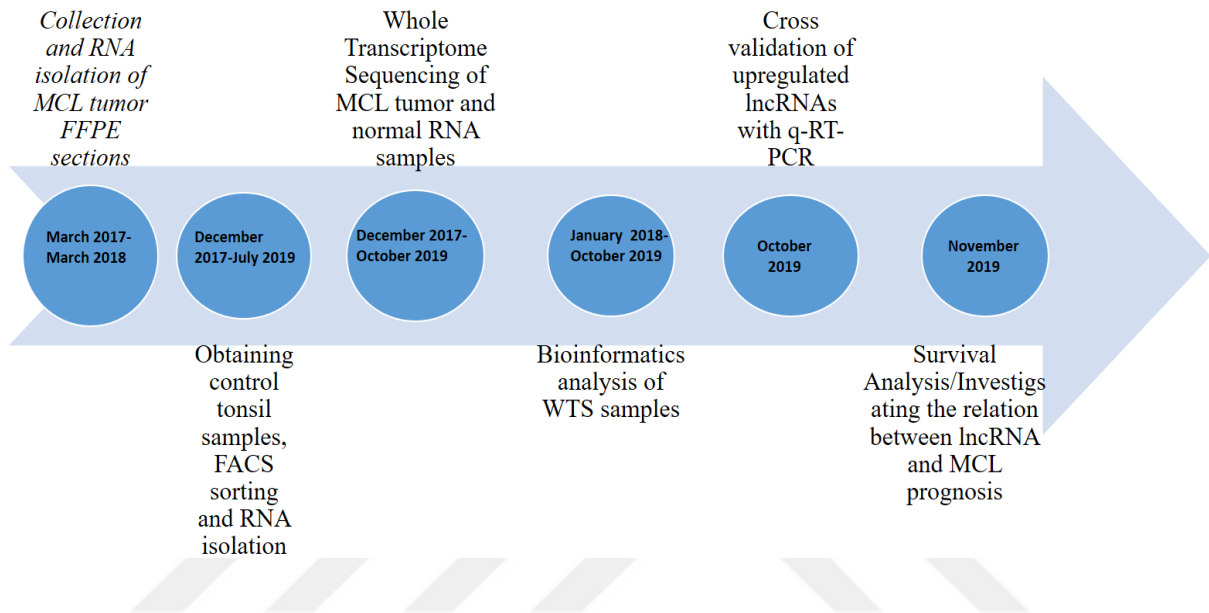
Pathway analysis was conducted to examine whether the most DEmRNA genes are involved in signalling pathways or biological processes that may be related to mantle cell lymphoma. Enrichr tool was used for acquiring significantly enriched Gene Ontology (GO) terms, Kyoto Encyclopedia of Genes and Genomes (KEGG) pathways and Reactome analysis using the differentially expressed upregulated and downregulated mRNAs, separately. (Kuleshov et al., 2016) (Croft et al., 2014).

3.6.11. Survival Analysis

To investigate the relationship between irregularly expressed lncRNAs and mRNAs and patient prognosis survival analysis was conducted. The lncRNAs showing different levels of expression between MCL patients and normal B cell subset groups were evaluated in the light of the clinical course of MCL patients. First of all, the ROC (Receiver Operating Characteristic) analysis was conducted to determine the diagnostic value of selected DElncRNAs and DEmRNAs. Afterwards, Kaplan-Meier survival graphs were generated to determine the prognostic value of lncRNAs. Kaplan-Meier graphs are known to be good estimators of censored data, e.g. patients who do not have a follow-up clinical data (Efron, 1988). Overall

survival (the time period between the diagnosis and death of the patient) demonstrated in Kaplan-Meier graphs using Graphpad Prism 8 (GraphPad Software, Inc, San Diego, CA).

3.7. Study Plan and Calendar



3.8. Data Evaluation

Prognostic value of lncRNAs was evaluated by generating Kaplan-Meier survival graphs using Graphpad Prism 8 (GraphPad Software, Inc, San Diego, CA). For differential expression analysis log₂ fold change >2 and FDR (False Discovery Rate) < 0.01 was considered as cut off of significantly differentially expressed genes. And *P*-value of less than 0.05 was considered to be statistically significant.

3.9. Limitations of the Study

The main goal of this study was the determination of dysregulated lncRNAs in MCL disease by RNA-seq method and investigation of the prognostic value of highly dysregulated lncRNAs in disease pathogenesis. To do so, 18 FFPE MCL tumor sections were compared with three control samples (2 naive B cells and 1 Memory cell). The main limitation of the study was the low number and low RNA amount of control samples. The nanodrop measurement was used to measure the quality and concentration of control samples before sending the samples for whole transcriptome sequencing where the quality of the RNA samples was measured with Bioanalyzer (Agilent Technologies) device. Unfortunately, the Bioanalyzer results showed a dramatical change in RNA concentration and most of the control samples sent for sequencing could not pass the library preparation step with Illumina Truseq Stranded kit. As a solution, four Naive B cell samples were merged and treated as one sample and the same was done with three Memory B-cell samples. Besides, library preparation of these merged samples was performed by NEBNext Ultra II RNA Library Prep Kit, being different than the 18 FFPE MCL samples and 1 Naive B cell library preparation kit (Illumina Truseq Stranded Total RNA kit).

3.10. Ethics Committee Approval

Our study, which was evaluated ethically and approved by the Noninvasive Research Ethics Board of Dokuz Eylul University School of Medicine; protocol no: 2525-GOA; decision no.: 2017/26-31 (Appendix 8.1).

4. RESULTS

4.1. FACS Analysis of Tonsil B cell Subtypes

Reactive tonsil fresh tissue samples which were used as control samples were obtained by routine tonsillectomy operations performed in DEU Otorhinolaryngology (ENT) department and processed promptly. Tonsil cells recovered from half of a pair of tonsils varied substantially among donors and tonsil cell suspension protocol, ACK lysis method gave a better yield than Ficoll-Hypaque method, in terms of tonsil cell suspension number.

Immunophenotypic staining of mononuclear cells present in tonsils was performed by antibodies. From each B cell subpopulation, at least 200,000 cells were sorted directly into 1ml RPMI or 1 ml of 1X PBS solution and cell sorting procedures were performed by FACS Aria III device. The sorting strategies can be briefly summarized as follows: Firstly, total lymphocytes were gated on a forward scatter (FSC) and side scatter (SSC) and DAPI + dead cells were excluded. Then, IgD+, CD23- Naive B cells were selected from viable cells. and finally, IgD-, CD38- Memory B cells were selected. Flow cytometry data were analysed using BD FACSDiva 6.0 and FlowJo software (FlowJo, Ashland, OR, USA) as demonstrated in

Figure 8.

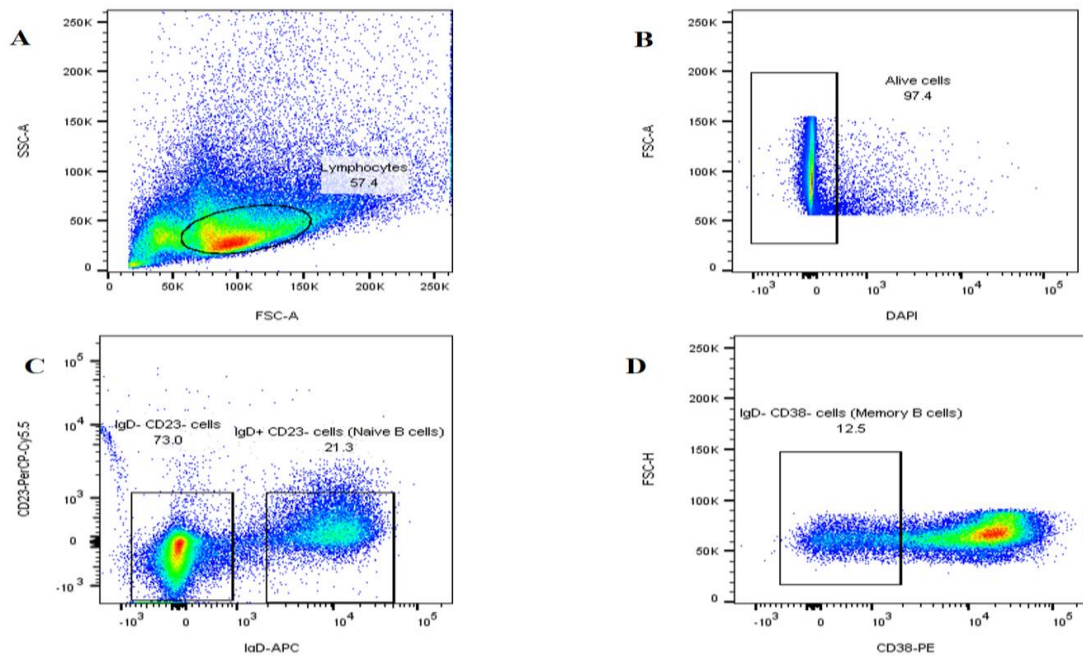


Figure 8: Sorting gates strategies used in multicolor FACS analysis to isolate B-cell subsets. **A)** Total lymphocytes were gated on a forward scatter (FSC) and side scatter (SSC) **B)** DAPI + dead cells were excluded. **C)** IgD+, CD23- Naive B cells were selected from viable cells. **D)** Finally, IgD-, CD38-Memory B cells were selected. Flow cytometry data were analysed

using BD FACSDiva 6.0 and FlowJo software (FlowJo, Ashland, OR, USA). The percentages of gated populations are indicated above the FACS graph.

4.2. Quality control of raw sequence data

High throughput sequencing instruments produce vast quantities- tens of millions of sequences- of data in a single run. Before starting the analysing the sequence data and reaching biological conclusions, it is necessary to assess the quality of the high-throughput sequencing data obtained from the sequencing instrument (Ewing & Green, 1998; Nakamura et al., 2011).

Quality control (QC) of raw data reads were assessed with the **FASTQC** (v 0.72+galaxy1) tool. FASTQC tool summarizes the raw sequence data by generating summary plots and tables to evaluate the quality. The HTML output file maintains the following results:

- Basic Statistics
- Per base sequence quality
- Per sequence quality scores
- Per base sequence content
- Per base GC content
- Per sequence GC content
- Per base N content
- Sequence Length Distribution
- Sequence Duplication Levels
- Overrepresented sequences
- Kmer Content

To rank the quality assessment, precious information is obtained from the change in the Phred value between sequential bases, which eventually the quality scores of reads will drop at the 3' end of the reads as a consequence of sequence by synthesis methods of Illumina sequencing platforms (Ewing & Green, 1998).

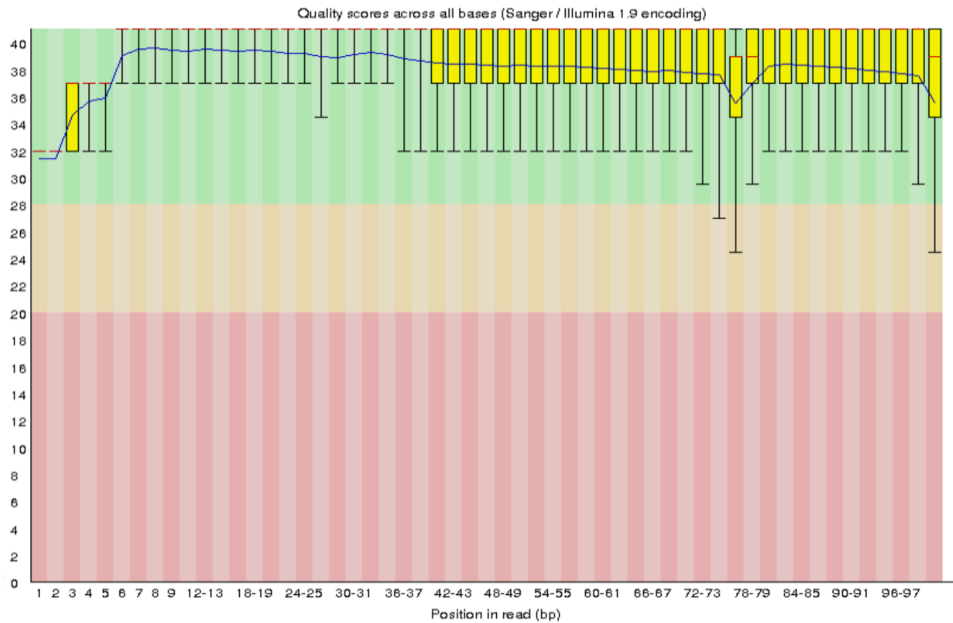


Figure 9: Per base sequence quality of MCL41 sample

Figure 9 demonstrates the Per Base Sequence Quality box-whisker plot which overviews the range of quality scores all bases for each position in the of MCL41 sample raw data (FASTQ) file. In this figure, central red line represents the median value, the yellow box represents the interquartile range (25-75%), blue line represent the mean quality and the upper and lower whiskers represent the 10% and 90% points. The X-axis shows the position in read (bp) and the Y-axis show the Phred quality values. Higher the quality score indicates the higher the base call. The background of the chart divides the y-axis into high-quality searches (green), reasonable-quality searches (orange), and low-quality searches (red).

Phred quality score (Q) is logarithmically related to the probability of error for each base-call. It is calculated as $Q = -10 \times \log_{10}(P)$ where P is the probability of erroneous base calling. For example, a Phred quality score of 30 indicates the chance that this base is called incorrectly is 1 in 1,000. Reads with Phred scores lower than 20 generally discarded before further analysis due to the high rate of error probability (probability of incorrect base call of 1 in 100).

It is normal for all Illumina sequencers to have a median quality score less than the initial 5-7 bases and then increase. The reading quality on most platforms is reduced at the end of the reading. This is usually caused by signal decay or phasing during sequencing (Ewing & Green, 1998; Li, Nair, Wang, & Wang, 2015; Mbandi, Hesse, Rees, & Christoffels, 2014; Nakamura et al., 2011).

4.3. Confirming the strand specificity orientation of the RNA-seq data

Infer Experiment (Galaxy version 2.6.4.1) module of RSeQC tool was used to confirm the strand specificity orientation of the RNA-seq data. The bam file of HISAT2 was used as input and “hg38_RefSeq.bed.gz” file (<https://www.ncbi.nlm.nih.gov/refseq/>) was used as reference gene model.

Below results confirmed that RNA-seq reads are strand-specific and in FR First-Strand (RF) setting. Strandness of read2 is consistent with that of the gene model, while strandness of read1 is opposite to the strand of the reference gene model.

```
=====  
This is PairEnd Data  
Fraction of reads failed to determine: 0.0087  
Fraction of reads explained by "1++,1--,2+-,2-+": 0.0184  
Fraction of reads explained by "1+-,1-+,2++,2--": 0.9729  
=====
```

4.4. Read mapping and Quality Control

Quality control of HISAT2-aligned reads using **MultiQC tool** (Galaxy Version 1.7) (Ewels, Magnusson, Lundin, & Källner, 2016). Alignment rate for each one of the RNA-seq reads against the human genome (hg38) is demonstrated in **Figure 10** with the number of reads among samples (Figure 10A) and percentages of reads among samples (Figure 10B).

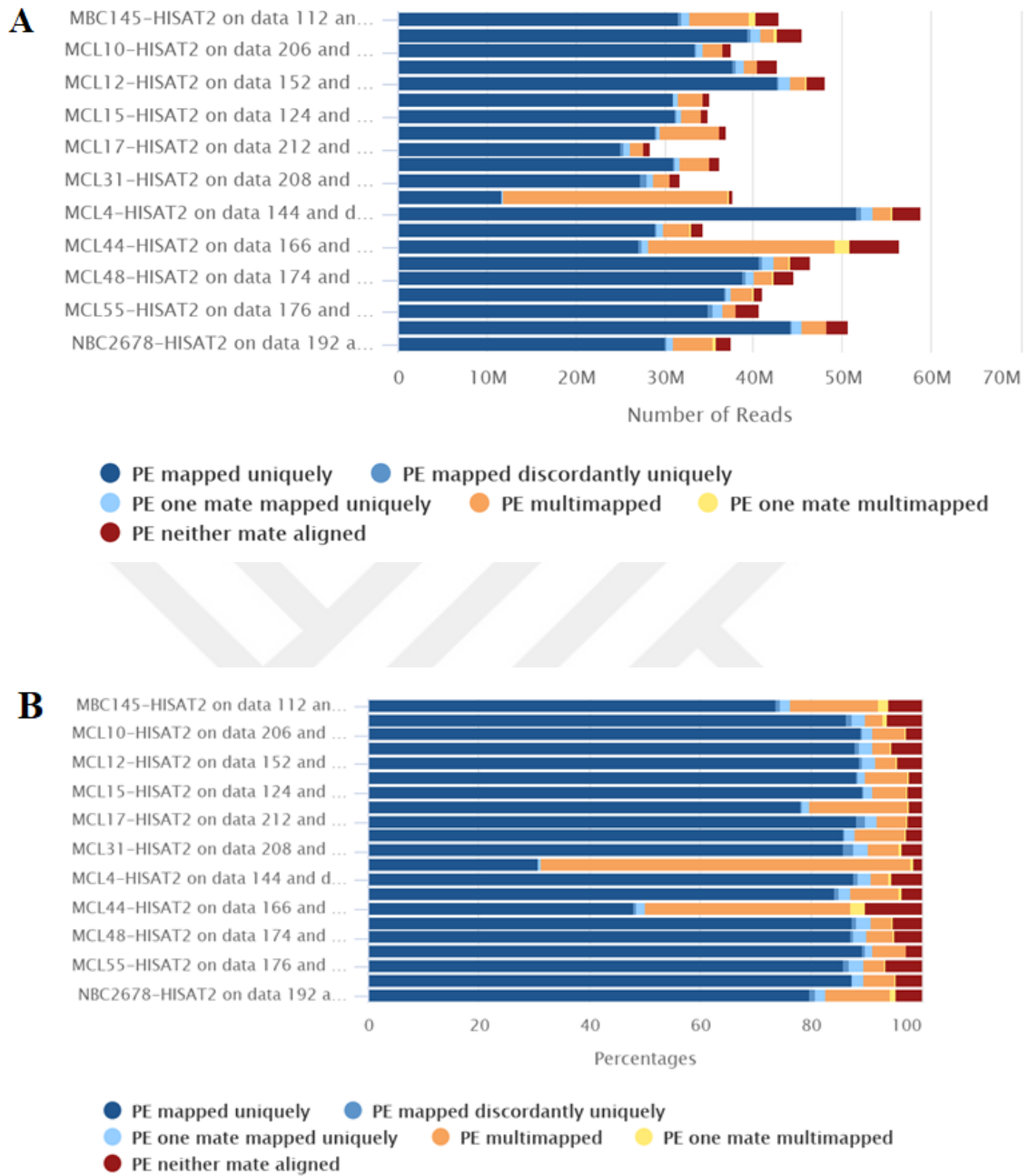


Figure 10: MultiQC results of HISAT2 alignment scores. **A)** The number of reads among samples. **B)** Percentages of reads among samples.

4.5. Identification of differentially expressed lncRNAs in MCL cases

Whole transcriptome sequencing was used to identify the differentially expressed lncRNAs (DElncRNAs) in 18 MCL cases compared to 3 control samples (2 Naive B cells and 1 memory B cells). DESeq2 tool was used for the expression level comparisons of genes and transcripts.

Significantly differentially expressed genes identified upon meeting the following criteria: **1)** P value < 0.05; **2)** P-adjusted value (False Discovery Rate(FDR)) < 0.01; **3)** absolute log₂ fold change [abs(log₂FC)] >2 for up and down regulation.

A total of **1149** significantly DElncRNAs was detected from all samples with **322** of upregulated and **827** of lncRNAs downregulated.

Table 8 shows the top 20 upregulated lncRNAs (FDR < 0.05; log₂FC > 2) and **Table 9** show the top 20 downregulated lncRNAs (FDR < 0.05; log₂FC < 2) according to DESeq2 results file.

Table 9: The top 20 upregulated DElncRNAs in MCL

Gene name	Type of Gene	log ₂ Fold Change	P-value	FDR
AC010983.1	lncRNA	9.768525416	8.25E-15	1.04E-12
AC090125.1	lncRNA	9.084380078	6.48E-15	8.66E-13
NR2F2-AS1	lncRNA	7.910221056	2.19E-12	1.63E-10
LINC01268	lncRNA	7.44237927	5.98E-12	3.99E-10
AC108025.2	lncRNA	7.104103613	1.94E-09	6.32E-08
LINC01197	lncRNA	6.885281384	1.23E-09	4.26E-08
PWRN2	lncRNA	6.756151163	1.18E-08	3.15E-07
MAST4-IT1	lncRNA	6.743395037	1.06E-14	1.32E-12
LINC01515	lncRNA	6.65649692	1.33E-07	2.59E-06
CARMN	lncRNA	6.627087331	1.11E-18	4.91E-16
MAGI1-IT1	lncRNA	6.419210477	2.55E-08	6.14E-07
MAGI2-AS3	lncRNA	6.289161794	1.51E-13	1.55E-11
LINC01105	lncRNA	6.279407413	2.59E-05	0.000244949
AC016251.1	lncRNA	6.213545989	5.69E-08	1.23E-06
ADAMTS9-AS2	lncRNA	5.987194047	1.49E-07	2.85E-06
DNM3OS	lncRNA	5.962427457	1.05E-10	4.81E-09
DANT2	lncRNA	5.838617184	8.11E-06	8.99E-05
MIR100HG	lncRNA	5.838306989	1.38E-19	7.52E-17
FENDRR	lncRNA	5.101933439	3.24E-05	0.000297485
LIFR-AS1	lncRNA	5.028761872	7.33E-06	8.29E-05

*FDR: False Discovery Rate

Table 10: The top 20 downregulated DElncRNAs in MCL

Gene name	Type of Gene	log2 Fold Change	P-value	FDR
AF111167.1	lncRNA	-8.924144823	2.27E-27	5.36E-24
AC011446.2	lncRNA	-8.871619307	9.74E-18	3.28E-15
AC044849.1	lncRNA	-8.315720702	3.07E-39	2.17E-35
AC093484.3	lncRNA	-8.129432151	2.12E-15	3.19E-13
AL160408.2	lncRNA	-8.114371042	1.63E-07	3.06E-06
AC005944.1	lncRNA	-7.810052903	1.58E-05	0.00016
AC026202.3	lncRNA	-7.570155821	6.34E-13	5.61E-11
AC004528.2	lncRNA	-7.529753343	5.53E-10	2.07E-08
AP001046.1	lncRNA	-7.40074677	7.29E-15	9.38E-13
AC002401.1	lncRNA	-7.31567243	1.83E-11	1.04E-09
DDIT4-AS1	lncRNA	-7.26343141	2.14E-05	0.000208
PRMT5-AS1	lncRNA	-7.223460781	2.88E-17	8.16E-15
Z83844.2	lncRNA	-7.209709138	2.03E-15	3.13E-13
AC124014.1	lncRNA	-6.948216472	2.06E-11	1.16E-09
AL031846.2	lncRNA	-6.871443422	1.39E-10	6.12E-09
CTBP1-AS	lncRNA	-6.675919813	6.53E-13	5.70E-11
AC006441.3	lncRNA	-6.650412015	4.69E-09	1.38E-07
LINC01783	lncRNA	-6.639387545	2.83E-11	1.55E-09
AL031600.3	lncRNA	-6.634888661	0.000337432	0.00211
AC008894.2	lncRNA	-6.615218275	1.15E-12	9.34E-11

*FDR: False Discovery Rate

Besides the gene list and normalized count matrix of genes, DESeq2 analysis gives a graphical summary of the results, that includes the following plots which are used for the quality assessment of the experiment

Heatmap of the sample-to-sample distances of lncRNA annotated MCL and control samples

A beneficial initial step in a WTS analysis is often to evaluate the overall similarity within samples. This similarity evaluation is very useful for assessing the experimental design of samples. For instance, does tumor samples and control samples different to each other according to sample distance matrix? Hence, heatmap of distance matrix was drawn to visualize the sample-to-sample distances which outline the similarities and dissimilarities between

samples (**Figure 11**). According to this heatmap, lncRNA annotated MCL samples were clustered closer together and control samples cluster distantly from them as expected.

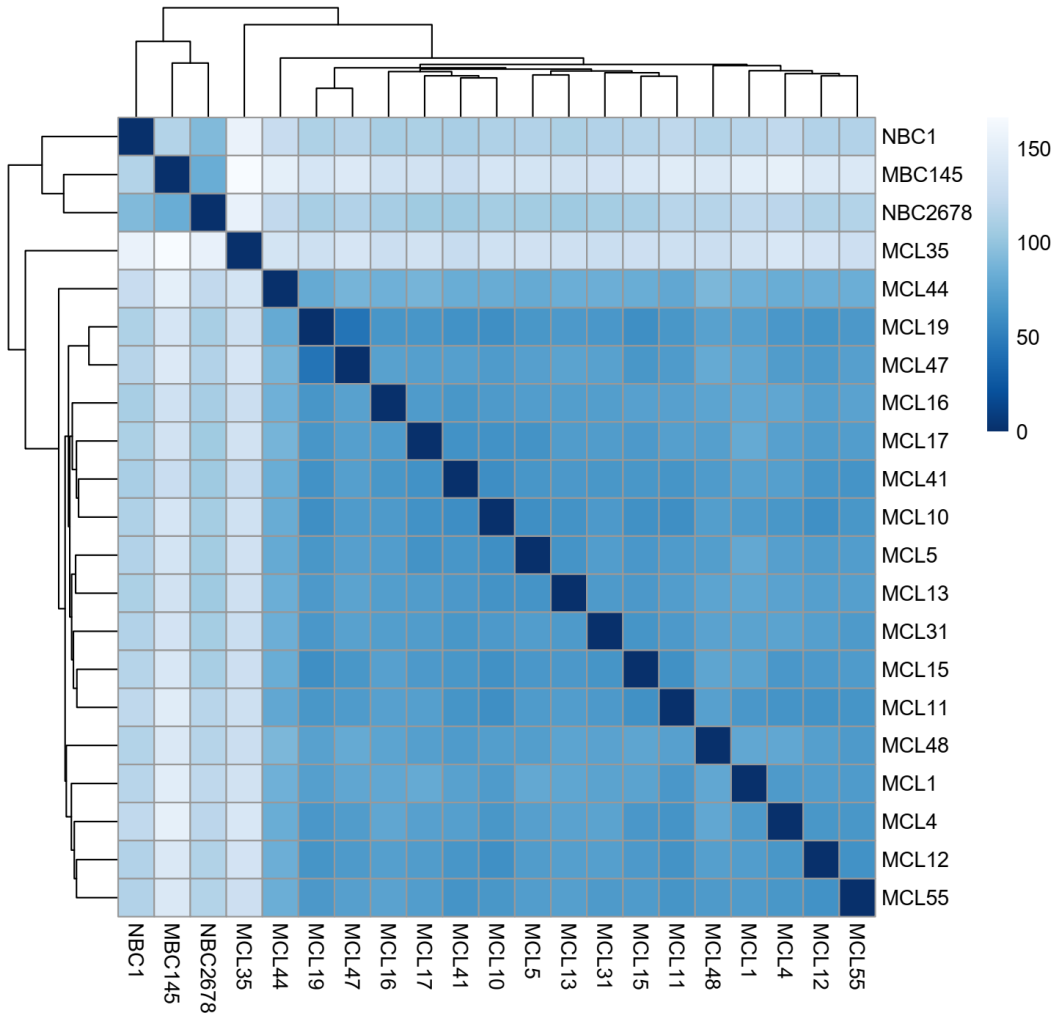


Figure 11: Heatmap of sample-to-sample distances of lncRNA annotated MCL and control samples (*Darker blue colors indicate more similarity*)

PCA plot of lncRNA annotated MCL and control samples

PCA (Principal component analysis) plot is another way of visualizing the sample-to-sample distances which demonstrated the separation between group 1 (MCL_lncRNA) and group 1 (Control_lncRNA). PCA plots are useful for assessing the overall effect of batch effects and experimental covarities between samples. The samples are reflected in the 2D plane and spread in two directions that explain most of the differences (**Figure 12**). PC1 is indicated in

the x-axis and indicates the direction which separates the samples the most, and PC2 in the y-axis indicates the dimension which separates the data second-most. According to the PCA plot at Figure 12 MCL samples cluster together and control samples cluster together and these two groups cluster distantly from each other as expected. With the exception of MCL35 samples which acted as an outlier.

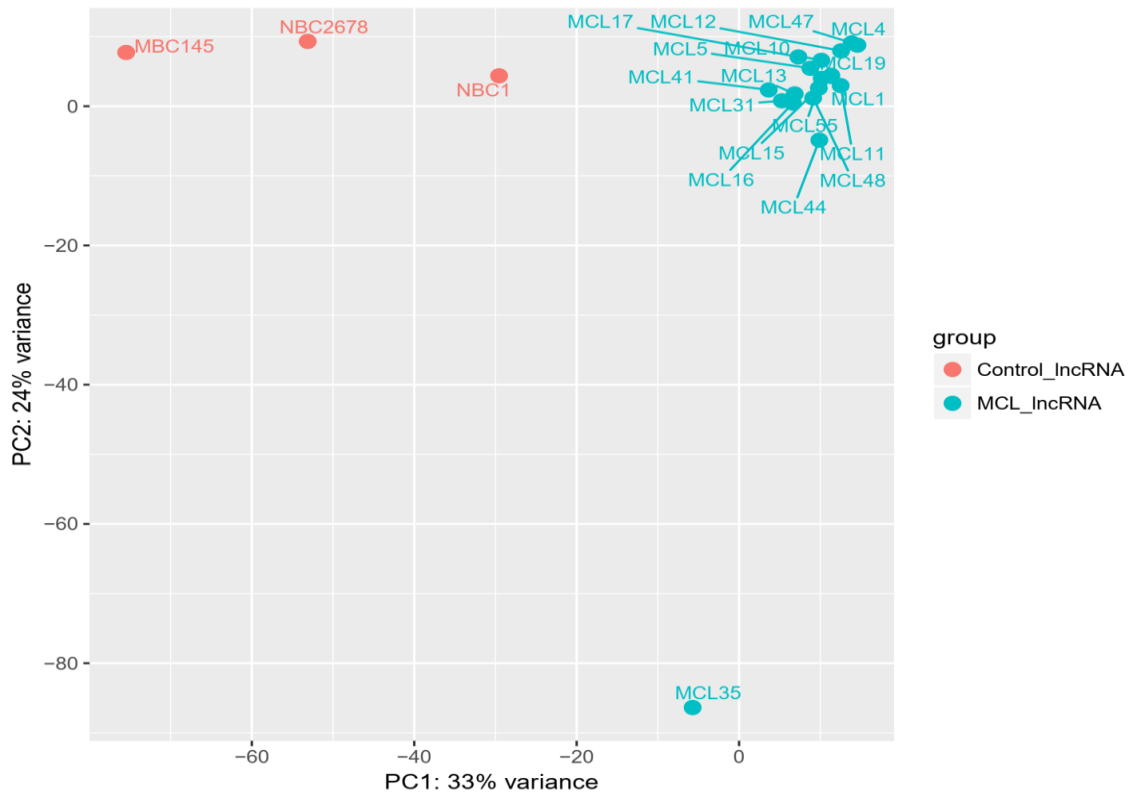


Figure 12: PCA plot of lncRNA annotated MCL and control samples

MA-Plot of lncRNA annotated MCL and control samples

MA plot (also known as Bland-Altman plot or mean-difference plot) is often used for visualization of differences between measurements taken in two samples by transforming the data onto log scale. “M” on the y-axis indicates the log ratio (expression change) and “A” on the x-axis indicates the mean average scales (**Figure 13**). The red points in the MA-plot indicates the genes with adjusted P-value (FDR) < 0.1. In general, differentially expressed genes have a high fold change and highly expressed.

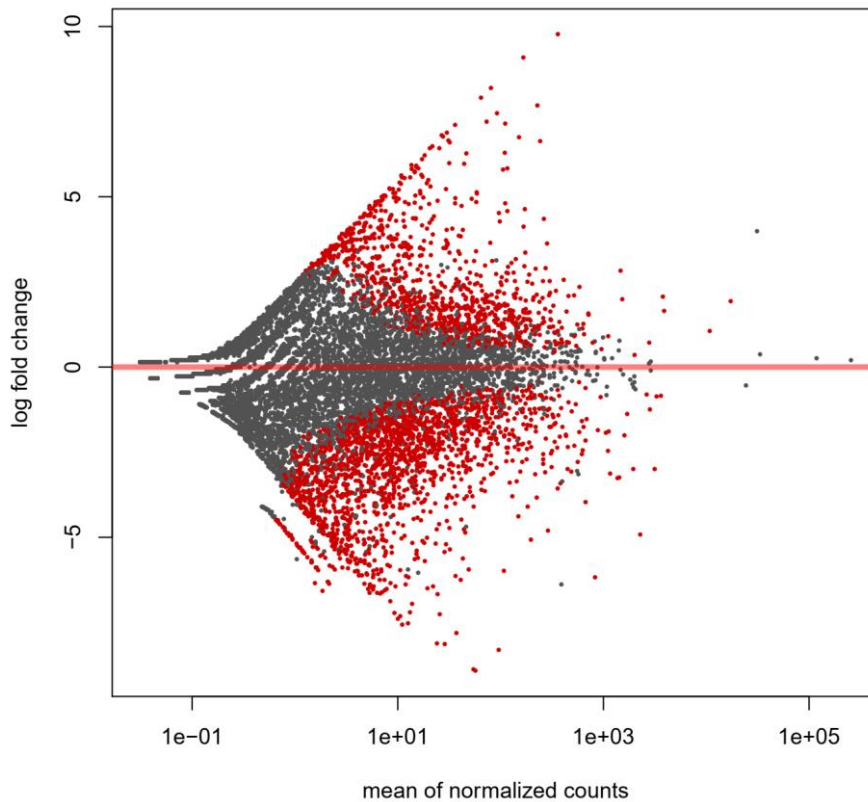


Figure 13: MA-plot of lncRNA annotated MCL and control samples

4.6. Identification of differentially expressed mRNAs

Similar strategy was followed for the identification of differentially expressed mRNAs (DEmRNAs) in 18 MCL cases compared to 3 control samples (2 Naive B cells and 1 memory B cells). DEmRNAs were considered significant upon meeting the following criteria: **1)** P value < 0.05; **2)** P-adjusted value (False Discovery Rate-FDR) < 0.01; **3)** absolute log₂ fold change [abs(log₂FC)] >2 for up and down regulation. Following this criteria, a total of **4275** significantly DEmRNAs was detected from all samples with **2924** of upregulated and **1351** of downregulated.

Table 10 shows the most dysregulated DE mRNA genes in MCL patients samples compared to control samples (P < 0.05; FDR < 0.01; log₂FC > 2) according to DESeq2 results file.

Table 11: The most dysregulated DEmRNAs in MCL

Gene name	Type of Gene	log2 Fold Change	P-value	FDR	Status
CCND1	mRNA	5.469476521	4.63E-57	4.28E-53	Up
NFIB	mRNA	8.327682654	2.01E-35	2.66E-32	Up
SOX11	mRNA	9.615993663	1.43E-34	1.65E-31	Up
IGFBP3	mRNA	7.508334178	9.39E-29	5.92E-26	Up
CXCL12	mRNA	8.63266257	1.35E-27	7.47E-25	Up
IL33	mRNA	8.082458817	2.66E-21	5.96E-19	Up
NR2F2	mRNA	9.004711294	2.43E-20	4.87E-18	Up
MXRA5	mRNA	7.772030495	1.60E-18	2.34E-16	Up
SVEP1	mRNA	8.880366904	4.25E-18	5.72E-16	Up
FZD4	mRNA	7.194490502	3.49E-17	3.87E-15	Up
IGLV3-21	mRNA	-5.817536917	5.53E-16	4.81E-14	Down
XKR4	mRNA	8.071985624	1.32E-15	1.03E-13	Up
PREX2	mRNA	8.750312673	3.33E-15	2.41E-13	Up
ADGRF5	mRNA	8.987382286	3.99E-15	2.81E-13	Up
CDH5	mRNA	8.913347395	6.39E-15	4.24E-13	Up
SLC22A3	mRNA	9.035012161	6.68E-15	4.41E-13	Up
ART4	mRNA	8.574188871	8.08E-15	5.21E-13	Up
NOVA1	mRNA	7.208182531	1.02E-14	6.46E-13	Up
CACNA2D1	mRNA	8.459159275	3.31E-14	1.91E-12	Up
ROBO2	mRNA	8.270324935	7.54E-14	4.09E-12	Up
IL21R	mRNA	-2.856446009	7.88E-13	3.58E-11	Down
MYOCD	mRNA	8.135622626	1.40E-11	4.75E-10	Up
ZACN	mRNA	-6.31073628	2.00E-10	5.07E-09	Down
ARHGAP6	mRNA	4.181197227	1.59E-09	3.32E-08	Up
RAB33A	mRNA	-3.557515433	7.89E-09	1.37E-07	Down
SLAMF1	mRNA	-3.189312354	4.04E-08	5.88E-07	Down
CD8B2	mRNA	-4.583483566	1.03E-06	1.02E-05	Down
BCAR3	mRNA	-2.055567443	5.69E-06	4.59E-05	Down
CCDC173	mRNA	-4.641615253	5.32E-05	0.0003217	Down
IL24	mRNA	-4.72752451	0.000887	0.0036811	Down

Besides the gene list and normalized count matrix of genes, DESeq2 analysis gives a graphical summary of the results, that includes the following plots which are used for the quality assessment of the experiment.

Heatmap of the sample-to-sample distances based on mRNA expression

Heatmap of distance matrix was drawn to visualize the sample-to-sample distances which outline the similarities and dissimilarities between samples (**Figure 14**). According to this heatmap, MCL samples were clustered closer together and control samples cluster distantly from them as expected.

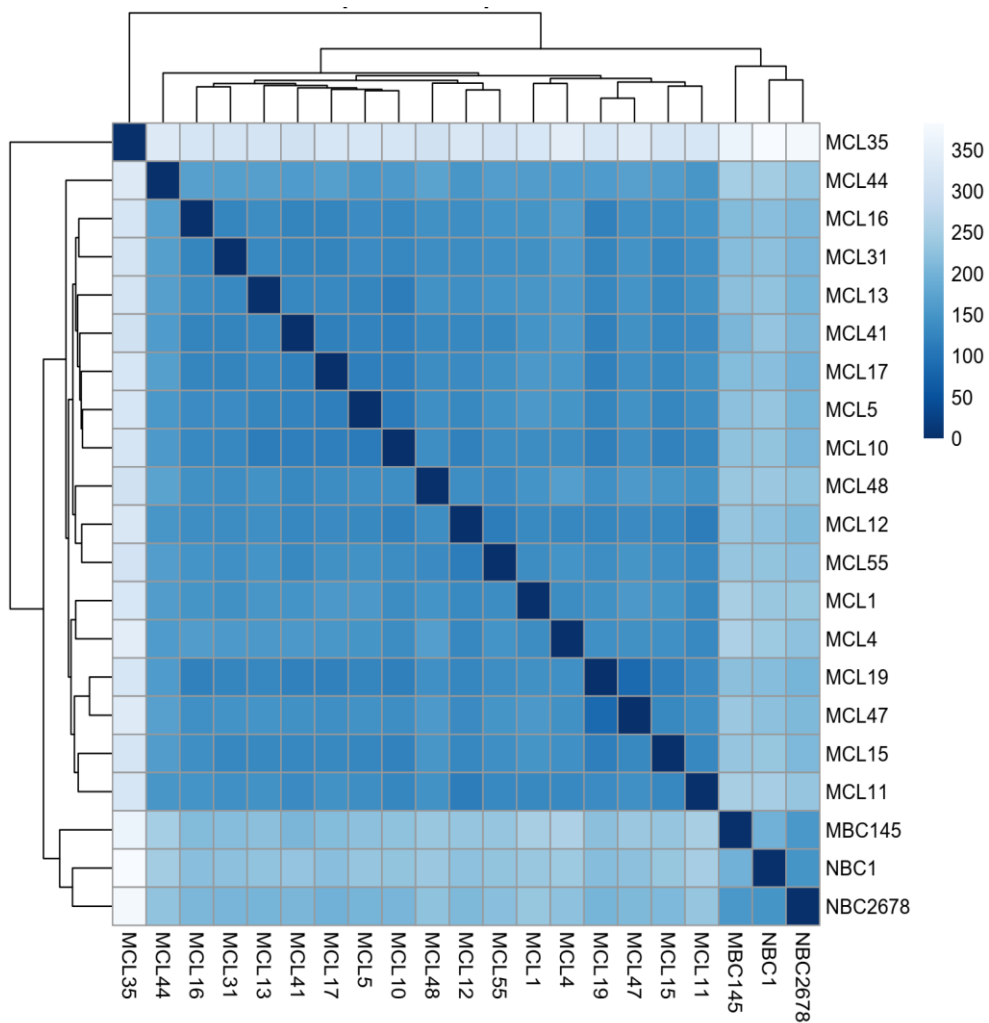


Figure 14: Heatmap of sample-to-sample distances (Darker blue colors indicate more similarity)

PCA plot of MCL and control samples based on mRNA expression

PCA plot below (**Figure 15**) demonstrates the sample-to-sample distances group 1 (MCL) and group 2 (Control) with 64% variance of group 1. According to the PCA plot at MCL samples cluster together and control samples cluster together and these two groups cluster distantly from each other as expected. Similar to the lncRNA PCA plot, “MCL35” sample acted as an outlier.

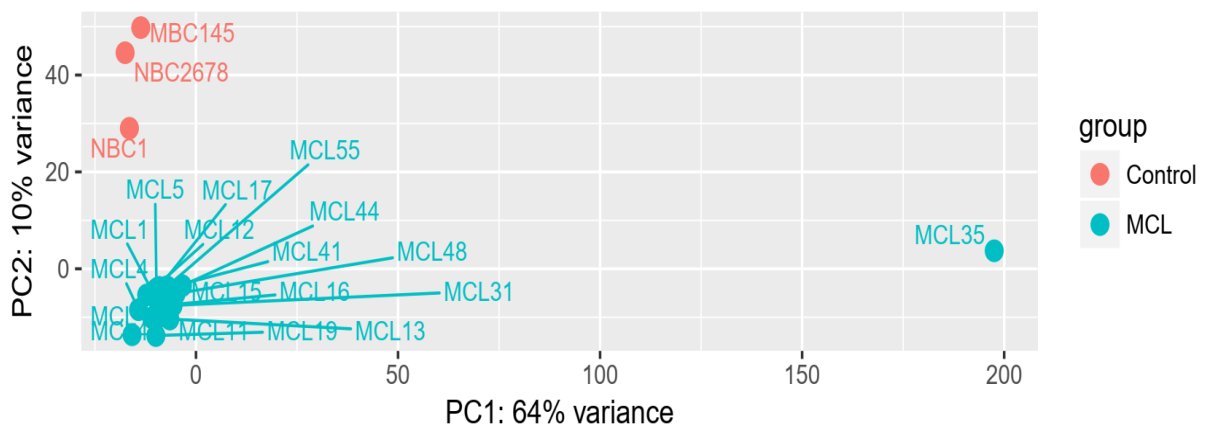


Figure 15:PCA plot of MCL and control samples

MA-Plot based on mRNA expression

MA plot below demonstrates the relationship between expression change (M) and average expression strength (A) of samples (**Figure 16**). The red points in the MA-plot indicate the genes with adjusted P-value (FDR) < 0.1. In general, differentially expressed genes have a high fold change and highly expressed.

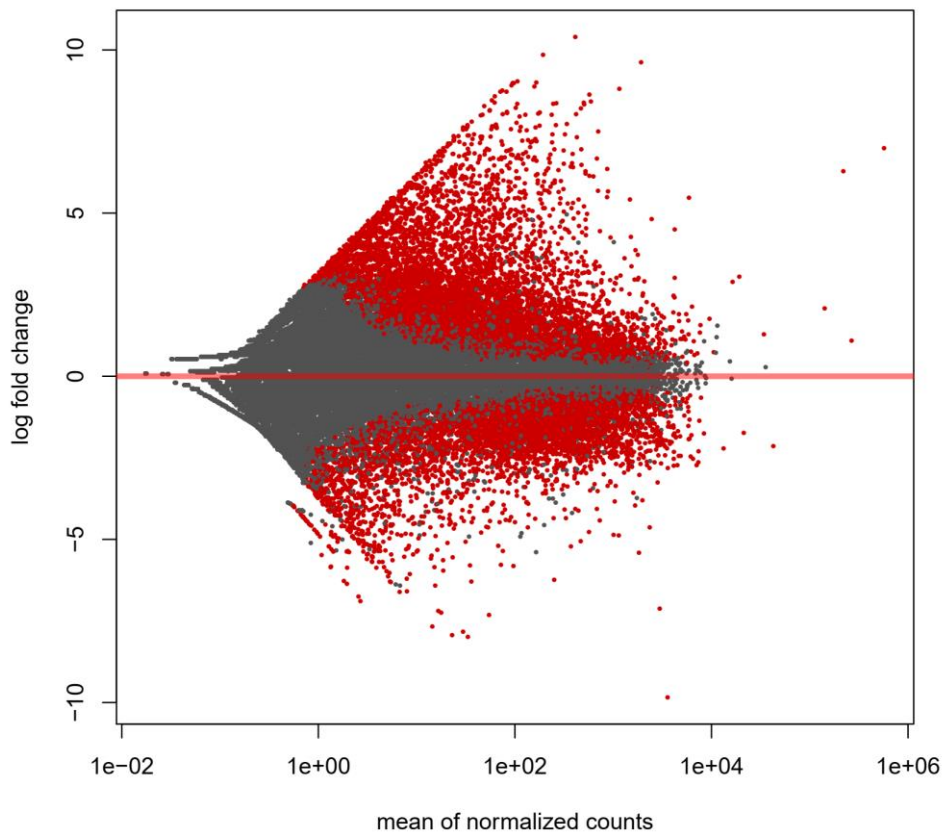


Figure 16: MA-plot of MCL and control samples

4.7. Quality control of transcript expression analysis of whole transcriptome data obtained with RNA-Seq

FPKM values obtained from whole transcriptome sequence analyzes using Cufflinks computational bioinformatics workflow in the context of normalization. However, for co-analysis of different RNA-Seq samples, additional normalization methods between samples are required. One of these methods is normalization, taking into account the expression of the housekeeping gene or genes. When the amounts of RNA are equal, the housekeeping gene expression of different samples is considered unchanged. Because all MCL cases underwent formalin fixation and paraffin embedding (FFPE), the quality of isolated total RNAs was inherently lower. As a result of whole transcriptome data analyzes, housekeeping gene FPKM data were lower in MCL cases compared to naive B cell FPKM data. Pearson correlation

analysis of different housekeeping gene FPKM values in pairs showed that housekeeping gene expressions had high positive correlation among themselves (data not shown).

The Pearson correlation (R) values of RPL13A, GAPDH, RPS13, and HPRT1 housekeeping genes were 0.99, 0.98, 0.98, and 0.85 in a total of 19 WTS samples (18 MCL and 1 NBC), respectively. In order to compare FFPE MCL cases with NBC sample separated from FACS by reactive tonsil tissue, Cufflinks results were examined and housekeeping gene normalization results were added.

RNA-Seq mRNA expression of CCND1 and SOX11 genes characterizing MCL tumors

The quality control of transcript expression analysis of whole transcriptome data obtained with RNA-Seq was performed by identifying the expressions of CCND1 and SOX11 proto-oncogenes in MCL cases compared to B cells. The fact that the immunoglobulin heavy chain (IGH) enhancer comes closer to the CCND1 gene, leading to high expression of this gene is a genetic aberration that characterizes mantle cell lymphoma (MCL) tumors (Menke et al., 2017).

When Cufflinks FPKM data were examined, it was observed that CCND1 gene was expressed more in MCL cases than naïve B cells (**Figure 17A**). When levels of CCND1 FPKM transcript were normalized to RPS13 or GAPDH housekeeping gene expressions for each sample, it was also observed that the CCND1 gene was upregulated in MCL cases as expected (**Figure 17B, 17C**). In terms of high expression in MCL tumor tissues, the most important gene after CCND1 is the SOX11 gene. SOX11 oncogene is not expressed in normal B cells but upregulated in MCL cases. When FPKM values of SOX11 mRNA were examined, SOX11 mRNA was upregulated in MCL cases compared to NBC sample, as for CCND1 (**Figure 17D-F**).

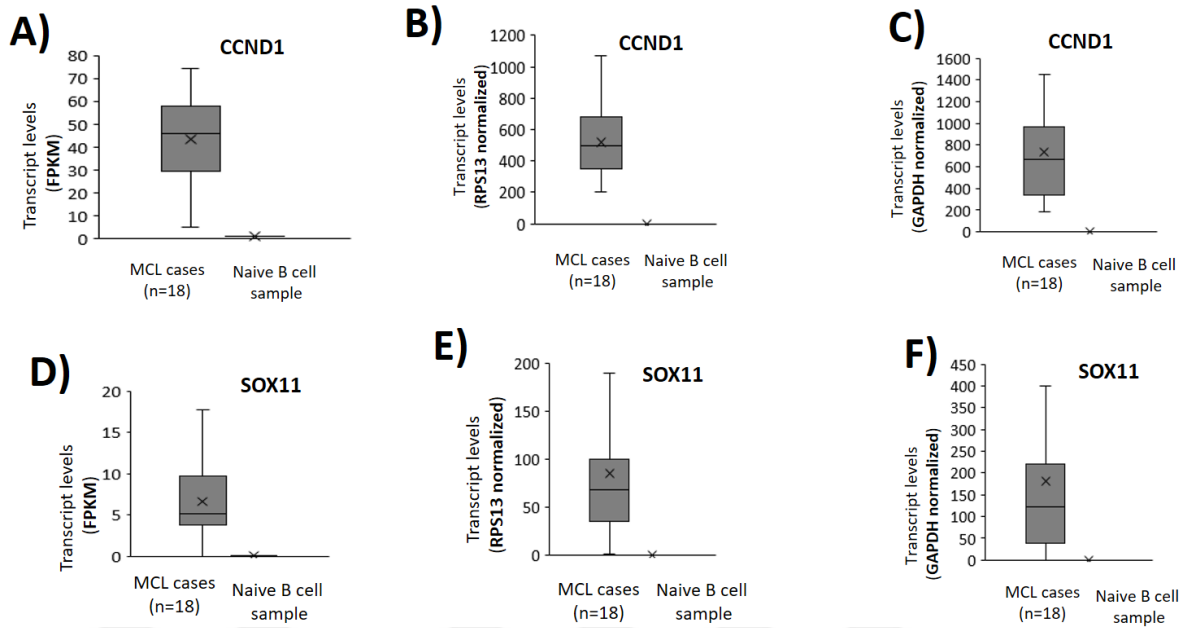


Figure 17: RNA-Seq expression of CCND1 and SOX11 transcripts in MCL cases. CCND1 and SOX11 mRNAs in 18 MCL cases were compared with levels of FPKM (A, D), RPS13 (B, E) or GAPDH (C, F) in normalized naïve B cell and plotted as a box whisker plot.

RNA-seq analysis of dysregularly expressed MALAT1 and SNHG5 lncRNAs in MCL tumors

There are few reports of irregularly expressed lncRNAs in MCL cases. In one of these publications, although there were large differences in expression between samples, it was observed that expression of MALAT1 lncRNA was higher than that in normal B cells (X. Wang et al., 2016). When we analyzed whole the transcriptome sequence analysis FPKM data, we did not observe a significant increase in MALAT1 lncRNA expression in MCL cases (**Figure 18A**). However, when we normalized MALAT1 levels to RPS13 or GAPDH levels, it was observed that MALAT1 was higher than reactive tonsil naïve B cells (**Figure 18B, 18C**). SNHG5 lncRNA was observed to suppress MYC oncoprotein expression in MCL cell lines. However, a study that analyzes SNHG5 expression in MCL patient tumor samples has not yet been reported (Hu, Zhang, & Gupta, 2019). When we examined the whole transcriptome sequence Cufflinks FPKM values, we observed that the expression of SNHG5 lncRNA decreased significantly in MCL cases compared to the NBC sample (**Figure 18D**). In all cases (n=19) SOX11 FPKM values were higher in MCL cases compared to NBC samples when normalized to RPS13 or GAPDH housekeeping gene FPKM values (**Figure 18E, 18F**).

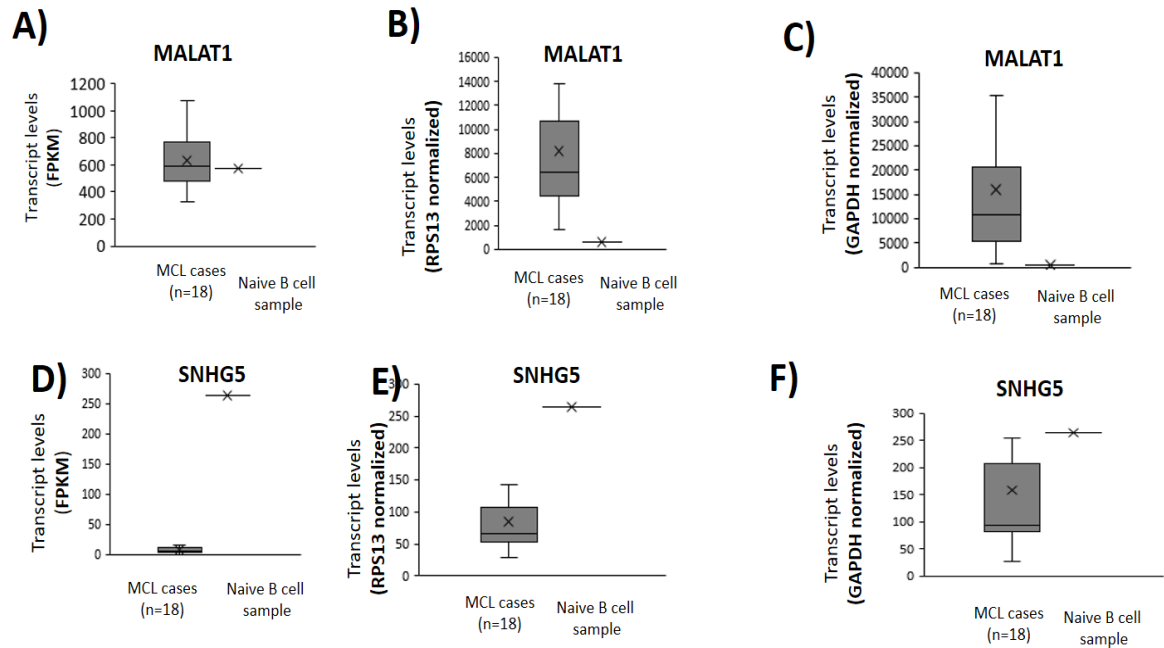


Figure 18: RNA-Seq expression of MALAT1 and SNHG5 lncRNAs in MCL cases. Boxes were plotted against the levels of MALAT1 and SNHG5 lncRNAs in 18 MCL cases in the normalized naïve B cell FPKM (A, D), RPS13 (B, E) or GAPDH (C, F).

4.8. Cross-validation of selected lncRNA transcripts' expression by qRT-PCR

Next, quantitative PCR analysis was performed to validate the WTS results for the selected differentially expressed lncRNA transcripts. As a result of the gradient PCR optimization of the annealing temperatures (54 ° C-64 ° C) of the primer pairs, qRT-PCR procedures were started by using the MALAT1 and SNHG5 qRT-PCR primer pairs. RPS13 housekeeping gene was used for the expression normalization.

The primer pair RPS13-qRT-PCR produces 77 bp amplicon. The RPS13 primers were designed to span through sequential exons to perform cDNA amplification only. The cDNA amplification of the qRT-PCR assay of 18 MCL samples with WTS data analyzed from reactive tonsil tissues, memory B cells and naïve B cells of three different cases were performed on the LightCycler 480 qPCR instrument (Roche company) with Maxima SYBR Green qPCR Master Mix (ThermoFisher Scientific company).

SNHG5 and MALAT1 lncRNA expression for each sample was normalized to RPS13 housekeeping gene expression. SNHG5 and MALAT1 expressions in MCL cases were calculated as relative fold change compared to naïve B cell or memory B cell. The $2^{-\Delta\Delta CT}$ method was used for the quantification of relative expression of lncRNAs. Besides, the melting curve (dissociation curve) analysis was performed for the evaluation of the specificity of qPCR amplification.

According to WTS data analysis results, SNHG5 lncRNA with decreased expression in MCL cases was subjected to cross-validation by quantitative reverse transcriptase PCR (qRT-PCR). As a result of these analyzes, as in WTS data (**Figure 19A, 19B**), qRT-PCR experiments showed that the SNHG5 transcript values were lower in MCL cases compared to levels in naïve B cells (**Figure 19C, 19D**). Similarly, SNHG5 levels in MCL cases were lower than those in memory B cells (**Figure 19E**). SNHG5 FPKM values were also low in MCL cases when normalized by RPS13 and GAPDH housekeeping gene transcripts (**Figure 19E, F**). These results suggest that SNHG5 may be a tumor suppressor lncRNA related to MCL development.

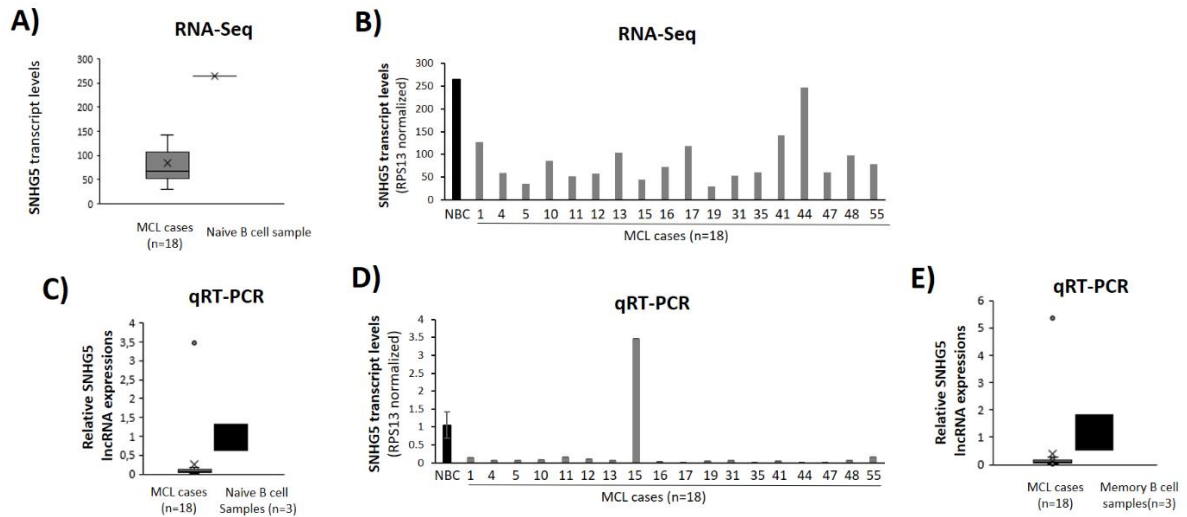


Figure 19: Comparison of SNHG5 expression levels in MCL cases by RNA-Seq and qRT-PCR methods. In 18 MCL cases and a naïve B cell (NBC) sample, SNHG5 transcript levels determined by whole transcriptome sequencing are shown as box-whisker plot (A) and bar graph (B). Box-whisker plot (C, E) and bar graphs (D) of SNGH5 expressions determined by qRT-PCR in memory B cell samples as well as the same samples.

According to q-RT-PCR results MALAT1 transcript values were higher in MCL cases compared to levels in naïve B cells except MCL 16 sample (Figure 20). However, this increase is not significant.

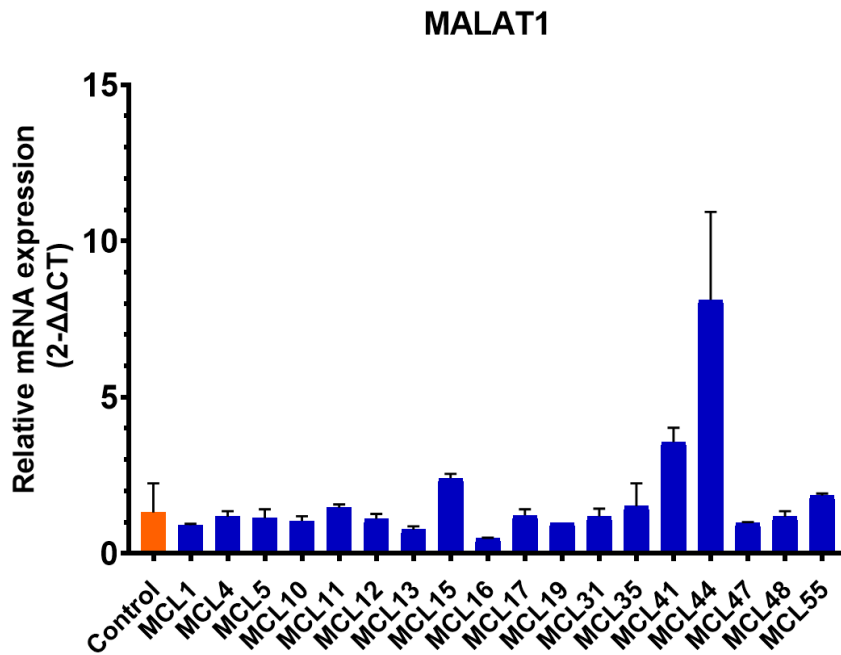


Figure 20: Relative MALAT1 expression in MCL samples (n=18) compared to control samples (n=3)

4.9. Pathway analysis of MCL-related genes

Pathway analysis was conducted to examine whether the most DEmRNA genes are involved in signalling pathways or biological processes that may be related to mantle cell lymphoma. Enrichr tool was used for acquiring significantly enriched GO terms KEGG pathways and Reactome analysis using the differentially expressed upregulated and downregulated mRNA, separately (Kuleshov et al., 2016) (Croft et al., 2014).

Firstly, as input for GO enrichment and KEGG pathway analysis the top 150 significantly upregulated DEmRNAs were used. **Figure 21** depicts the top 10 significantly enriched pathways ranked by p-value, through KEGG analysis. The length of the bar represents the significance of that specific term. In addition, the brighter the color, the more significant that term is. In the KEGG pathway analysis, upregulated DEmRNAs are found to be mostly enriched in “PI3K-Akt signaling pathway” (hsa04151), “Pathways in cancer” (hsa05200) which are known to be related with mantle cell lymphoma and cancer disease itself, respectively (Yu et al., 2018). The other two most significantly enriched pathways were related to cell motility:

“Focal adhesion” (hsa04510) and “ECM-receptor interaction” (hsa04512) which might play a role in cancer cell invasion and metastasis.

KEGG Pathway Analysis

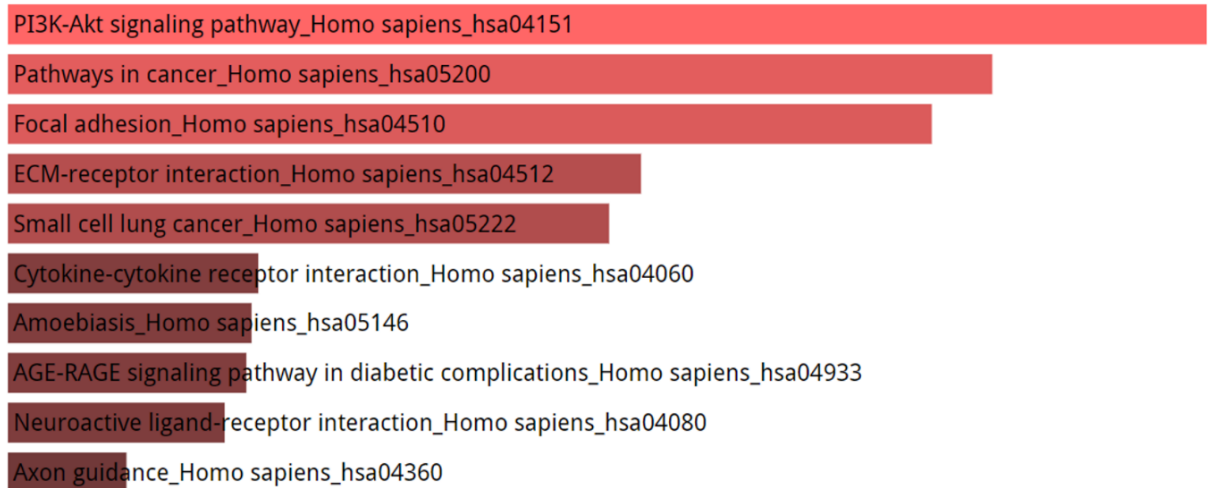
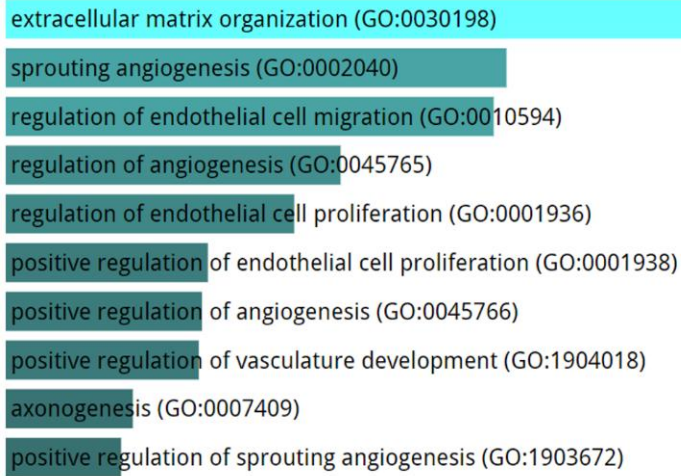


Figure 21: KEGG Pathway analysis of upregulated differentially expressed mRNAs in MCL. The brighter the color of the bar, the more significant that term is ($p < 0.01$).

GO analysis with respect to biological process, the most enriched GO terms of upregulated differentially expressed mRNAs were associated with extracellular matrix (ECM) organization and angiogenesis (**Figure 22A**). For, molecular function integrin binding and the collagen binding were the most enriched GO terms (**Figure 22B**). As for the cellular component, most of the upregulated mRNAs revealed to be associated with the extracellular part. (**Figure 22C**).

A

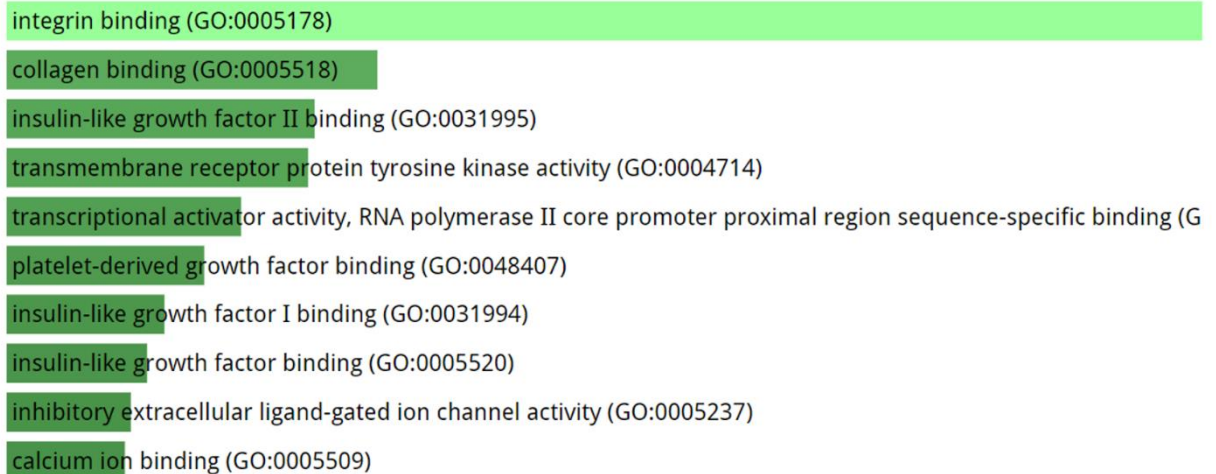
GO Analysis- Biological Process



extracellular matrix organization (GO:0030198)
sprouting angiogenesis (GO:0002040)
regulation of endothelial cell migration (GO:0010594)
regulation of angiogenesis (GO:0045765)
regulation of endothelial cell proliferation (GO:0001936)
positive regulation of endothelial cell proliferation (GO:0001938)
positive regulation of angiogenesis (GO:0045766)
positive regulation of vasculature development (GO:1904018)
axonogenesis (GO:0007409)
positive regulation of sprouting angiogenesis (GO:1903672)

B

GO Analysis- Molecular Function



integrin binding (GO:0005178)
collagen binding (GO:0005518)
insulin-like growth factor II binding (GO:0031995)
transmembrane receptor protein tyrosine kinase activity (GO:0004714)
transcriptional activator activity, RNA polymerase II core promoter proximal region sequence-specific binding (GO:0005518)
platelet-derived growth factor binding (GO:0048407)
insulin-like growth factor I binding (GO:0031994)
insulin-like growth factor binding (GO:0005520)
inhibitory extracellular ligand-gated ion channel activity (GO:0005237)
calcium ion binding (GO:0005509)

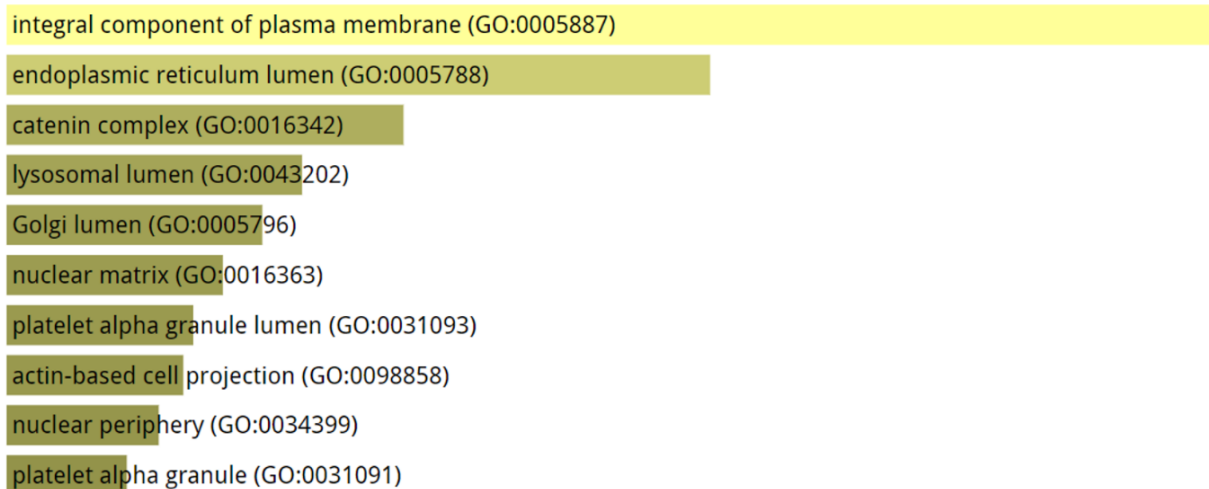
C**GO Analysis- Cellular Component**

Figure 22: Gene Ontology analysis of upregulated differentially expressed mRNAs with the most enriched GO term associated with the biological process (A), molecular function (B), and cellular component (C). The brighter the color of the bar, the more significant that term is ($p < 0.01$).

Pathway analysis of downregulated DEmRNAs

Furthermore, the top 120 significantly downregulated DEmRNAs were used as input for GO enrichment and KEGG pathway analysis. **Figure 23** depicts the top 10 significantly enriched pathways ranked by p-value, through Reactome annotations. The length of the bar represents the significance of that specific term. In addition, the brighter the color, the more significant that term is. In the KEGG pathway analysis, downregulated DEmRNAs are found to be mostly enriched in “Senescence-Associated Secretory Phenotype”, “DNA Damage-Telomere Stress Induced Senescence” and “HDACs deacetylase histones” pathways.

GO analysis with respect to biological process, the most enriched GO terms of downregulated differentially expressed mRNAs were associated with complement activation, classical pathway and humoral immune responses mediated with circulating immunoglobins (**Figure 24A**). For, molecular function serine-type endopeptidase activity and transcriptional repressor activity were the most enriched GO terms (**Figure 24B**). As for the cellular component, most of the upregulated mRNAs revealed to be associated with nuclear chromatin (**Figure 24C**).

Reactome Pathway Analysis

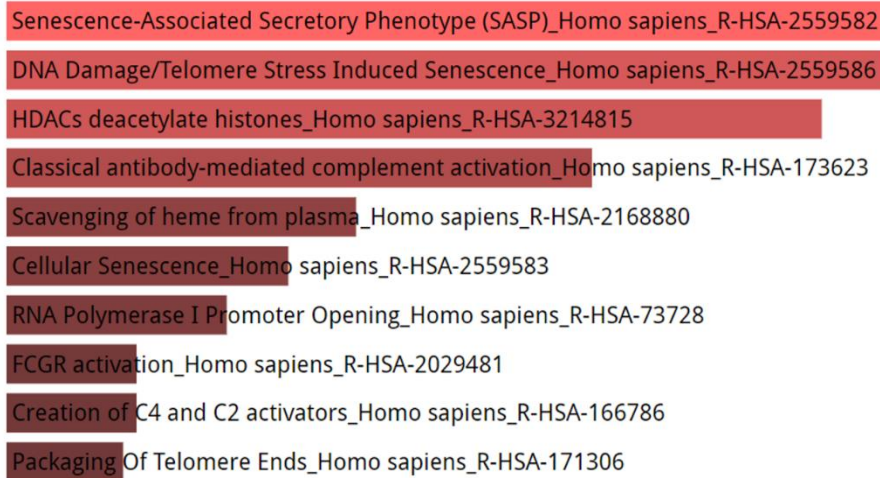
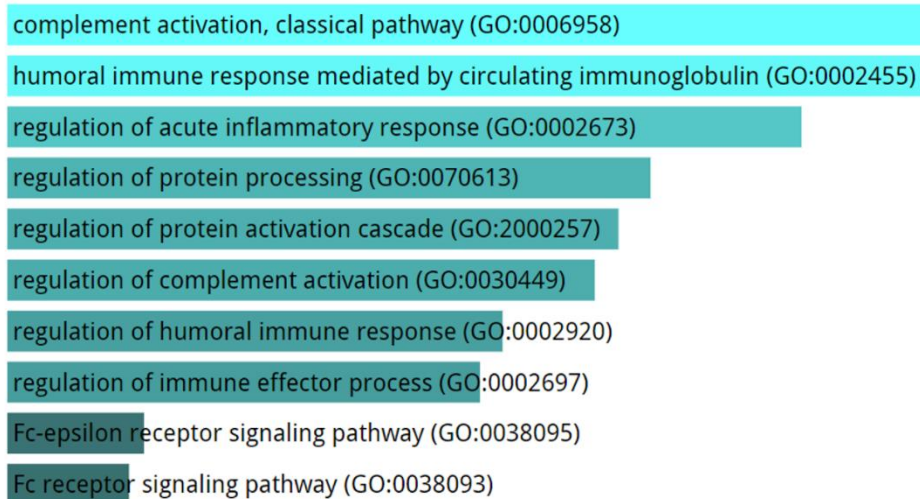


Figure 23: Reactome pathway analysis of downregulated differentially expressed mRNAs in MCL. The brighter the color of the bar, the more significant that term is ($p < 0.01$).

A

GO Analysis- Biological Process



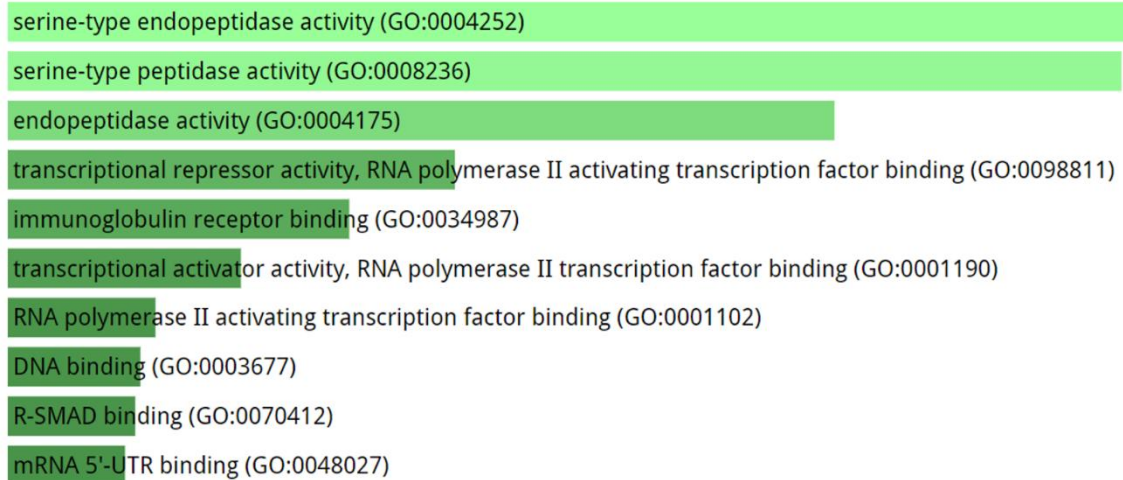
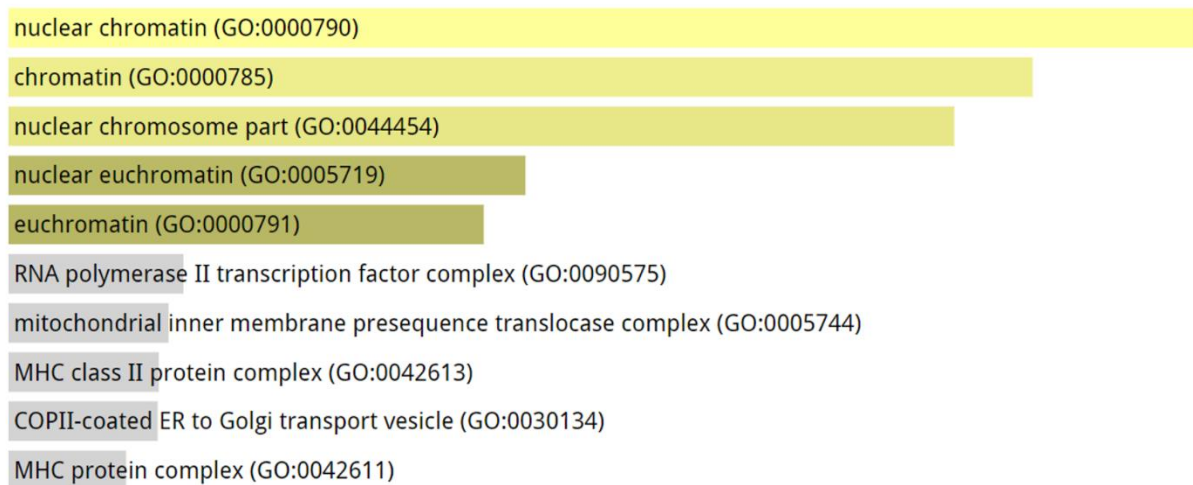
B**GO Analysis- Molecular Function****C****GO Analysis- Cellular Component**

Figure 24: Gene Ontology analysis of downregulated differentially expressed mRNAs with the most enriched GO term associated with the biological process (A), molecular function (B), and cellular component (C). The brighter the color of the bar, the more significant that term is. Only the grey bars indicate p values greater than 0.05.

4.10. ROC and Survival Analysis

To investigate the relationship between irregularly expressed lncRNAs and mRNAs with patient prognosis, survival analysis was performed. At first, the diagnostic value of selected DElncRNAs and DEmRNAs were determined by ROC (Receiver Operating Characteristic) analysis using the FPKM normalized count data of 15 MCL patients.

Four of the top upregulated DElncRNAs (AC010983.1, LINC01268, PWRN2, MAGI1-IT1) which were first shown at Table 8 were chosen and Graphpad Prism 8 (GraphPad Software, Inc, San Diego, CA) was used to conduct ROC analysis. ROC curves of AC010983.1, LINC01268, PWRN2, MAGI1-IT1 lncRNAs are depicted in **Figure 25**. Moreover, the specificity and sensitivity values and other important values are summarized in **Table 11**.

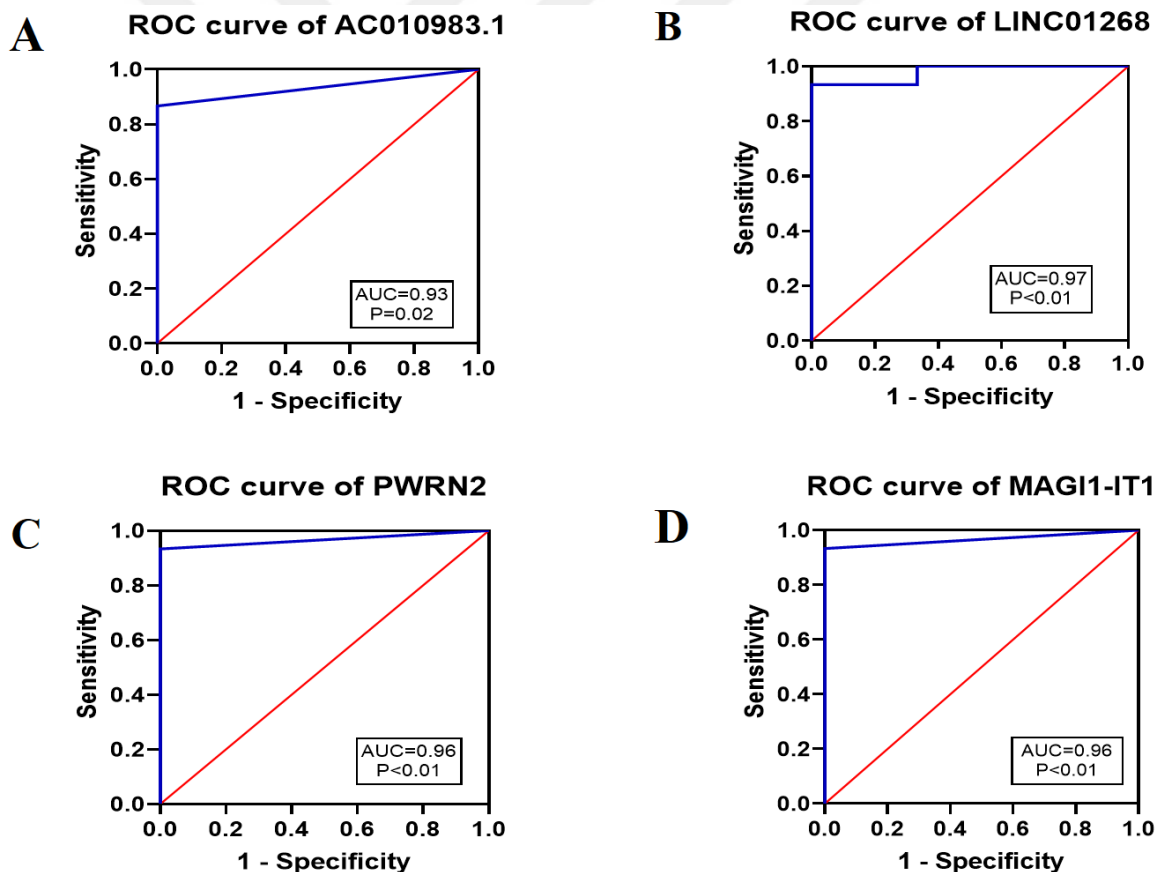


Figure 25: ROC Curves of AC010983.1 (A), LINC01268 (B), PWRN2 (C), MAGI1-IT1 (D) lncRNAs (AUC: area under the ROC curve)

Table 12: Details of the ROC Curve Analysis of Upregulated DElncRNAs

lncRNA	AUC	Cut-off	Sensitivity	Specificity	95% CI	P-value
AC010983.1	0.9333	> 0.8616 FPKM	86.67%	100%	0.8154-1.000	0.0209
LINC01268	0.9778	> 0.07311 FPKM	93.33%	100%	0.9129-1.000	0.0109
PWRN2	0.9667	> 0.01922 FPKM	93.33%	100%	0.8842 to 1.000	0.0129
MAGI1-IT1	0.9667	> 0.05455 FPKM	93.33%	100%	0.8842 to 1.000	0.0129

Abbreviations: AUC: Area under curve; CI: Confidence Interval

Similarly, we also examined the diagnostic value of the three of the upregulated mRNAs (SOX11, EZH2 and IL33) by ROC analysis with again using the FPKM normalized data and by using the Graphpad Prism 8 (GraphPad Software, Inc, San Diego, CA). ROC curves of SOX11, EZH2 and IL33 mRNAs are depicted in **Figure 26**. and the important values of the analysis are depicted in **Table 12**.

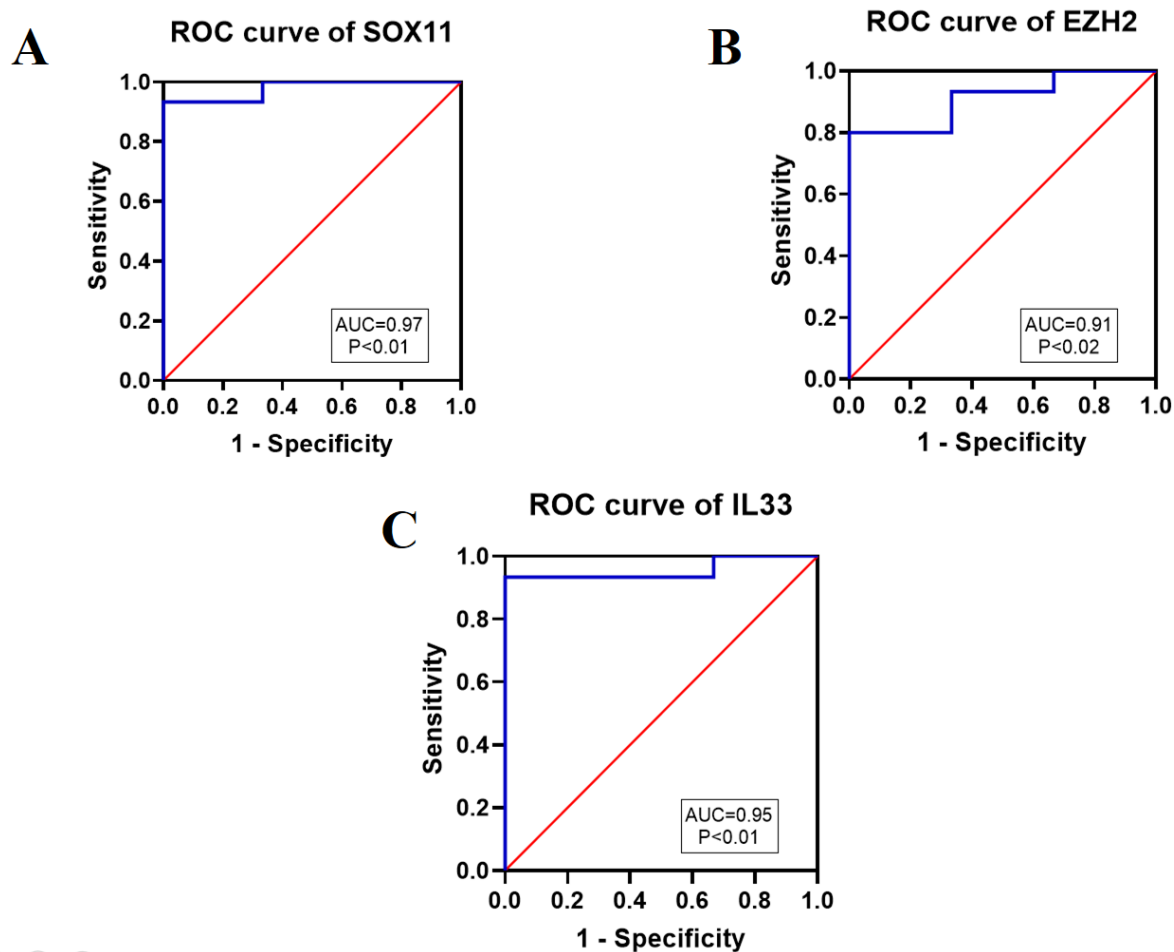


Figure 26: ROC curves of SOX11(A), EZH2 (B), and IL33 (C) mRNAs (AUC: area under the ROC curve)

Table 13: Details of the ROC Curve Analysis of Upregulated DEmRNAs

mRNA	AUC	Cut-off	Sensitivity	Specificity	95% CI	P-value
SOX11	0.9778	> 0.6272	93.33%	100%	0.9129 to 1.000	0.0109
EZH2	0.9111	< 1.952	73.33%	100%	0.7648 to 1.000	0.0284
IL33	0.9556	> 0.3080	93.33%	100%	0.8579 to 1.000	0.0152

Abbreviations: AUC: Area under curve; CI: Confidence Interval

Next, AUC (Area Under Curve), Sensitivity and Specificity of the ROC curves were examined. Based on the calculated cut-off value selected differentially expressed lncRNAs and/or mRNAs were divided into low and high expressed groups. And the prognostic value of the Kaplan–Meier analysis was used to estimate survival curves by Graphpad Prism 8 (GraphPad Software, Inc, San Diego, CA). Figure 27 demonstrates the overall survival curves of AC010983.1 (**Figure 27A**) LINC01268 (**Figure 27B**) PWRN2 (**Figure 27C**) MAGI1-IT1 (**Figure 27D**) lncRNAs. Overall survival curves of SOX11(**Figure 28A**), EZH2 (**Figure 28B**), and IL33 (**Figure 28C**) mRNAs are depicted in Figure 28. The estimated Log-rank (Mantel-Cox) test p values are depicted on the graphs.

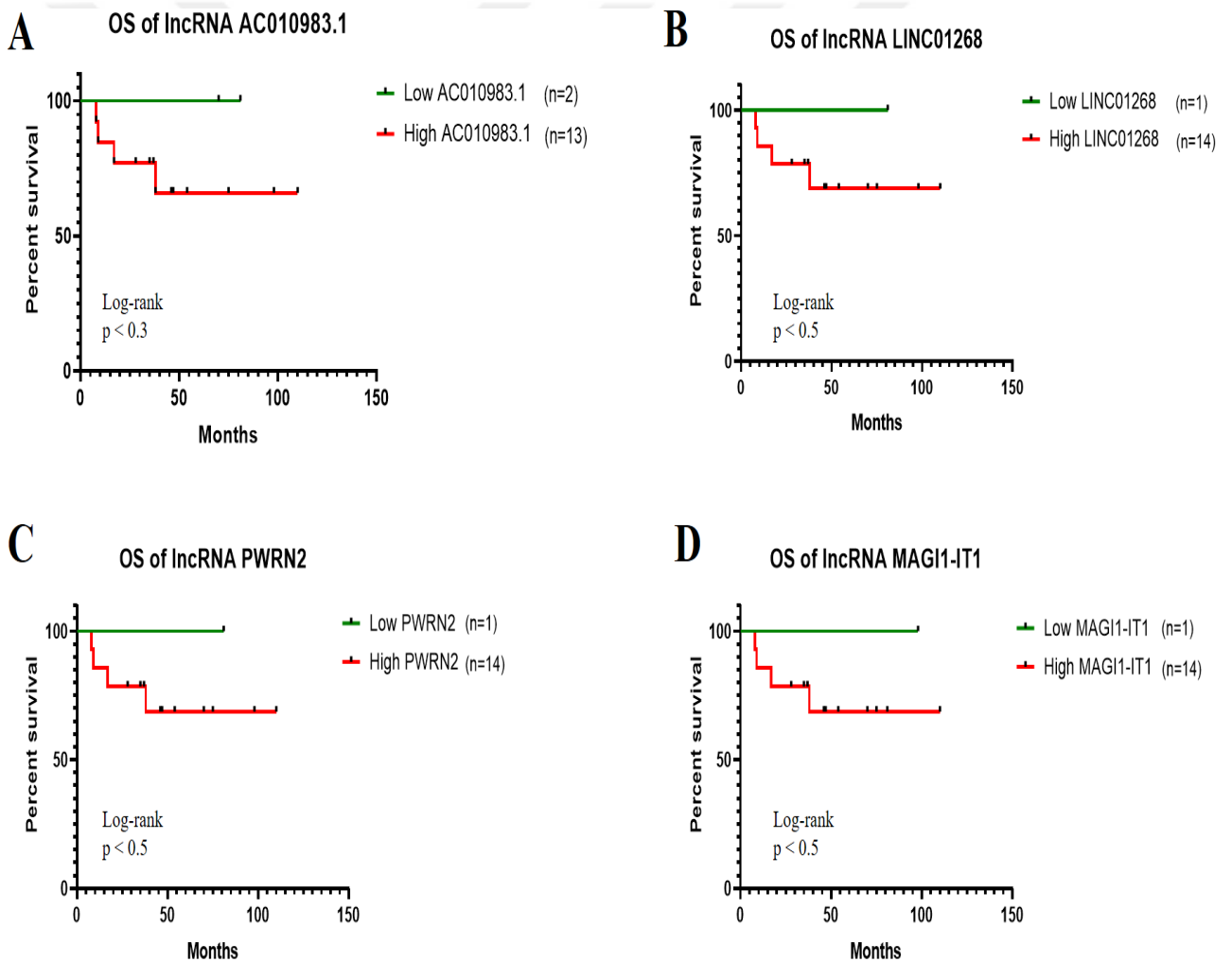


Figure 27: Kaplan Meier graphs of AC010983.1 (**A**) LINC01268 (**B**) PWRN2 (**C**) MAGI1-IT1 (**D**) lncRNAs

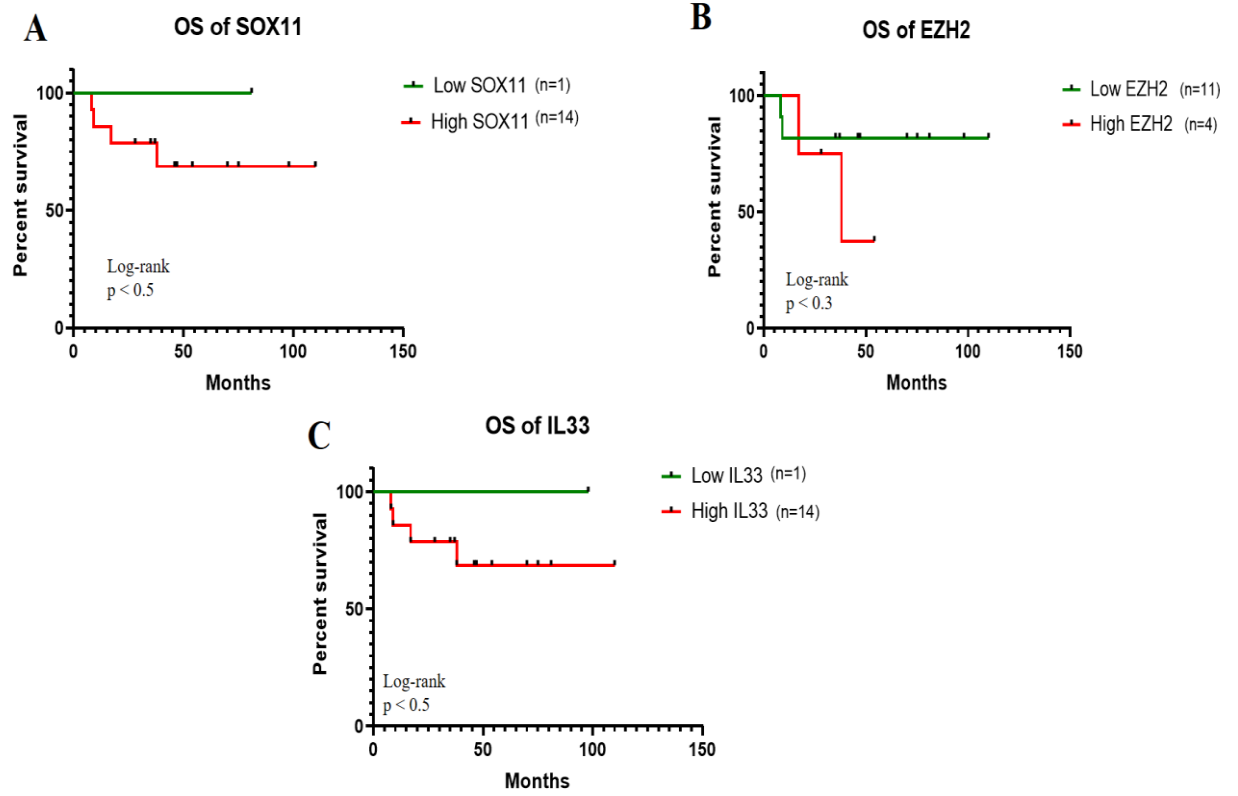


Figure 28: Kaplan Meier graphs of SOX11(A), EZH2 (B), and IL33 (C) mRNAs

5. DISCUSSION

Mantle cell lymphoma (MCL) is a B-cell non-Hodgkin's lymphoma (NHL) which is considered as an incurable lymphoid neoplasm with a continuous relapse pattern and a median survival of only 3-5 years (Jares et al., 2007; Swerdlow et al., 2016). Therefore, there is an urgent need to elucidate the MCL disease pathobiology and identification of novel biomarkers and therapeutic target to optimize the treatment and improve the prognosis of MCL patients (Ahmed et al., 2016). Long noncoding RNAs (lncRNAs) have been shown to involve the development of many cancers and some of them are used as novel biomarkers (Huarte, 2015). However, there are very few reports of lncRNAs that are related to the MCL pathogenesis and prognosis. In this study, we aimed to identify lncRNAs that have the potential to be novel diagnostic, prognostic biomarkers or therapeutic targets in MCL through whole-transcriptome sequencing.

The primary oncogenic event and also the genetic hallmark of MCL is the chromosomal translocation which causes juxtaposition of CCND1 (also known as BCL1), a cell cycle gene at chromosome 11q13 and IgH chain gene at chromosome 14q32. This reciprocal translocation, t(11;14)(q13;q32), is present in more than 90% of the MCL cases and, and leads to constitutive expression of CCND1 gene which is not expressed in normal B cells (Jares et al., 2007; Rosenwald et al., 2003). Our RNA-seq results confirm CCND1 mRNA upregulation in MCL cases compared to naive B cell sample.

In terms of high expression in MCL tumor tissues, the most important gene after CCND1 in the SOX11 gene. SOX11 oncogene is not expressed in normal B cells but upregulated in conventional (cMCL) cases. cMCL is the most common subtype of MCL which follows an aggressive clinical course and generally represent epigenetically naive B cell-like signature (Fernández et al., 2010; Vegliante et al., 2013). When FPKM values of SOX11 mRNA were examined, SOX11 mRNA was upregulated in MCL cases compared to control sample, as for CCND1.

There are few reports of irregularly expressed lncRNAs in MCL cases. In one of these publications, although there were large differences in expression between samples, it was observed that expression of MALAT1 lncRNA was higher than that in normal B cells (X. Wang et al., 2016). When we analyzed whole the transcriptome sequence analysis FPKM data, we did not observe a significant increase in MALAT1 lncRNA expression in MCL cases. However, when we normalize MALAT1 levels to RPS13 or GAPDH levels, it was observed that MALAT1 was higher than reactive tonsil naive B cells. SNHG5 lncRNA was observed to suppress MYC oncoprotein expression in MCL cell lines (Hu et al., 2019). However, a study that analyzes SNHG5 expression in MCL patient tumor samples has not yet been reported. When we examined the whole transcriptome sequence Cufflinks FPKM values, we observed that the expression of SNHG5 lncRNA decreased significantly in MCL cases compared to the NBC sample.

In the KEGG pathway analysis, downregulated DE mRNAs are found to be mostly enriched in “Senescence-Associated Secretory Phenotype”, “DNA Damage-Telore Stress Induced Senescence” and “HDACs deacetylase histones” pathways. GO analysis with respect to biological process, the most enriched GO terms of downregulated differentially expressed mRNAs were associated with complement activation, classical pathway and humoral immune responses mediated with circulating immunoglobins which might suggest a relation with tumors avoiding immune destruction.

Among the top upregulated DE lncRNAs, AC010983.1, LINC01268, PWRN2, MAGI1-IT1 lncRNAs were chosen to conduct ROC. The top differentially upregulated lncRNA was AC010983.1 which previously did not associate with any type of cancer. However, LINC01268 lncRNA was related to glioma malignancy (Matjasic, Popovic, Matos, & Glavac, 2017). Huang et al showed that Prader-Willi region non-protein-coding RNA 2 (PWRN2) was up-regulated in the patients with polycystic ovary syndrome (Huang, Hao, Bao, Wang, & Dai, 2016). MAGI1-IT1 lncRNA promoted the invasion and metastasis of epithelial ovarian cancer (Gao et al., 2019). ROC is a probability curve and AUC represents the degree or measure of separability. It tells how much model is capable of distinguishing between classes. Then, we evaluated the area under curve (AUC) value which represents degree or measure of separability and found a high separation value (more than 0.9) for all selected transcripts.

Similarly, we also examined the diagnostic value of the three of the upregulated mRNAs (SOX11, EZH2 and IL33) by ROC analysis. SOX11 and EZH2 association with MCL were already well-founded in the literature (Queirós et al., 2016; X. Wang et al., 2016). However, there is not yet a study that shows the relation of interleukin 33 (IL33) gene with MCL. Besides, the pro-tumorigenic effect of IL33 gene with many types of cancers was shown including colorectal cancer (Cui et al., 2018), hepatocellular carcinoma (P. Zhang et al., 2012) and glioma (J. Zhang, Wang, Ji, Ding, & Lu, 2017). AUC values found to be high. Based on the calculated cut-off value selected differentially expressed lncRNAs and/or mRNAs were divided into low and high expressed groups. And the prognostic value of the Kaplan–Meier analysis was used to estimate survival curves. Despite a high diagnostic test value, and disposition of overexpressed transcripts with inferior survival the estimated Log-rank (Mantel-Cox) test of selected transcripts were not significant ($P > 0.05$) which might be explained by the low sample number ($n=15$).

In summary, our present study showed the potent value of significantly differentially expressed lncRNAs and mRNAs on MCL patient prognosis. With an increase of sample number and further functional analysis may shed light on the prognostic, diagnostic and therapeutic biomarker potential of lncRNAs in MCL.

6. CONCLUSION AND FUTURE ASPECTS

As a conclusion, we identified a total of 1149 significantly DElncRNAs of which 322 of lncRNAs upregulated and 827 of lncRNAs downregulated in MCL. Among DEmRNAs 2924 of mRNAs upregulated and 1351 of mRNAs downregulated. GO and KEGG analysis indicated that upregulated mRNAs were mainly involved in angiogenesis and pathways in cancer. We analyzed the SNHG5 expression in MCL patient tumor samples which has not yet been reported, before. We examined the diagnostic value of differentially expressed AC010983.1, LINC01268, PWRN2, MAGI1-IT1 lncRNAs and SOX11, EZH2 and IL33 mRNAs. Despite a high AUC value of selected transcripts, according to the log-rank test of Kaplan Meier curves, P-value was not significant ($P > 0.05$). However, our present study showed the potential value of significantly differentially expressed lncRNAs and mRNAs on MCL patient prognosis. Therefore, we suggest that the prognostic, diagnostic and therapeutic values of selected differentially expressed transcripts should be further investigated with functional assays and also improved in silico analysis.

7. REFERENCES

- Abbas, Abul K, Lichtman, Andrew H, Pillai, S. (2018). *Celular and Molecular Immunology. Ninth Edition*. Retrieved from <http://weekly.cnbnews.com/news/article.html?no=124000>
- Ahmed, M., Zhang, L., Nomie, K., Lam, L., & Wang, M. (2016). Gene mutations and actionable genetic lesions in mantle cell lymphoma. *Oncotarget*, 7(36), 58638–58648. <https://doi.org/10.18632/oncotarget.10716>
- Andrews, S. (2010). *FastQC: a quality control tool for high throughput sequence data*. Babraham Bioinformatics, Babraham Institute, Cambridge, United Kingdom.
- Antica, M., Paradzik, M., Novak, S., Dzebro, S., & Dominis, M. (2010). Gene expression in formalin-fixed paraffin-embedded lymph nodes. *Journal of Immunological Methods*, 359(1–2), 42–46. <https://doi.org/10.1016/j.jim.2010.05.010>
- Bea, S., Valdes-Mas, R., Navarro, A., Salaverria, I., Martin-Garcia, D., Jares, P., ... Campo, E. (2013). Landscape of somatic mutations and clonal evolution in mantle cell lymphoma. *Proceedings of the National Academy of Sciences*, 110(45), 18250–18255. <https://doi.org/10.1073/pnas.1314608110>
- Belder, N., Coskun, Ö., Doganay Erdogan, B., Ilk, O., Savas, B., Ensari, A., & Özdağ, H. (2016). From RNA isolation to microarray analysis: Comparison of methods in FFPE tissues. *Pathology Research and Practice*, 212(8), 678–685. <https://doi.org/10.1016/j.prp.2015.11.008>
- Bertoni, F., & Ponzoni, M. (2007). The cellular origin of mantle cell lymphoma. *International Journal of Biochemistry and Cell Biology*, 39(10), 1747–1753. <https://doi.org/10.1016/j.biocel.2007.04.026>
- Blankenberg, D., Gordon, A., Von Kuster, G., Coraor, N., Taylor, J., Nekrutenko, A., & Team, G. (2010). Manipulation of FASTQ data with galaxy. *Bioinformatics*, 26(14), 1783–1785. <https://doi.org/10.1093/bioinformatics/btq281>
- Bohmann, K., Hennig, G., Rogel, U., Poremba, C., Mueller, B. M., Fritz, P., ... Schaefer, K. L. (2009). RNA extraction from archival formalin-fixed paraffin-embedded tissue: A comparison of manual, semiautomated, and fully automated purification methods. *Clinical Chemistry*, 55(9), 1719–1727. <https://doi.org/10.1373/clinchem.2008.122572>
- Bowzyk Al-Naeeb, A., Ajithkumar, T., Behan, S., & Hodson, D. J. (2018). Non-Hodgkin lymphoma. *BMJ (Online)*, 362(August), 1–7. <https://doi.org/10.1136/bmj.k3204>
- Campo, E. (2014). Mantle Cell Lymphoma Elías. *Hematopathology Section, Department of Anatomic Pathology*, (1), 1–5. <https://doi.org/10.1007/s13398-014-0173-7.2>
- Cheah, C. Y., Gairdner, C., Wang, M. L., & Seymour, J. F. (2016). JOURNAL OF CLINICAL ONCOLOGY Mantle Cell Lymphoma. *J Clin Oncol*, 34(11), 1256–1269. <https://doi.org/10.1200/JCO.2015.63.5904>
- Cortelazzo, S., Ponzoni, M., Ferreri, A. J. M., & Dreyling, M. (2012). Mantle cell lymphoma. *Critical Reviews in Oncology/Hematology*, 82(1), 78–101. <https://doi.org/10.1016/j.critrevonc.2011.05.001>

- Cossarizza, A., Chang, H. D., Radbruch, A., Akdis, M., Andrä, I., Annunziato, F., ... Zimmermann, J. (2017). Guidelines for the use of flow cytometry and cell sorting in immunological studies. *European Journal of Immunology*, 47(10), 1584–1797. <https://doi.org/10.1002/eji.201646632>
- Croft, D., Mundo, A. F., Haw, R., Milacic, M., Weiser, J., Wu, G., ... D'Eustachio, P. (2014). The Reactome pathway knowledgebase. *Nucleic Acids Research*, 42(D1), 472–477. <https://doi.org/10.1093/nar/gkt1102>
- Cui, G., Yuan, A., Pang, Z., Zheng, W., Li, Z., & Goll, R. (2018). Contribution of IL-33 to the pathogenesis of colorectal cancer. *Frontiers in Oncology*, 8(NOV), 1–8. <https://doi.org/10.3389/fonc.2018.00561>
- De Silva, N. S., & Klein, U. (2015). Dynamics of B cells in germinal centres. *Nature Reviews Immunology*, 15(3), 137–148. <https://doi.org/10.1038/nri3804>
- Deben, C., Zwaenepoel, K., Boeckx, C., Wouters, A., Pauwels, P., Peeters, M., ... Deschoolmeester, V. (2013). Expression Analysis on Archival Material Revisited. *Diagnostic Molecular Pathology*, 22(1), 59–64. <https://doi.org/10.1097/pdm.0b013e318269de3b>
- Del Fabbro, C., Scalabrin, S., Morgante, M., & Giorgi, F. M. (2013). An Extensive Evaluation of Read Trimming Effects on Illumina NGS Data Analysis. *PLOS ONE*, 8(12), e85024. Retrieved from <https://doi.org/10.1371/journal.pone.0085024>
- Dreyling, M., Kluin-Nelemans, H. C., Beà, S., Hartmann, E., Salaverria, I., Hutter, G., ... Hoster, E. (2011). Update on the molecular pathogenesis and clinical treatment of mantle cell lymphoma: report of the 10th annual conference of the European Mantle Cell Lymphoma Network. *Leukemia & Lymphoma*, 52(12), 2226–2236. <https://doi.org/10.3109/10428194.2011.600488>
- E., H., M., D., W., K., C., G., A., V. H., H.C., K.-N., ... M., U. (2008). A new prognostic index (MIPI) for patients with advanced-stage mantle cell lymphoma. *Blood*, 111(2), 558–565. <https://doi.org/10.1182/blood-2007-06-095331> LK - http://emory-primoprod.hosted.exlibrisgroup.com/openurl/01EMORY/01EMORY_services_page?sid=EMBASE&issn=00064971&id=doi:10.1182%2Fblood-2007-06-095331&atitle=A+new+prognostic+index+%28MIPI%29+for+patients+with+advanced-stage+mantle+cell+lymphoma&stitle=Blood&title=Blood&volume=111&issue=2&spage=558&epage=565&aualast=Hoster&aufirst=Eva&aunit=E.&aufull=Hoster+E.&coden=BLOOA&isbn=&pages=558-565&date=2008&aunit1=E&aunitm=
- Efron, B. (1988). Logistic Regression, Survival Analysis, and the Kaplan-Meier Curve. *Journal of the American Statistical Association*, 83(402), 414–425. <https://doi.org/10.1080/01621459.1988.10478612>
- Evans, L. S., & Hancock, B. W. (2003). *Non-Hodgkin lymphoma*. 362, 139–146.
- Ewels, P., Magnusson, M., Lundin, S., & Käller, M. (2016). MultiQC: Summarize analysis results for multiple tools and samples in a single report. *Bioinformatics*, 32(19), 3047–3048. <https://doi.org/10.1093/bioinformatics/btw354>
- Ewing, B., & Green, P. (1998). Base-Calling of Automated Sequencer Traces Using Phred. II. Error Probabilities. *Genome Research*, 8(3), 186–194. <https://doi.org/10.1101/gr.8.3.186>

- Fan, Z., Wang, X., Li, P., Mei, C., Zhang, M., & Zhao, C. (2019). Overexpression of lncRNA GATA6-AS inhibits cancer cell proliferation in mantle cell lymphoma by downregulating GLUT1. *Oncology Letters*, 2443–2447. <https://doi.org/10.3892/ol.2019.10540>
- Fernández, V., Salamero, O., Espinet, B., Solé, F., Royo, C., Navarro, A., ... Campo, E. (2010). Genomic and gene expression profiling defines indolent forms of mantle cell lymphoma. *Cancer Research*, 70(4), 1408–1418. <https://doi.org/10.1158/0008-5472.CAN-09-3419>
- Galy, A., Travis, M., Cen, D., & Chen, B. (1995). Human T, B, natural killer, and dendritic cells arise from a common bone marrow progenitor cell subset. *Immunity*, 3(4), 459–473. [https://doi.org/10.1016/1074-7613\(95\)90175-2](https://doi.org/10.1016/1074-7613(95)90175-2)
- Gao, H., Li, X., Zhan, G., Zhu, Y., Yu, J., Wang, J., ... Guo, X. (2019). Long noncoding RNA MAGI1-IT1 promoted invasion and metastasis of epithelial ovarian cancer via the miR-200a/ZEB axis. *Cell Cycle*, 18(12), 1393–1406. <https://doi.org/10.1080/15384101.2019.1618121>
- Goecks, J., Nekrutenko, A., Taylor, J., & The Galaxy Team. (2010). Galaxy: a comprehensive approach for supporting accessible, reproducible, and transparent computation research in the life sciences. *Genome Biol*, 11(8), R86.
- Hanahan, D., & Weinberg, R. A. (2011). Hallmarks of cancer: The next generation. *Cell*, 144(5), 646–674. <https://doi.org/10.1016/j.cell.2011.02.013>
- Hess, C., Wardemann, H., Ehlers, M., Hess, C., Winkler, A., Lorenz, A. K., ... Ehlers, M. (2013). *Google-Ergebnis für* <http://www.impactaging.com/papers/v4/n6/full/100465/Figure3.jpg>. 123(9), 3788–3796. <https://doi.org/10.1172/JCI65938.3788>
- Hoster, E. (2011). Prognostic Relevance of Clinical Risk Factors in Mantle Cell Lymphoma. *Seminars in Hematology*, 48(3), 185–188. <https://doi.org/10.1053/j.seminhematol.2011.06.001>
- Hou, Z., Jiang, P., Swanson, S. A., Elwell, A. L., Nguyen, B. K. S., Bolin, J. M., ... Thomson, J. A. (2015). A cost-effective RNA sequencing protocol for large-scale gene expression studies. *Scientific Reports*, 5, 1–5. <https://doi.org/10.1038/srep09570>
- Hu, G., Gupta, S. K., Troska, T. P., Nair, A., & Gupta, M. (2017). Long non-coding RNA profile in mantle cell lymphoma identifies a functional lncRNA ROR1-AS1 associated with EZH2/PRC2 complex. *Oncotarget*, 8(46), 80223–80234. <https://doi.org/10.18632/oncotarget.17956>
- Hu, G., Zhang, Y., & Gupta, M. (2019). RIP sequencing in mantle cell lymphoma identifies functional long non-coding RNAs associated with translation machinery. *Blood Cancer Journal*, 9(8), 10–13. <https://doi.org/10.1038/s41408-019-0216-6>
- Huang, X., Hao, C., Bao, H., Wang, M., & Dai, H. (2016). Aberrant expression of long noncoding RNAs in cumulus cells isolated from PCOS patients. *Journal of Assisted Reproduction and Genetics*, 33(1), 111–121. <https://doi.org/10.1007/s10815-015-0630-z>
- Huarte, M. (2015). The emerging role of lncRNAs in cancer. *Nature Medicine*, 21(11), 1253–

1261. <https://doi.org/10.1038/nm.3981>

- Inamdar, A. A., Goy, A., Ayoub, N. M., Attia, C., Oton, L., Taruvai, V., ... Suh, K. S. (2016). Mantle cell lymphoma in the era of precision medicine-diagnosis, biomarkers and therapeutic agents. *Oncotarget*, 7(30), 48692–48731. <https://doi.org/10.18632/oncotarget.8961>
- Iqbal, J., Shen, Y., Liu, Y., Fu, K., Jaffe, E. S., Liu, C., ... Chan, W. C. (2012). Genome-wide miRNA profiling of mantle cell lymphoma reveals a distinct subgroup with poor prognosis. *Blood*, 119(21), 4939–4948. <https://doi.org/10.1182/blood-2011-07-370122>
- Jares, P., Colomer, D., & Campo, E. (2007). Genetic and molecular pathogenesis of mantle cell lymphoma: Perspectives for new targeted therapeutics. *Nature Reviews Cancer*, 7(10), 750–762. <https://doi.org/10.1038/nrc2230>
- Jares, P., Colomer, D., & Campo, E. (2012). Review series Molecular pathogenesis of mantle cell lymphoma. *Jci*, 122(10). <https://doi.org/10.1172/JCI61272.3416>
- Jiang, M., Bennani, N. N., & Feldman, A. L. (2017). Lymphoma classification update: B-cell non-Hodgkin lymphomas. *Expert Review of Hematology*, 10(5), 405–415. <https://doi.org/10.1080/17474086.2017.1318053>
- Kim, D., Langmead, B., & Salzberg, S. L. (2015). HISAT: a fast spliced aligner with low memory requirements. *Nature Methods*, 12, 357. Retrieved from <https://doi.org/10.1038/nmeth.3317>
- Klein, U., & Dalla-Favera, R. (2008). Germinal centres: Role in B-cell physiology and malignancy. *Nature Reviews Immunology*, 8(1), 22–33. <https://doi.org/10.1038/nri2217>
- Kridel, R., Meissner, B., Rogic, S., Boyle, M., Telenius, A., Woolcock, B., ... Gascoyne, R. D. (2012). Plenary paper Whole transcriptome sequencing reveals recurrent NOTCH1 mutations in mantle cell lymphoma. *Blood*, 119(9), 1963–1971. <https://doi.org/10.1182/blood-2011-11-391474>.
- Kridel, R., Meissner, B., Rogic, S., Boyle, M., Telenius, A., Woolcock, B., ... Gascoyne, R. D. (2012). Whole transcriptome sequencing reveals recurrent NOTCH1 mutations in mantle cell lymphoma. *Blood*, 119(9), 1963–1971. <https://doi.org/10.1182/blood-2011-11-391474>
- Kuleshov, M. V., Jones, M. R., Rouillard, A. D., Fernandez, N. F., Duan, Q., Wang, Z., ... Ma'ayan, A. (2016). Enrichr: a comprehensive gene set enrichment analysis web server 2016 update. *Nucleic Acids Research*, 44(W1), W90–W97. <https://doi.org/10.1093/nar/gkw377>
- Küppers, R. (2005). Mechanisms of B-cell lymphoma pathogenesis. *Nature Reviews Cancer*, 5(4), 251–262. <https://doi.org/10.1038/nrc1589>
- Lebien, T. W. (2000). *Review article Fates of human B-cell precursors*. 96(1), 9–23.
- Lebien, T. W., Thomas, *, & Tedder, F. (2008). *B lymphocytes: how they develop and function*. <https://doi.org/10.1182/blood>
- Leshchenko, V. V., Kuo, P. Y., Shaknovich, R., Yang, D. T., Gellen, T., Petrich, A., ... Parekh, S. (2010). Genomewide DNA methylation analysis reveals novel targets for drug

- development in mantle cell lymphoma. *Blood*, *116*(7), 1025–1034.
<https://doi.org/10.1182/blood-2009-12-257485>
- Levin, J. Z., Yassour, M., Adiconis, X., Nusbaum, C., Thompson, D. A., Friedman, N., ... Regev, A. (2010). Comprehensive comparative analysis of strand-specific RNA sequencing methods. *Nature Methods*, *7*(9), 709–715.
<https://doi.org/10.1038/nmeth.1491>
- Li, X., Nair, A., Wang, S., & Wang, L. (2015). Quality control of RNA-seq experiments. In *RNA Bioinformatics* (pp. 137–146). Springer.
- Liao, Y., Smyth, G. K., & Shi, W. (2014). FeatureCounts: An efficient general purpose program for assigning sequence reads to genomic features. *Bioinformatics*, *30*(7), 923–930. <https://doi.org/10.1093/bioinformatics/btt656>
- Love, M. I., Huber, W., & Anders, S. (2014). Moderated estimation of fold change and dispersion for RNA-seq data with DESeq2. *Genome Biology*, *15*(12), 1–21.
<https://doi.org/10.1186/s13059-014-0550-8>
- Luckey, C. J., Bhattacharya, D., Goldrath, A. W., Weissman, I. L., Benoist, C., & Mathis, D. (2006). *Memory T and memory B cells share a transcriptional program of self-renewal with long-term hematopoietic stem cells.*
- Matjasic, A., Popovic, M., Matos, B., & Glavac, D. (2017). Expression of LOC285758, a Potential Long Non-coding Biomarker, is Methylation-dependent and Correlates with Glioma Malignancy Grade. *Radiology and Oncology*, *51*(3), 331–341.
<https://doi.org/10.1515/raon-2017-0004>
- Matthias, P., & Rolink, A. G. (2005). Transcriptional networks in developing and mature B cells. *Nature Reviews Immunology*, *5*(6), 497–508. <https://doi.org/10.1038/nri1633>
- Mbandi, S., Hesse, U., Rees, D. J., & Christoffels, A. (2014). A glance at quality score: implication for de novo transcriptome reconstruction of Illumina reads . *Frontiers in Genetics* , Vol. 5, p. 17. Retrieved from
<https://www.frontiersin.org/article/10.3389/fgene.2014.00017>
- Menke, J. R., Vasmatazis, G., Murphy, S., Yang, L., Menke, D. M., Tun, H. W., ... Sukov, W. R. (2017). Mantle cell lymphoma with a novel t(11;12)(q13;p11.2): a proposed alternative mechanism of CCND1 up-regulation. *Human Pathology*, *64*, 207–212.
<https://doi.org/10.1016/j.humpath.2017.01.001>
- Mesin, L., Ersching, J., & Victora, G. D. (2016, September 20). Germinal Center B Cell Dynamics. *Immunity*, Vol. 45, pp. 471–482.
<https://doi.org/10.1016/j.immuni.2016.09.001>
- Mills, K. D., Ferguson, D. O., & Alt, F. W. (2003). The role of DNA breaks in genomic instability and tumorigenesis. *Immunological Reviews*, *194*, 77–95.
<https://doi.org/10.1034/j.1600-065x.2003.00060.x>
- Morton, L. M., Turner, J. J., Cerhan, J. R., Linet, M. S., Treseler, P. A., Clarke, C. A., ... Weisenburger, D. D. (2007). Proposed classification of lymphoid neoplasms for epidemiologic research from the Pathology Working Group of the International Lymphoma Epidemiology Consortium (InterLymph). *Blood*, *110*(2), 695–708.

<https://doi.org/10.1182/blood-2006-11-051672>

- Mu, G., Liu, Q., Wu, S., Xia, Y., & Fang, Q. (2019). Long noncoding RNA HAGLROS promotes the process of mantle cell lymphoma by regulating miR-100/ATG5 axis and involving in PI3K/AKT/mTOR signal. *Artificial Cells, Nanomedicine, and Biotechnology*, 47(1), 3649–3656. <https://doi.org/10.1080/21691401.2019.1645151>
- Nakamura, K., Oshima, T., Morimoto, T., Ikeda, S., Yoshikawa, H., Shiwa, Y., ... Kanaya, S. (2011). Sequence-specific error profile of Illumina sequencers. *Nucleic Acids Research*, 39(13), e90–e90. <https://doi.org/10.1093/nar/gkr344>
- Navarro, A., Clot, G., Prieto, M., Royo, C., Vegliante, M. C., Amador, V., ... Hernández, L. (2013). MicroRNA expression profiles identify subtypes of mantle cell lymphoma with different clinicobiological characteristics. *Clinical Cancer Research*, 19(12), 3121–3129. <https://doi.org/10.1158/1078-0432.CCR-12-3077>
- Nemazee, D. (2006). Receptor editing in lymphocyte development and central tolerance. *Nature Reviews Immunology*, 6(10), 728–740. <https://doi.org/10.1038/nri1939>
- Nodit, L., Bahler, D. W., Jacobs, S. A., Locker, J., & Swerdlow, S. H. (2003). Indolent Mantle Cell Lymphoma With Nodal Involvement and Mutated Immunoglobulin Heavy Chain Genes. *Human Pathology*, 34(10), 1030–1034. [https://doi.org/10.1053/S0046-8177\(03\)00410-6](https://doi.org/10.1053/S0046-8177(03)00410-6)
- Pelanda, R., & Torres, R. M. (2012). Central B-cell tolerance: where selection begins. *Cold Spring Harbor Perspectives in Biology*, 4(4), a007146. <https://doi.org/10.1101/cshperspect.a007146>
- Punt, J., Stranford, S., Jones, P., & Owen, J. (2018). *Kuby immunology*. Macmillan Higher Education.
- Queirós, A. C., Beekman, R., Vilarrasa-Blasi, R., Duran-Ferrer, M., Clot, G., Merkel, A., ... Martín-Subero, J. I. (2016). Decoding the DNA Methylome of Mantle Cell Lymphoma in the Light of the Entire B Cell Lineage. *Cancer Cell*, 30(5), 806–821. <https://doi.org/10.1016/j.ccell.2016.09.014>
- Recaldin, T., & Fear, D. J. (2016). Transcription factors regulating B cell fate in the germinal centre. *Clinical and Experimental Immunology*, 183(1), 65–75. <https://doi.org/10.1111/cei.12702>
- Rolink, A., & Melchers, F. (1991). *Molecular and Cellular Origins of B Lymphocyte Diver* & 66, 1081–1094.
- Rosenwald, A., Wright, G., Wiestner, A., Chan, W. C., Connors, J. M., Campo, E., ... Staudt, L. M. (2003). The proliferation gene expression signature is a quantitative integrator of oncogenic events that predicts survival in mantle cell lymphoma. *Cancer Cell*, 3(2), 185–197. [https://doi.org/10.1016/S1535-6108\(03\)00028-X](https://doi.org/10.1016/S1535-6108(03)00028-X)
- Royo, C., Navarro, A., Clot, G., Salaverria, I., Giné, E., Jares, P., ... Beà, S. (2012). Non-nodal type of mantle cell lymphoma is a specific biological and clinical subgroup of the disease. *Leukemia*, 26(8), 1895–1898. <https://doi.org/10.1038/leu.2012.72>
- Schatz, D. G., & Ji, Y. (2011). Recombination centres and the orchestration of V(D)J recombination. *Nature Reviews Immunology*, 11(4), 251–263.

<https://doi.org/10.1038/nri2941>

- Schmitt, A. M., & Chang, H. Y. (2016). Long Noncoding RNAs in Cancer Pathways. *Cancer Cell*, 29(4), 452–463. <https://doi.org/10.1016/j.ccell.2016.03.010>
- Shankland, K. R., Armitage, J. O., & Hancock, B. W. (2012). Linfoma : Causas, sintomas, tratamientos. *The Lancet*, 380(9844), 848–857. [https://doi.org/10.1016/S0140-6736\(12\)60605-9](https://doi.org/10.1016/S0140-6736(12)60605-9)
- Shen, Y., Iqbal, J., Xiao, L., Lynch, R. C., Rosenwald, A., Staudt, L. M., ... Chan, W. C. (2004). Distinct gene expression profiles in different B-cell compartments in human peripheral lymphoid organs. *BMC Immunology*, 5. <https://doi.org/10.1186/1471-2172-5-20>
- Song, S., & Matthias, P. D. (2018, September 5). The transcriptional regulation of germinal center formation. *Frontiers in Immunology*, Vol. 9. <https://doi.org/10.3389/fimmu.2018.02026>
- Swerdlow, S. H., Campo, E., Pileri, S. A., Harris, N. L., Stein, H., Siebert, R., ... Jaffe, E. S. (2016). The 2016 revision of the World Health Organization classification of lymphoid neoplasms. *Blood*, 127(20), 2375–2391. <https://doi.org/10.1182/blood-2016-01-643569>.The
- Swerdlow, S. H., Campo, E., Pileri, S. A., Harris, N. L., Stein, H., Siebert, R., ... Jaffe, E. S. (2017). 2016 WHO Classification of lymphoid neoplasms. *The Blood Journal*, 127(20), 453–462. <https://doi.org/10.1182/blood-2016-01-643569>.The
- Teras, L. R., DeSantis, C. E., Cerhan, J. R., Morton, L. M., Jemal, A., & Flowers, C. R. (2016). 2016 US lymphoid malignancy statistics by World Health Organization subtypes. *CA: A Cancer Journal for Clinicians*, 66(6), 443–459. <https://doi.org/10.3322/caac.21357>
- Trapnell, C., Pachter, L., & Salzberg, S. L. (2009). TopHat: Discovering splice junctions with RNA-Seq. *Bioinformatics*, 25(9), 1105–1111. <https://doi.org/10.1093/bioinformatics/btp120>
- Tung, J. W., Parks, D. R., Moore, W. A., Herzenberg, L. A., & Herzenberg, L. A. (2004). New approaches to fluorescence compensation and visualization of FACS data. *Clinical Immunology*, 110(3), 277–283. <https://doi.org/10.1016/j.clim.2003.11.016>
- Vegliante, M. C., Palomero, J., Pérez-Galán, P., Roué, G., Castellano, G., Navarro, A., ... Amador, V. (2013). SOX11 regulates PAX5 expression and blocks terminal B-cell differentiation in aggressive mantle cell lymphoma. *Blood*, 121(12), 2175–2185. <https://doi.org/10.1182/blood-2012-06-438937>
- Veloza, L., Ribera-Cortada, I., & Campo, E. (2019). Mantle cell lymphoma pathology update in the 2016 WHO classification. *Annals of Lymphoma*, 3(cMCL), 3–3. <https://doi.org/10.21037/aol.2019.03.01>
- Victoria, G. D., Dominguez-Sola, D., Holmes, A. B., Deroubaix, S., Dalla-Favera, R., & Nussenzweig, M. C. (2012). Identification of human germinal center light and dark zone cells and their relationship to human B-cell lymphomas. *Blood*, 120(11), 2240–2248. <https://doi.org/10.1182/blood-2012-03-415380>

- von Ahlfen, S., Missel, A., Bendrat, K., & Schlumpberger, M. (2007). Determinants of RNA quality from FFPE samples. *PLoS ONE*, 2(12), 1–7. <https://doi.org/10.1371/journal.pone.0001261>
- Vos, Q., Lees, A., Wu, Z. Q., Snapper, C. M., & Mond, J. J. (2000). B-cell activation by T-cell-independent type 2 antigens as an integral part of the humoral immune response to pathogenic microorganisms. *Immunological Reviews*, 176, 154–170. <https://doi.org/10.1034/j.1600-065X.2000.00607.x>
- Vose, J. M. (2017). Mantle cell lymphoma: 2017 update on diagnosis, risk-stratification, and clinical management. *American Journal of Hematology*, 92(8), 806–813. <https://doi.org/10.1002/ajh.24797>
- Wang, X., Sehgal, L., Jain, N., Khashab, T., Mathur, R., & Samaniego, F. (2016). Lncrna malat1 promotes development of mantle cell lymphoma by associating with ezh2. *Journal of Translational Medicine*, 14(1), 1–14. <https://doi.org/10.1186/s12967-016-1100-9>
- Wang, Z., Gerstein, M., & Snyder, M. (2010). *RNA-Seq : a revolutionary tool for transcriptomics*. 10(1), 57–63. <https://doi.org/10.1038/nrg2484>.RNA-Seq
- Wojcik, S. E., Rossi, S., Shimizu, M., Nicoloso, M. S., Cimmino, A., Alder, H., ... Calin, G. A. (2010). *Non-codingRNA sequence variations in human chronic lymphocytic leukemia and colorectal cancer*. 31(2), 208–215. <https://doi.org/10.1093/carcin/bgp209>
- Wu, C., de Miranda, N. F., Chen, L., Wasik, A. M., Mansouri, L., Jurczak, W., ... Pan-Hammarström, Q. (2016). Genetic heterogeneity in primary and relapsed mantle cell lymphomas: Impact of recurrent CARD11 mutations. *Oncotarget*, 7(25), 38180–38190. <https://doi.org/10.18632/oncotarget.9500>
- Yu, D., Zhang, Y., Chen, G., Xie, Y., Xu, Z., Chang, S., ... Shi, J. (2018). Targeting the PI3K/Akt/mTOR signaling pathway by pterostilbene attenuates mantle cell lymphoma progression. *Acta Biochimica et Biophysica Sinica*, 50(8), 782–792. <https://doi.org/10.1093/abbs/gmy070>
- Zhang, J., Wang, P., Ji, W., Ding, Y., & Lu, X. (2017). Overexpression of interleukin-33 is associated with poor prognosis of patients with glioma. *The International Journal of Neuroscience*, 127(3), 210–217. <https://doi.org/10.1080/00207454.2016.1175441>
- Zhang, P., Liu, X.-K., Chu, Z., Ye, J. C., Li, K.-L., Zhuang, W.-L., ... Jiang, Y.-F. (2012). Detection of interleukin-33 in serum and carcinoma tissue from patients with hepatocellular carcinoma and its clinical implications. *The Journal of International Medical Research*, 40(5), 1654–1661. <https://doi.org/10.1177/030006051204000504>
- Zhang, Y., Lu, P., Du, H., & Zhang, L. (2019). LINK-a lncRNA promotes proliferation and inhibits apoptosis of mantle cell lymphoma cell by upregulating survivin. *Medical Science Monitor*, 25, 365–370. <https://doi.org/10.12659/MSM.912141>
- Zhong, S., Joung, J. G., Zheng, Y., Chen, Y. R., Liu, B., Shao, Y., ... Giovannoni, J. J. (2011). High-throughput illumina strand-specific RNA sequencing library preparation. *Cold Spring Harbor Protocols*, 6(8), 940–949. <https://doi.org/10.1101/pdb.prot5652>

8. APPENDIX

8.1. Curriculum Vitae

Deniz KURŞUN

Date of Birth:	25.11.1994
Contact Address:	Onur Mah. Begonya Sokak No:28/2 Balçova/İzmir
Phone:	+90 5387432342
e-mail:	deniz.kursun@msfr.ibg.edu.tr

EDUCATIONAL BACKGROUND

Country	University	Faculty/Instutite	Department	Degree	Graduation Year
T.C	Yıldız Technical University	Chemical and Metallurgical Faculty	Bioengineering (100% Eng)	BSc (GPA:3.57/4.00)	2016
T.C	Dokuz Eylul University	Izmir Biomedicine Genome Institute	Molecular Biology and Genetics	MSc (GPA:4.00/4.00)	2019

ACADEMIC / PROFESSIONAL EXPERIENCE

Organization	Country	City	Department / Unit	Task Type	Duty Period
Medical Park Göztepe Hospital	T.C	Istanbul	Rotation in Hematology, Biochemistry & Microbiology Departments	Devices and their working principles, applied tests, result analyses, laboratory management	June 2014 – July 2014

APS Packaging - Cosmetics and Cleaning Products AŞ	T.C	Istanbul	Production Engineering	Process management, applied engineering skills	July 2015 – August 2015
-------------------------------------------------------------	-----	----------	---------------------------	------------------------------------------------------------	----------------------------

RESEARCH FIELDS

Research Fields

Functional genomics, RNA-seq analysis, lymphoid cancer malignancies, Mantle cell lymphoma

PUBLICATIONS

Articles published in SCI, SSCI, AHCI indexes

KURŞUN, D., & KÜÇÜK, C. (2019). Systematic analysis of the frequently amplified 2p15-p16. 1 locus reveals PAPOLG as a potential proto-oncogene in follicular and transformed follicular lymphoma. *Turkish Journal of Biology*, 43(2), 124-132.

Publications in the proceedings of refereed conferences / symposiums

Burcu Akman, **Deniz Kurşun**, Tefvik Hatipoğlu, Xiaozhou Hu, Wing C. Chan, Can Küçük “CD25 is a direct transcriptional target of PRDM1 in activated human natural killer cells” American Society of Hematology 2018 annual meeting

Burcu Akman, Hongling Huan, **Deniz Kurşun**, Xiaozhou Hu, Markus Muschen, Wing C. Chan, Can Küçük “CD25 is a direct transcriptional target of PRDM1 in activated human natural killer cells” 6th International Congress of the Molecular Biology Association of Turkey, Izmir, 2018

Burcu Akman, Ahmet Şeyhanlı, Xiaozhou Hu, Doğuş Türkyılmaz, Aybüke Olgun, Hongling Yuan, **Deniz Kurşun**, Taner K. Erdağ, G. Hayri Özsan, Can Küçük “Sox7 Tümör Baskılayıcı Gen Adayının Multipl Myelom Olgularında Tanı ve Nüks Esnasındaki Rolünün İncelenmesi” 45. Ulusal Hematoloji kongresi

8.2. Ethics Comittee

DOKUZ EYLÜL ÜNİVERSİTESİ
GİRİŞİMSEL OLMAYAN ARAŞTIRMALAR ETİK KURULU

Konu:
Sayı :

27.10.2017

Sayın Yard.Doç.Dr.Can KÜÇÜK,

Kurulumuz tarafından 26.10.2017 tarih ve 2525-GOA protokol numaralı 2017/26-31 karar numarası ile görüşülen “**Mantle Hücreli Lenfomalarda Özgün Tanı, Prognoz Belirteci Veya Tedavi Hedefi Olma Potansiyeline Sahip Uzun Kodlamayan RNA'ların Tüm Transkriptom Dizi Analizi Yoluyla Belirlenmesi**” konulu araştırmanıza ilişkin Kurulumuz kararı ekte sunulmuştur.

Bilgilerinizi ve gereğini rica ederim

Prof.Dr.Banu ÖNVURAL
Başkan

Dokuz Eylül Üniversitesi Sağlık Yerleşkesi İnciraltı 35340 TÜRKİYE
Tel:0 232 4122254 - 0 232 4122258 Faks: 0232 4122243 Elektronik posta:etikkurul@deu.edu.tr

BELGELER

rica dilekçesi

16.10.2017

Türkçe

İngilizce

Diğer

DOKUZ EYLÜL ÜNİVERSİTESİ
GİRİŞİMSSEL OLMAYAN ARAŞTIRMALAR ETİK KURUL KARARI

ETİK KOMİSYONUNUN ADI	DOKUZ EYLÜL ÜNİVERSİTESİ GİRİŞİMSSEL OLMAYAN ARAŞTIRMALAR ETİK KURULU
AÇIK ADRES	Dokuz Eylül Üniversitesi Tıp Fakültesi Dekanlığı 2. Kat İnciraltı-İZMİR
TELEFON	0 232 412 22 54-0 232 412 22 58
FAKS	0 232 412 22 43
E-POSTA	etikkurul@deu.edu.tr

BAŞVURU BİLGİLERİ	DOSYA NO:	2525-GOA
	ARAŞTIRMA	UZMANLIK TEZİ <input type="checkbox"/> AKADEMİK AMAÇLI <input type="checkbox"/>
	ARAŞTIRMANIN AÇIK ADI	Mantle Hücreli Lenfomalarda Özgün Tanı, Prognoz Belirteci veya Tedavi Hedefi Olma Potansiyeline Sahip Uzun Kodlamayan RNA'ların Tüm Transkriptom Dizi Analizi Yoluyla Belirlenmesi
	ARAŞTIRMA PROTOKOL KODU	
	SORUMLU ARAŞTIRMACI ÜNVANI/ADI/SOYADI ve UZMANLIK ALANI	Yrd.Doç.Dr.Can KÜÇÜK Biyotıp ve Genom Enstitüsü
	DESTEKLEYİCİ VE AÇIK ADRESİ	-
	DESTEKLEYİCİNİN YASAL TEMSİLCİSİ VE ADRESİ	-
	ARAŞTIRMAYA KATILAN MERKEZLER	TEK MERKEZ <input checked="" type="checkbox"/> ÇOK MERKEZLİ <input type="checkbox"/>

DEĞERLENDİRİLEN BELGELER	Belge Adı	Tarihi	Versiyon Numarası	Dili		
				Türkçe <input checked="" type="checkbox"/>	İngilizce <input type="checkbox"/>	Diğer <input type="checkbox"/>
	Araştırmacı dilekçesi	16.10.2017		Türkçe <input checked="" type="checkbox"/>	İngilizce <input type="checkbox"/>	Diğer <input type="checkbox"/>

KARAR BİLGİLERİ	Karar No:2017/25-31	Tarih:26.10.2017
	Yrd.Doç.Dr.Can KÜÇÜK'ün sorumlusu olduğu "Mantle Hücreli Lenfomalarda Özgün Tanı, Prognoz Belirteci veya Tedavi Hedefi Olma Potansiyeline Sahip Uzun Kodlamayan RNA'ların Tüm Transkriptom Dizi Analizi Yoluyla Belirlenmesi" isimli klinik araştırmaya ait 16.10.2017 tarihli araştırmacı dilekçesine ilişkin olarak; - Normal B hücrelerinin izolasyonu için on adet kanser olmayan bireyden tonsillektomi sırasında alınmış taze reaktif tonsil dokusu kesiti kullanımı ile ilgili belgeler incelenerek bilgi edinilmiş ve uygun bulunmuştur.	
ETİK KURUL BİLGİLERİ		
ÇALIŞMA ESASI	Dokuz Eylül Üniversitesi Girişimsel Olmayan Araştırmalar Etik Kurulu İşleyiş Yönergesi İyi Klinik Uygulamaları Kılavuzu	
ETİK KURUL ÜYELERİ		

Unvanı/Adı/Soyadı	Uzmanlık Alanı	Kurumu	Cinsi yet	Araştırma ile ilişkili mi?		İmza
				E <input type="checkbox"/>	H <input checked="" type="checkbox"/>	
Prof.Dr.Banu ÖNVURAL (Başkan)	Tıbbi Biyokimya	DEU Tıp Fakültesi Tıbbi Biyokimya Anabilim Dalı	Kadın	E <input type="checkbox"/>	H <input checked="" type="checkbox"/>	
Prof.Dr.Ş.Reyhan UÇKU (Başkan Yardımcısı)	Halk Sağlığı	DEU Tıp Fakültesi Halk Sağlığı A.D.	Kadın	E <input type="checkbox"/>	H <input checked="" type="checkbox"/>	
Prof.Dr.Nejat SARIOSMANOĞLU	Kalp Damar Cerrahisi	DEU Tıp Fakültesi Kalp Damar Cerrahisi Anabilim Dalı	Erkek	E <input type="checkbox"/>	H <input checked="" type="checkbox"/>	
Prof.Dr.Sevineç ERASLAN	Endokrinoloji	DEU Tıp Fakültesi İç Hastalıkları Anabilim Dalı	Kadın	E <input type="checkbox"/>	H <input checked="" type="checkbox"/>	
Prof.Dr.Äyşe Aydan ÖZKÜTÜK	Tıbbi Mikrobiyoloji	DEU Tıp Fakültesi Tıbbi Mikrobiyoloji Anabilim Dalı	Kadın	E <input type="checkbox"/>	H <input checked="" type="checkbox"/>	
Prof.Dr.Müge KIRAY	Fizyoloji	DEU Tıp Fakültesi Fizyoloji Anabilim Dalı	Kadın	E <input type="checkbox"/>	H <input checked="" type="checkbox"/>	
Prof.Dr.Sevda ÖZKARDEŞLER	Anesteziyoloji	DEU Tıp Fakültesi Anesteziyoloji ve Reanimasyon A.D.	Kadın	E <input type="checkbox"/>	H <input checked="" type="checkbox"/>	
Prof.Dr.Sülen SARIOĞLU	Patoloji	DEU Tıp Fakültesi Tıbbi Patoloji A.D.	Kadın	E <input type="checkbox"/>	H <input checked="" type="checkbox"/>	
Prof.Dr.Bilge KARA	Fizik Tedavi ve Rehabilitasyon	DEU Fizik Tedavi ve Rehabilitasyon Yüksek Okulu	Kadın	E <input type="checkbox"/>	H <input checked="" type="checkbox"/>	
Prof.Dr.Sefa KIZILDAĞ	Tıbbi Biyoloji ve Genetik	DEU Tıp Fakültesi Tıbbi Biyoloji ve Genetik A.D.	Erkek	E <input type="checkbox"/>	H <input checked="" type="checkbox"/>	
Prof.Dr.Ayhan ABACI	Pediyatrik Endokrinoloji ve Metabolizma Hastalıkları	DEU Tıp Fakültesi Çocuk Sağlığı ve Hastalıkları Anabilim Dalı	Erkek	E <input type="checkbox"/>	H <input checked="" type="checkbox"/>	
Doç.Dr.M.Aylin ARICI	Tıbbi Farmakoloji	DEU Tıp Fakültesi Tıbbi Farmakoloji Anabilim Dalı	Kadın	E <input type="checkbox"/>	H <input checked="" type="checkbox"/>	
Doç.Dr.Murat BEKTAŞ	Çocuk Sağlığı ve Hastalıkları Hemşireliği	DEU Hemşirelik Fakültesi Çocuk Sağlığı ve Hastalıkları Hemşireliği	Erkek	E <input type="checkbox"/>	H <input checked="" type="checkbox"/>	
Uzm.Dr.Ahmet Can BILGIN	Hukuk	DEU Tıp Tarihi ve Etik A.D.	Erkek	E <input type="checkbox"/>	H <input checked="" type="checkbox"/>	
Mehmet Erhan ÖZKUL	Sağlık mensubu olmayan üye	D.E.U Tıp Fakültesi İdari Mali İşler	Erkek	E <input type="checkbox"/>	H <input checked="" type="checkbox"/>	